Multiuser Detection for DS-CDMA Systems Using Optimization Methods

by

Xianmin Wang
M.Sc, Beijing University of Posts & Telecomm., 1999
B.Sc, Beijing University of Posts & Telecomm., 1996

A Dissertation Submitted in Partial Fulfillment of the Requirements
for the Degree of

DOCTOR OF PHILOSOPHY

in the Department of Electrical and Computer Engineering

Supervisor: Dr. A. Antoniou and Dr. W.-S. Lu

ABSTRACT

Several new multiuser detectors are developed for different direct-sequence code-division multiple-access (DS-CDMA) application environments. The first detector is based on a *semidefinite-programming* (SDP) relaxation technique. In this detector, maximum likelihood (ML) detection is achieved by 'relaxing' the associated combinatorial problem into an SDP problem, which leads to a detector of polynomial complexity. It is shown that the SDP-relaxation (SDPR) based detector can be obtained by solving a dual SDP problem which leads to improved efficiency. Computer simulations demonstrate that the SDPR detector offers near-optimal performance with much reduced computational complexity compared with that of the ML detector proposed by Verdù for both synchronous and asynchronous DS-CDMA systems.

The second detector is based on a *recursive convex programming* (RCP) approach. In this detector, ML detection is carried out in two steps: first, the combinatorial problem associated with ML detection is relaxed to a convex programming problem, and then a recursive approach is used to obtain an approximate solution for ML detection. Efficient unconstrained relaxation approach is proposed for the proposed detector to reduce the involved computational complexity. Computer simulations demonstrate that the proposed detectors offer near-optimal detection performance which is superior to that offered by many other suboptimal detectors including the SDPR detector. However, the computational complexity involved in the proposed detectors is much lower relative to that involved in Verdù's ML detector as well as our SDPR detector.

The third detector entails a *subspace estimation-based constrained optimization* approach for channel estimation in DS-CDMA systems with multipath propagation channels. The proposed approach offers an improved approximation for the noise

subspace compared with that offered by several existing algorithms. Computer simulations show that the performance of the proposed detector offers nearly the same performance as that of existing subspace detectors but leads to a significant reduction in the amount of computation. Relative to some existing constrained optimization methods, the proposed detector offers a significantly improved performance while requiring a comparable amount of computation.

The fourth detector is proposed based on a *vector constant-modulus* (VCM) approach. This detector is designed for DS-CDMA systems with multipath propagation channels where the effective signatures observed at receiver are distorted by multipath propagation and aliasing concurrently. In this detector, detection is carried out by solving a linear constrained optimization problem whose objective function is formulated based on the VCM criterion. Two adaptation algorithms, namely, the constrained stochastic gradient algorithm and the recursive vector constant-modulus algorithm, are developed. Analysis are presented to investigate the performance of the proposed detector. Computer simulations show that the proposed detectors are able to suppress multiuser interference and inter-symbol interference effectively. More importantly, they offer robust detection performance against the effective signature distortion caused by aliasing at the receiver.

Table of Contents

Abstract ii

Table of Contents v

List of Tables ix

List of Figures x

List of Abbreviations xii

Acknowledgement xv

1 Introduction 1

1.1 Previous Work 4

1.1.1 Linear Multiuser Detectors 6

1.1.2 Nonlinear Multiuser Detectors 7

1.1.3 MUI Suppression Using Smart Antenna 8

1.2 Scope and Contributions of This Thesis 9

2 Fundamentals of DS-CDMA and Multiuser Detection 12

2.1 Introduction 12

2.2 Mobile Communication Channel 12

2.2.1 Doppler Spread: Time-Selective Fading 14

2.2.2 Delay Spread: Frequency Selective Fading 16

2.2.3 Classifications of Mobile Communication Channel 17

2.3 DS-CDMA System 19

2.3.1 Code Division Multiple Access 19
2.3.2 Conventional Detection 21
2.4 Multiuser Detection 28
2.4.1 Maximum Likelihood Multiuser Detection 29
2.4.2 Linear Multiuser Detectors 31
2.4.2.1 Decorrelating Detector 32
2.4.2.2 MMSE Detector 34
2.4.2.3 Blind Detection 36
2.4.3 Nonlinear Multiuser Detectors 42
2.4.3.1 Generalized MMSE Detector 42
2.4.3.2 Bound-Constrained Detector 43
2.5 Conclusion 44

3 New Suboptimal ML Detectors Based on Semidefinite Programming Relaxation 46

3.1 Introduction 46
3.2 New Multiuser Detector Based on SDP Relaxation 48
3.2.1 Semidefinite Programming 48
3.2.2 SDP Relaxation of MAX-CUT Problem 48
3.2.3 Primal SDP-Relaxation Based Detector 51
3.2.4 Binary Solution 52
3.2.5 Optimality of Solution 54
3.3 Dual SDP-Relaxation Based Detector 55
3.4 Simulation Results 59
3.5 Conclusions 62

4 Multiuser Detector Based on Recursive Convex Programming 68

4.1 Introduction 68
4.2 Convex Relaxation of ML Detection 69

4.3 Recursive CP-based Multiuser Detection 72
4.3.1 Recursive ML Approach for Multiuser Detection 73
4.3.2 RCP-Based Multiuser Detection 75
4.3.3 Relationship Between RCP Detector and SDPR Detectors . . 78
4.4 Improved RCP Detector 80
4.5 Simulation Results 84
4.6 Conclusions 87

5 Subspace Estimation Based Multiuser Detector for Multipath DS-CDMA Channels **94**
5.1 Introduction 94
5.2 Relationship between Subspace Methods and Constrained Optimization Methods 96
5.3 Constrained Optimization Method Based on Subspace Estimation . . 98
5.4 Simulations 100
5.5 Conclusions 101

6 VCM Multiuser Detector for DS-CDMA Systems with Multipath Fading Channels **104**
6.1 Introduction 104
6.2 Signal Model 106
6.3 VCM-Based Blind Multiuser Detectors 107
6.4 Adaptation Algorithms 111
6.5 Analysis of the Proposed Adaptation Algorithms 113
6.6 Simulation Results 116
6.7 Conclusions 118

7 Conclusions and Future Work **119**

7.1 Conclusions 119
7.1.1 SDPR Detector 119
7.1.2 RCP Detector 120
7.1.3 SED Detector 121
7.1.4 VCM Detector 122
7.2 Future Work 123
7.2.1 RCP Detectors 123
7.2.2 RCP Detectors for Asynchronous DS-CDMA Systems 124
7.2.3 SED Detector 124

Bibliography **126**

Appendix A Proof of Propostion 4.2 **134**

Appendix B Proof of Proposition 4.4 **137**

Appendix C A Sufficient Condition for Global Convexity of the Problem in (6.19) **140**

List of Tables

Table 4.1 Recursive CP Detector 77
Table 4.2 Improved Recursive CP Detector 81

Table 6.1 Definitions of $\bar{A}_k$, $\bar{b}_k^i$, and $\bar{\mathbf{h}}_k$ in (6.4) 108
Table 6.2 Constrained Stochastic Gradient Algorithm 112
Table 6.3 Recursive VCM Algorithm 113

List of Figures

Figure 1.1 Three multiple access schemes: FDMA, TDMA, and CDMA. . 2

Figure 2.1 A tap-delayed model for multipath propagation channels. . . . 13

Figure 2.2 Classification of multipath propagation channels depending on (a) coherence time (or delay spread) and (b) coherence bandwidth (or Doppler spread). 18

Figure 2.3 Signal model for DS-CDMA systems. 21

Figure 2.4 Conventional detector for asynchronous DS-CDMA systems over AWGN channels. 23

Figure 2.5 Conventional detector for DS-CDMA system using an L-element antenna array. 26

Figure 2.6 An M-branch RAKE receiver for DS-CDMA systems over frequency-selective fading channels. 27

Figure 2.7 Multiuser detector for synchronous DS-CDMA systems. 29

Figure 3.1 BER versus SNR for a six-user synchronous DS-CDMA system over AWGN channel. 63

Figure 3.2 BER versus SNR for an eight-user synchronous DS-CDMA system over flat Rayleigh fading channel. 64

Figure 3.3 Near-far performance in a six-user synchronous DS-CDMA system over AWGN channel. 65

Figure 3.4 BER versus SNR for a four-user asynchronous DS-CDMA system over AWGN channel. 66

Figure 3.5 Computational complexity of the demodulation for ML, PS-DPR, DSDPR detectors. 67

Figure 4.1 Feasible regions defined by (4.1b) (labeled with small circles) and by (4.13b) for $p = 20$ (denoted as I), $p = 3$ (I+II), $p = 2$ (I+II+III) and $p = 1$ (I+II+III+IV). 73

Figure 4.2 BERs of the seven-user system for $\alpha = 0.95$. 86

Figure 4.3 BERs of the seven-user system for $\alpha = 0.80$. 87

Figure 4.4 BERs of the seven-user system for $\alpha = 0.50$. 88

Figure 4.5 BERs of the fifteen-user system for $\alpha = 0.95$. 89

Figure 4.6 BERs of the fifteen-user system for $\alpha = 0.80$. 90

Figure 4.7 BERs of the fifteen-user system for $\alpha = 0.50$. 91

Figure 4.8 BERs of the fifteen-user system for $\alpha = 0.30$. 92

Figure 4.9 Computational complexity of various detectors. 93

Figure 5.1 MSE of the estimation of the channel impulse response in Example 1. 102

Figure 5.2 MSE of the estimation of the channel impulse response in Example 2. 103

Figure 6.1 The BERs of various detectors in the first example. 115

Figure 6.2 The BERs of various detectors in the second example. 116

Figure 6.3 Demodulation BERs obtained in the first example. 117

Figure 6.4 Demodulation BERs obtained in the second example. 118

List of Abbreviations

AWGN	Additive white Gaussian noise
BC	Bound constraint
BPSK	Binary phase-shift-key
BER	Bit-error rate
BS	Base station
CCI	Co-channel interference
CDMA	Code-division multiple-access
CM	Constant-modulus
CMOE	Constrained minimum-output-energy
COM	Constrained optimization method
CP	Convex programming
CQP	Convex quadratic programming
CSG	Constrained stochastic gradient
DF	Decision feedback
DD	Decorrelating detector
DOA	Direction of arrival
DS-CDMA	Direct-sequence code-division multiple-access
ED	Eigenvalue decomposition
FDMA	Frequency-division multiple-access
GMMSE	Generalized minimum mean-squared-error
IMT-2000	International mobile telecommunication 2000
IS-95	Interim standard 95
IS-665	Interim standard 665

ISI	Inter-symbol interference
ITU	International telecommunication union
KKT	Karush-kuhn-tucker
LMI	Linear matrix inequality
LMMSE	Linear minimum mean-squared-error
LMS	Least-mean-square
LOS	Line of sight
MA	Multiple access
MAI	Multiple-access interference
MF	Matched filter
MFB	Matched filter bank
ML	Maximum likelihood
MMSE	Minimum mean-squared-error
MRC	Maximum ratio combination
MSE	Mean-squared-error
MUI	Multi-user interference
NF	Near-far
NP	Non-polynomial
PDF	Probability density function
PIC	Parallel interference cancellation
QP	Quadratic programming
RCP	Recursive convex programming
RF	Radio frequency
RLS	Recursive-least-square
r.v.	Random variable
RVCM	Recursive vector constant-modulus
SECO	Subspace-estimation-based comstrained optimization
SDP	Semidefinite programming

SDPR	Semidefinite programming relaxation
SDPR-D	Semidefinite programming relaxation dual
SDPR-P	Semidefinite programming relaxation primal
SIC	Successive interference cancellation
SINR	Signal-to-interference-plus-noise ratio
SM	Subspace method
SNR	Signal-to-noise ratio
SS	Spread spectrum
SSMA	Spread-spectrum multiple-access
TDMA	Time-division multiple-access
UMTS	Universal mobile telecommunication system
UR	Unconstrained relaxation
VCM	Vector constant-modulus

Acknowledgement

First, I would take this opportunity to express deep gratitude to my co-supervisors, Dr. Andreas Antoniou and Dr. Wu-Sheng Lu, for their insightful thoughts that foresee the topic of this thesis and guide me through the entire journey toward the accomplishment of my Ph. D degree. Their continuous encouragement and support along the way of my Ph. D study are invaluable to me.

I thank Dr. Pan Agathoklis, Dr. Dale Olesky and Dr. Wei-Ping Zhu for being on my thesis committee, and for their contribution of precious time in providing suggestions, comments, and questions that greatly help improve the quality of this thesis.

I wish to thank our staff Ms. Catherine Chang, Ms. Lynne Barrett, Ms. Vicky Smith, Ms. Moneca Bracken, and Ms. Mary-Anne Teo, and my colleahues Dr. Xiaofeng Wang, Dr. M. Watheq El-Kharashi, Dr. Tarek Nasser, Yajun Kou, Nanyan Wang, Mingjie Cai, Manjinder Mann, Rafik Mikhael, Rajeev Nongpiur, Sabbir Ahmad, Stuart Bergen, Deepali Arora, Paramesh Ramachandran, Mohamed S. Yasein, Brad Riel, David Guindon, and many others whose names do not appear here for their generous friendship, enlightening discussion, and productive cooperation.

I also thank micronet, NSERC, and PMC-Sierra Inc. sponsoring the project of this thesis. The financial support from these sources is greatly appreciated.

I am greatly indebted to my parents for their love, deep understanding, and continuous strong support on the pursuit of my Ph. D degree that culminated this thesis.

Finally I wish to express my deepest gratefulness to my wife, Zhiwei, who has been accompanying and supporting me walking through the journey of many years. Without her encouragement and support, I could not have come even close to what I have achieved today.

Chapter 1

Introduction

The history of modern wireless communications can be dated back to more than one hundred years ago when *Guglie Marconi* first invented radio telegraph in 1897 [1]. Since then, wireless communication technology has witnessed steady and continuous progress. In the late 1980s, personal mobile communications began to be widely accepted by the general public. In the last twenty years, both academic and industrial societies have contributed tremendous efforts to the development of wireless communications.

The rapid progress in wireless communications has brought about many low-cost services to the public. In the past ten years, however, most of these services were restricted to narrow-band communications such as voice telephony and low-speed data transmission. Due to an increasing demand for wideband applications, wideband, or even broadband wireless communications become the focus of next-generation wireless communication systems.

In the development of wireless communications, radio spectrum has been considered as one of the most precious resources [1, 2, 3]. In order to improve the spectrum efficiency and system capacity, several multiple access (MA) schemes have been proposed for wireless communications, which can be classified into three categories: frequency-division multiple access (FDMA), time-division multiple access (TDMA), and code-division multiple access (CDMA).

Three MA schemes are illustrated in Fig. 1.1. In the FDMA scheme, user sig-

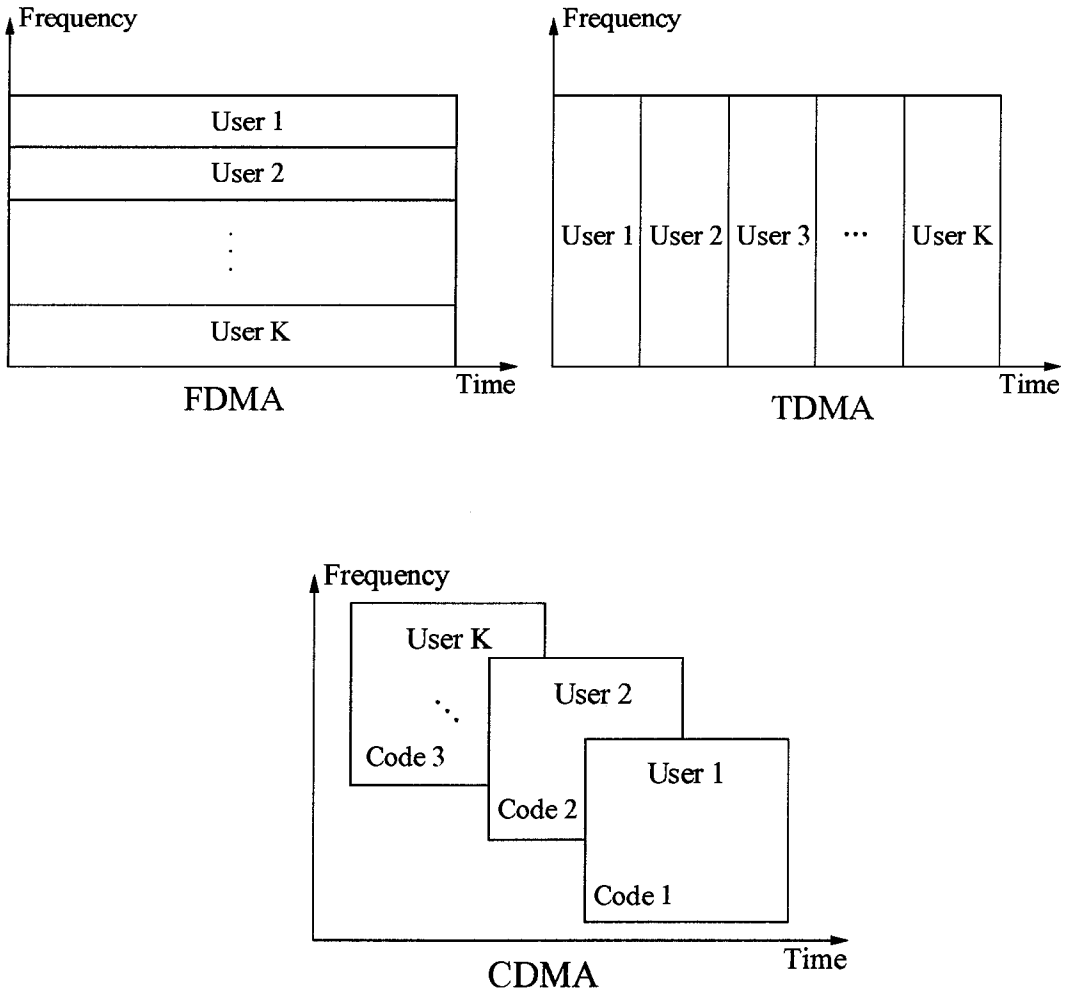

Figure 1.1. *Three multiple access schemes: FDMA, TDMA, and CDMA.*

nals are separated by non-overlapping transmission frequency bands; in the TDMA scheme, user signals are separated by non-overlapping transmission time slots; and in CDMA scheme, user signals are separated by different signature waveforms [1, 4]. Since the frequency bandwidth of CDMA signals is often much wider relative to that of the transmitted signals, the CDMA scheme is also referred to as the *spread spectrum multiple access* (SSMA) scheme [3, 5, 6, 7]. Compared with FDMA and TDMA, the CDMA scheme offers many advantages to mobile communications such as soft system capacity, soft hand-off, anti-jamming, low power consumption, and low

narrow-band interference to other wireless systems. Therefore, the CDMA scheme has been adopted in many air interface standards in the second and third generation wireless communications such as IS-95, IS-665, CDMA2000, and IMT-2000.

One of the most popular CDMA schemes is the direct-sequence CDMA (DS-CDMA). In this scheme, the signal of each user is first spread by multiplying the information-bearing symbols by a specific signature waveform. Then the spread signals of all users are transmitted through communication channels by simultaneously sharing the same frequency bandwidth. Therefore, the received signal is the superposition of the signals of all users plus ambient channel noise. At the receiver, the demodulation of each signal is carried out by passing the received signal through a so-called *matched filter* (MF) which correlates the received signal with the corresponding signature waveform. This process is called *despreading*. The transmitted information bits are then determined as the sign of the matched-filter's output.

If the signature waveforms of all users are orthogonal to each other, then the multiuser interference (MUI) present in the received signal can be completely removed by the MFs. In such a case, the demodulation performance of a DS-CDMA system is equivalent to that of a single-user communication system [9]. However, if the signature waveforms are not orthogonal to each other or the transmission is not completely synchronized, then the MUI may not be completely removed by the matched filters. The MUI present at the outputs of the MFs not only significantly impairs the demodulation performance of DS-CDMA systems, but it also causes the so-called *near-far* problem [1, 17]. That is, the far-end mobile signal (with weak power) may be largely immersed in the interference from a near-end mobile signal (with strong power). Since the signature waveforms are largely determined by the properties of the signature sequences, the design of signature sequences with good autocorrelation and crosscorrelation has been an active research topic for many years [10, 11, 12].

Other forms of MUI known as co-channel interference (CCI) and inter-symbol interference (ISI) also appear in the FDMA and TDMA schemes. Since the sources

of interference are primarily due to spectral and temporal overlap between adjacent transmitted signals, CCI and ISI can be easily alleviated by inserting guarding frequency bands or guarding time slot between adjacent transmitted signals. Other effective methods for CCI and ISI suppression can be found in [13, 14, 15]. Since the transmitted signals of all users share the same frequency bandwidth and the same time slot, MUI suppression is a non-trivial problem in DS-CDMA systems.

Multiuser detection is a technique for demodulating information-bearing symbols from mutually interfering digital streams. Techniques for multiuser detection have been exploited widely in many applications such as high-speed data transmission, digital television, satellite communications, and wireless communications. In these applications, the intrinsic structure of MUI signals is exploited by multiuser detection algorithms to help recover the transmitted information. In the past twenty years, multiuser detection for DS-CDMA systems has been one of the most active research areas in digital communications [17, 18, 19].

Many existing multiuser detectors have been developed based on optimization methods. Recent progress in this area has demonstrated that the performance and the computational complexity of multiuser detectors can be considerably improved by incorporating optimization concepts and efficient algorithms. In this thesis, new optimization-based multiuser detectors for DS-CDMA systems are developed with an objective to achieve improved performance and reduced computational complexity at the same time.

1.1 Previous Work

An implementation of any detection method is said to be a detector and it may assume a software or hardware form. A detector in software form would comprise one or more algorithms. In conventional DS-CDMA systems, transmitted information symbols are detected by using a bank of MFs, each of which is matched to the signature

waveform assigned for a specific user. By completely neglecting the existence of MUI, the transmitted information bits are demodulated as the sign of the MF outputs. This detection method is often referred to as the conventional detector and has been studied for many years. Although the conventional detector offers optimal demodulation performance in single-user communication systems over an additive white Gaussian noise (AWGN) channel [4], its performance is impaired by MUI. In addition, the performance of the conventional detector is seriously degraded when the near-far problem of DS-CDMA systems is serious.

To improve the performance, new multiuser detection methods and detectors have been investigated. An early multiuser detection method for DS-CDMA systems is the so-called maximum-likelihood (ML) method proposed by Verdù [20]. In this pioneering work, detection is achieved by maximizing the *joint a posteriori probability*, which is done by selecting the information-bearing waveform closest to the observed waveform in terms of *Euclidean* distance. The ML detection method has been shown by Verdù [20] to offer joint optimal demodulation performance and has been implemented by a number of researchers [20, 22, 23, 24, 25]. Implementations of the ML detection method are known collectively as ML detectors, and this family of detectors is often used as a comparison baseline for ML-based suboptimal as well as other types of suboptimal multiuser detectors. One disadvantage of ML detectors is that except for some special applications where the crosscorrelation matrix of the user signatures is well structured [24, 25], the detection has to be carried out by solving a combinatorial optimization problem which involves a quadratic objective function and binary constraints. Consequently, the worst-case computational complexity of ML detectors increase in an exponential manner with the number of users, and the implementation of these detectors becomes prohibitive even for DS-CDMA systems with a moderate number of users. To deal with this problem, various suboptimal ML detectors have been proposed, which offer reduced computational complexity relative to Verdù's ML detector [28, 63, 64, 84, 59, 60]. Other suboptimal detectors that are

not directly derived from the ML detectors include the minimum mean-squared-error (MMSE) detector, constrained minimum-output-energy (CMOE) detector, successive interference cancellation (SIC) detector, parallel interference cancellation (PIC) detector, etc. A detailed account of these and many other suboptimal detectors can be found in [17] and the references therein. Depending on whether linear transformations are applied to the received signal in detection, these detectors can be classified as linear or nonlinear multiuser detectors [17, 19].

1.1.1 Linear Multiuser Detectors

A linear multiuser detector exploits a linear transformation (mapping) to the outputs of the MF bank in order to reduce the MUI present in the transformed signal. Three well-known linear multiuser detectors are the decorrelating [28, 29, 30], the linear minimum mean-squared-error (LMMSE) [31, 32, 33], and the CMOE detectors [35].

In the decorrelating detector, the linear transformation is determined in order to completely eliminate the MUI present in the transformed signals without considering the presence of channel noise. Although the MUI can be completely cancelled by the decorrelating detector, the channel noise is enhanced by the linear transformation. Consequently, the decorrelating detector suffers significant performance degradation when the channel noise level is relatively high. Studies have been presented to show that the performance of a decorrelating detector is likely to be inferior to that of a conventional detector in DS-CDMA systems with low SNR.

The linear transformation used in the LMMSE detector is determined in order to minimize the mean-squared-error (MSE) between the transformed signals and transmitted information symbols. It can be shown that the requirement of suppressing MUI while not enhancing the effect of channel noise can be met by the resulting linear transformation. In most cases, an LMMSE detector offers better performance relative to that of a decorrelating detector especially when the channel noise is significant. One disadvantage of the LMMSE detector is that the power of the received

signals of all users and the level of channel noise has to be known for LMMSE detection. This requirement inevitably increases the whole system complexity. In order to avoid the problem, adaptive implementations of linear MMSE detectors using training sequences have been proposed [36, 37, 38]. In a fast time-varying communication channel, the repeated transmission of training sequences reduces spectrum efficiency. Subspace methods for deriving the decorrelating and LMMSE detectors were proposed in [39].

In a CMOE detector, the linear transformation is used to minimize the energy of the transformed signal by assuming that the projection of the received signal onto the desired user signature is fixed. It has been shown that the detection vector obtained for CMOE detection is the same as that obtained for LMMSE detection to within a scalar multiplier [35]. For this reason, the demodulation performance of a CMOE detector is considered the same as that of an LMMSE detector, and is superior relative to that of a decorrelating detector. Since the CMOE detector can be implemented adaptively without relying on training sequences and the information other than the signature of the desired user, it has received a great deal of attention since been proposed. One disadvantage of the CMOE detector is that its performance can degrade significantly when the desired user signature used at receiver is not the same as the one specified at transmitter [35]. This is very likely happen in DS-CDMA systems with multipath propagation channels where the signatures are distorted due to multipath propagation. Possible remedies are to estimate the impulse responses of multipath channels and reconstruct the effective signatures observed at the receiver for CMOE detection. This approach has been pursued by several authors using subspace methods [40, 41] and constrained optimization methods [42, 43, 44].

1.1.2 Nonlinear Multiuser Detectors

Nonlinear multiuser detectors are also very popular for DS-CDMA systems. Many nonlinear multiuser detectors, such as the SIC [45, 46, 51, 52], PIC [53, 54], multi-

stage [55, 56], and decision-feedback detectors [57, 58] detectors, are decision-aided multiuser detectors. The underlying principle in these detectors is that the soft or hard decisions obtained in previous stages are utilized to help improve the decisions in subsequent stages. Obviously, the performance of these detectors depends largely on initial decisions. Compared with linear multiuser detectors, nonlinear detectors are computationally less involved and are suitable for DS-CDMA systems using long signature codes. These advantages make them particularly useful for practical DS-CDMA systems.

Other recently proposed nonlinear multiuser detectors are suboptimal ML detectors, which include the generalized MMSE (GMMSE) [59, 60], bound-constraint (BC) [59, 60, 62], and semidefinite programming relaxation (SDPR) detectors [62, 63, 64, 84]. One common feature of these detectors is that they are developed by relaxing the ML detection problem into various optimization problems that can be solved more efficiently. The GMMSE and BC detectors will be briefly reviewed in chapter 2 and the SDPR detector will be carefully studied in chapter 3.

1.1.3 MUI Suppression Using Smart Antenna

In addition to using multiuser detection methods, the suppression of MUI has also been pursued by many researchers using smart antenna techniques [66]. In this technique, antenna arrays are equipped at receivers to exploit the spatial diversity of mobile users. Since mobile users are often located at different places, the directions-of-arrival (DOA) of the signals from distinct users are usually different. If the radiation pattern of the antenna array is designed such that the peaks and nulls of the radiation pattern are steered toward the DOA of the signal of the desired user and interferers, respectively, then the MUI present in the received signal can be suppressed. A more advanced approach to suppress MUI is to combine multiuser detection methods and smart antenna techniques together, which brings about the so-called *space-time multiuser detectors*. In general, the MUI suppression performance offered by space-time

multiuser detectors is superior to that achieved by using multiuser detection or smart antenna alone.

1.2 Scope and Contributions of This Thesis

This thesis is composed of seven chapters. In Chapter 2, a preliminary study on wireless and mobile communication channels, DS-CDMA systems, and several important multiuser detection methods is presented. Chapters 3-6 constitute the main part of the thesis where four new multiuser detectors are proposed. Chapter 7 provides concluding remarks and suggestions for future study.

In Chapter 3, new suboptimal detectors for DS-CDMA systems are proposed based on the semidefinite-programming relaxation approach [71]. It is shown that the ML detection can be carried out by 'relaxing' the associated combinatorial programming problem into an SDP problem where both the objective function and constraint functions are convex functions of continuous variables. This leads to a suboptimal ML detector, referred to in this thesis as the *primal SDP relaxation-based detector*, whose computational complexity is of polynomial order with respect to the number of users. Next, an efficient dual algorithm is proposed to solve the SDP problem in three steps. First, the primal SDP problem is converted into a dual problem based on the duality theory. Then the dual SDP problem is solved using the projective method [61] which leads to improved efficiency due to the reduced number of variables. Then, the solution of the primal SDP problem is expressed in terms of the solution of the dual SDP problem based on the Karush-Kuhn-Tucker (KKT) conditions and the central path concept. The dual algorithm obtained leads to a new detector referred to in this thesis as the *dual SDP relaxation-based detector*. Computer simulations are presented which demonstrate that the proposed detector offers near-optimal performance for both synchronous and asynchronous DS-CDMA systems as well as a significantly reduced computational complexity compared with that associated with the ML de-

tector proposed in [20]. In addition, it is demonstrated by our simulations that the proposed dual algorithm solves the SDP problem very efficiently without impairing the performance.

In Chapter 4, another new suboptimal ML detector is developed by using a *recursive convex programming* (RCP) approach. In this detector, the detection is carried out in two steps: first, the combinatorial optimization problem involved in ML detection is relaxed into a convex programming (CP) problem and then a recursive approach is applied to the CP problem to obtain an approximate solution of the ML detection problem. An efficient algorithm is developed for the proposed detector and the efficiency of the algorithm is investigated through analysis. Computer simulations demonstrate that the proposed detector outperforms many existing suboptimal ML detectors such as the GMMSE, bound-constrained, and our SDPR detectors. In particular, it offers comparable detection performance relative to that of Verdù's ML detector, yet it requires a significantly reduced amount of computation.

Chapter 5 is devoted to channel estimation problem in multiuser DS-CDMA systems with multipath propagation channels. A subspace estimation-based constrained optimization method is proposed in the chapter to estimate the impulse response of multipath propagation channels. This method entails a new algorithm that offers improved approximation for the noise subspace in a more robust manner than several existing methods. It is demonstrated that the proposed method can achieve nearly the same performance as the subspace methods in [40, 41] with much reduced computational complexity. Compared with the constrained optimization methods described in [42, 43, 44], our method offers a significantly improved performance while requiring a comparable amount of computation.

Chapter 6 is devoted to multiuser detection for DS-CDMA systems with multipath propagation channels. In such a case, the demodulation performance of the CMOE detector degrades severely if mismatched signature is used at the receiver for detection. Although several detection methods have been proposed using subspace

and constrained optimization approaches, their demodulation performance becomes unsatisfactory when signature distortion occurs due to aliasing at the receiver. In this chapter, a new multiuser detector is proposed where the detection is carried out by solving a linear constrained optimization problem whose objective function is formulated based on the vector constant-modulus (VCM) criterion. By treating the signals in the adjacent symbol durations as that from equivalent users in the current symbol duration, the ISI is treated as MUI in the received signal. Two adaptation algorithms are developed for solving the optimization problem and the performance of the proposed detector is investigated. Through computer simulations, it is demonstrated that the proposed detector can effectively suppress MUI and ISI simultaneously. More importantly, it is shown that when signatures are distorted by aliasing at receiver, the proposed detector offers superior performance to existing detectors using subspace and constrained optimization methods.

Chapter 2

Fundamentals of DS-CDMA and Multiuser Detection

2.1 Introduction

The objective of multiuser detection is to identify transmitted information from mutually interfering signal waveforms observed at the receiver. In DS-CDMA systems, the design of a multiuser detector depends on many considerations such as the availability of signal information, the system synchronization scheme used, the type of signature codes, and the characteristics of the wireless communication channel. In this chapter, some background knowledge, concepts, and terminology for the mobile communication channel, the DS-CDMA system, and multiuser detection are discussed. The chapter provides a basis on which the subsequent chapters are developed in a unified framework for various multiuser detection algorithms.

2.2 Mobile Communication Channel

In a mobile communication system, a transmission channel is referred to as a propagation path over which radio signals travel from a base station to a mobile (forward link), or from a mobile to a base station (reverse link) [26]. Typical mobile communication channels vary from simple line-of-sight (LOS) transmission channels to very

complicated ones that may be blocked by vehicles, mountains, and high-rise buildings. In addition, due to the relative motion of mobiles and other radio propagation media with respect to the base station, the received signals often exhibit a great deal of randomness. Consequently, mobile communication channels are often modeled using statistical methods.

Two important parameters associated with mobile communication channels are *time variation* and *time dispersion*. Time variation is due to varying radio signal propagation environment from the transmitter to the receiver such as movement of the transmitter, receiver, or other media that are relied on during signal propagation. Time dispersion is due to multiple reflections during signal propagation where different electromagnetic waves travel along different paths of varying lengths and arrive at the receiver with different time delays. In general, mobile communication channels can be described using a tap-delayed model presented in Fig. 2.1 [1, 26].

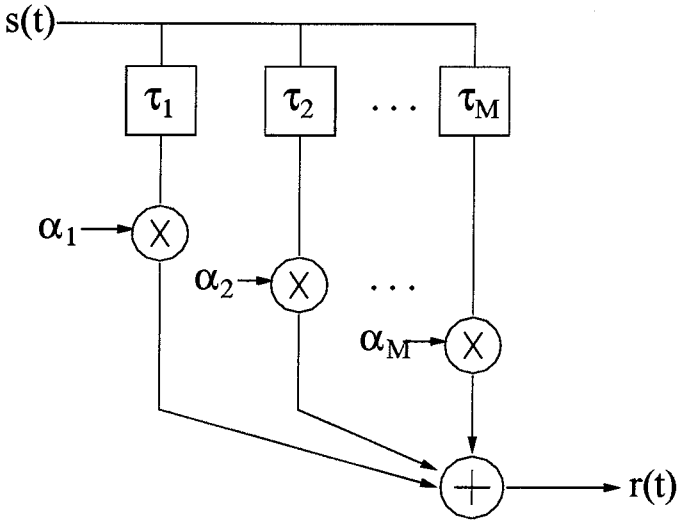

Figure 2.1. *A tap-delayed model for multipath propagation channels.*

The effects of time variation and time dispersion in mobile communication channels are represented by using variable path gain α_m and path delay τ_m in the channel model of Fig. 2.1. The impulse response of the multipath propagation channel de-

scribed in Fig. 2.1 is given by [1]

$$g(t) = \sum_{m=1}^{M} \alpha_m \exp(-j\theta_m)\delta(t - \tau_m) \tag{2.1}$$

where $\delta(t)$, M, α_m, τ_m, and θ_m denote the unit impulse function, the number of resolvable propagation paths, the real path gain, the excess path delay, and the additional phase shift of the mth propagation path, respectively.

2.2.1 Doppler Spread: Time-Selective Fading

In mobile communication systems, the power level of the received signals often exhibits fluctuations and variations. This phenomenon is called *fading* which is due to the relative motion of the mobile and other transmission media. Specifically, the effect of fading can be described as follows [1], i.e.,

$$\alpha(t) = \alpha_f(t) \cdot \alpha_s(t) \tag{2.2}$$

where $\alpha_f(t)$ represents the effect of fast fading and $\alpha_s(t)$ represents the effect of slow fading, respectively, and $\alpha(t)$ represents the total effect of channel fading.

Fast fading is caused by the scattering of transmitted radio signals by objects surrounding transmitters or receivers. In mobile communication systems that are operated in urban areas, radio transmission is very likely to be blocked by high-rise buildings or other obstructive objects. As a result, LOS transmission between transmitter and receiver is not available. In such a case, the signal observed at receiver is the superposition of a large number of scattered electromagnetic signals travelling along different propagation paths. Assume that a large number of signals arrive at receiver with random amplitudes and DOAs and the phase shifts of these signals are uniformly distributed over the range $[0, 2\pi)$, then $\alpha_f(t)$ in (2.2) can be modeled as a *Rayleigh* distributed random variable whose probability density function (PDF) is given by [26]

$$f(x) = x \cdot \exp(-x^2/2) \tag{2.3}$$

A fading channel whose path gains have a Rayleigh PDF [26] is referred to as a *Rayleigh fading channel.* When a direct LOS transmission is available between transmitter and receiver, the amplitude of the channel impulse response has a so-called *Rice* PDF [26], and the fading channel in this case is referred to as a *Rician fading channel.* Note that *Nakagami* distribution [26] is also frequently used to describe the effect of fast fading, and the fading channel in such a case is referred to as a *Nakagami fading channel.*

Slow fading is primarily due to signal shadowing by buildings or natural obstacles during radio signal propagation from transmitter to receiver. This effect is related to the local mean of that of fast fading. In a Rayleigh fading channel, the effect of slow fading, $\alpha_s(t)$, is modeled as a log normally distributed random variable whose PDF is given by

$$f(x) = \frac{20\log_{10} e}{x\sigma_p\sqrt{2\pi}} \exp\left(-\frac{(20\log_{10} x)^2}{2\sigma_p^2}\right) \tag{2.4}$$

Doppler spread is a measurement often used to describe the time varying nature of a mobile communication channel. Doppler spread is relevant to a phenomena that when a pure tone signal is transmitted through a time variant mobile communication channel, the received signal may spread over a finite spectral bandwidth. Specifically, Doppler spread is defined as the range of frequencies over which the spectrum of the received signal assumes non-zero values. In mobile communications, Doppler spread is related to the velocity of moving objects such as mobiles and other propagation media, and the angle between the direction of movement and the DOA of scattered electromagnetic signals [1].

Coherence time is a measurement used to describe the frequency dispersion nature of a mobile communication channel in the time domain. It represents the time duration over which the power levels of two received signals have strong correlation. This implies that the channel condition is essentially invariant within the coherent time. Numerically, coherence time is inversely proportional to the Doppler spread. In

mobile communication systems, coherence time is usually defined as the time duration over which the time correlation function is greater than 0.5,which can be roughly computed as

$$T_c = \frac{9}{16\pi f_m} \tag{2.5}$$

In (2.5), $f_m = v/\lambda$ denotes the *maximum Doppler shift* with v and λ being the velocity of the mobile relative to the base station and the wave length of the radio signal, respectively. A channel is said to be *slow fading* if the coherence time is much longer than the symbol duration of the transmitted signal. In such a case, the effect of Doppler spread at the receiver is simply negligible. On the other hand, if the coherence time is shorter than or comparable with the symbol duration of the transmitted signal, the channel is said to be a *fast fading* channel in which the effect of Doppler spread can not be ignored.

2.2.2 Delay Spread: Frequency Selective Fading

Delay spread is a measurement used to describe the time dispersion nature of a mobile communication channel. In mobile communications, the received signal is composed of several attenuated versions of transmitted signals, which, having been transmitted along different paths of different lengths, arrive at the receiver at different times. The parameters frequently used in quantifying the delay spread of a mobile communication channel are *mean excess delay*, *rms delay spread*, and *excess delay spread*, which are defined in [1]. In a typical mobile communication channel, the delay separation between adjacent propagation paths increases exponentially and the path amplitudes decay exponentially with respect to path delay [69, 70]. Delay spread often leads to *frequency selective fading*, i.e., the fading effect of the received signal depends on frequency.

Coherence bandwidth is a measurement of the range of frequencies over which propagation channels can pass all spectral components with approximately equal

gain and linear phase. This implies that the power levels of two signal frequencies are potentially correlated within the coherence bandwidth. If the coherence bandwidth is defined as the bandwidth over which the frequency correlation function is greater than 0.9, then it can be roughly computed as

$$f_c = \frac{1}{50\sigma_t} \tag{2.6}$$

where σ_t denotes the *rms* delay spread (see [1] for definition). A channel is said to be *frequency-flat fading* if the channel coherence bandwidth is greater than that of transmitted baseband signal. In such a case, the delay spread is insignificant relative to the symbol duration so that its effect can be neglected at the receiver. On the other hand, if the coherence bandwidth is smaller relative to the bandwidth of transmitted baseband signal, the channel is said to be a *frequency-selective fading* channel and the effects of delay spread at the receiver are considerable.

2.2.3 Classifications of Mobile Communication Channel

Mobile communication channels can be classified as slow fading or fast fading depending on the coherence time and Doppler spread, and as frequency-flat fading or frequency-selective fading depending on the delay spread and coherence bandwidth as shown in Fig. 2.2. In Fig. 2.2.(a), the classification is made based on coherence time and delay spread and in Fig. 2.2.(b), the classification is made based on coherence bandwidth and Doppler spread. It should be stressed that the coherence time (or Doppler spread) and the coherence bandwidth (or delay spread) in mobile communication channels are independent parameters.

In the study of multiuser detection in DS-CDMA systems, additive white Gaussian noise (AWGN) channels are often assumed as a starting point. In AWGN channels, only one propagation path is assumed whose path gain is invariant throughout the transmission. In addition, the ambient channel noise is modeled as an independent zero-mean Gaussian random process. Note that an AWGN channel can de regarded as

a special case of a frequency-selective fading channel where the number of propagation paths is reduced to one and the path gain remains constant during the transmission.

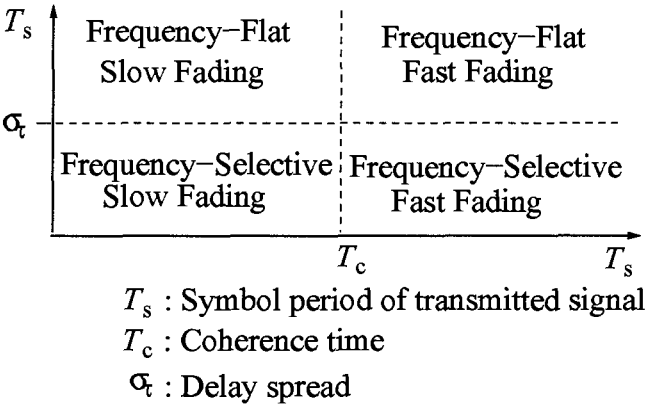

(a)

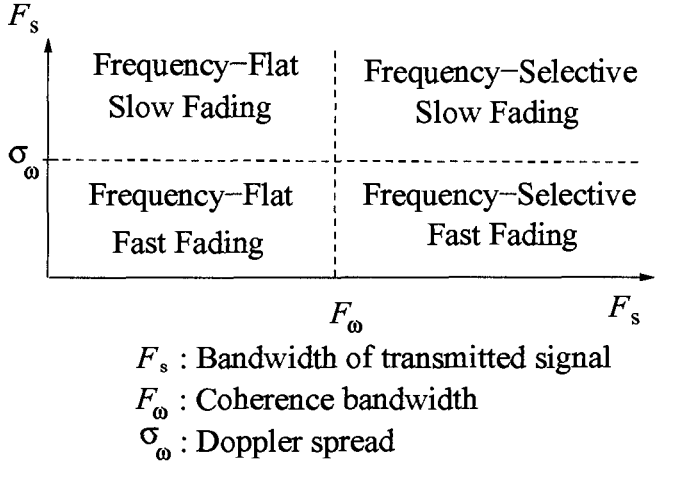

(b)

Figure 2.2. *Classification of multipath propagation channels depending on (a) coherence time (or delay spread) and (b) coherence bandwidth (or Doppler spread).*

2.3 DS-CDMA System

2.3.1 Code Division Multiple Access

In a DS-CDMA system, the signal of each user is multiplexed by multiplying the information-bearing symbols with a distinctively assigned signature waveform. This process is called *spreading*. The spread signals of multiple users are then transmitted by sharing the same bandwidth at the same time. In what follows, we present two DS-CDMA signal models in different channels: AWGN channel and frequency-selective fading channels.

We first consider DS-CDMA system with AWGN channel. At the transmitter, the ith information bit of user k, denoted as b_k^i, is multiplied by its own signature waveform, $s_k(t)$. The signature waveform is expressed as

$$s_k(t) = \sum_{i=1}^{N} c_k(i) p_{T_c}[t - (i-1)T_c] \quad \text{for } t \in [0,\ T_b] \tag{2.7}$$

where T_b denotes the symbol duration, T_c denotes the chip duration, $p_{T_c}(t)$ denotes the chip waveform which assumes a nonzero value between $0 \leq t \leq T_c$ and is zero elsewhere, $\mathbf{s}_k = [c_k(1)\ c_k(2)\ \cdots\ c_k(N)]^T$ is the *spreading sequence* assigned for user k, and $N = T_b/T_c$ denotes the length of the signature sequence, which is called *spreading gain*.

In the rest of this thesis, it is assumed that the transmitted information-bearing symbols, b_k^i, are binary antipodal signals which only assume the values of 1 and -1 with equal probability. The results obtained for antipodal signal transmission can be extended to other cases using QPSK or other modulation schemes. Following this assumption, the spreading sequence, $\mathbf{s}_k$, assumes real values. In addition, normalized signature waveforms are assumed for all users, i.e.,

$$||s_k(t)||^2 = \int_0^{T_b} s^2(t)\ dt = 1 \quad \text{for} \quad k = 1,\ 2,\ \ldots,\ K$$

The transmitted signal of user k is given by

$$x_k(t) = \sum_{i=-\infty}^{\infty} A_k^i b_k^i s_k(t - iT_b - \tau_k) \tag{2.8}$$

At the receiver, the observed signal waveform is the superposition of the signals of all users plus ambient channel noise and can be expressed as

$$y(t) = \sum_{i=-\infty}^{\infty} \sum_{k=1}^{K} A_k^i b_k^i s_k(t - iT_b - \tau_k) + n(t) \tag{2.9}$$

where τ_k is the transmission delay, A_k^i is the signal amplitude, and b_k^i is the information bit of the signal of user k, $n(t)$ is an AWGN process with zero-mean and variance σ^2.

In a synchronous DS-CDMA system, $\tau_1 = \tau_2 \cdots = \tau_K = 0$ is assumed. As a result, the detection of information bits only relies on the received signal of the current symbol period. In this case, (2.9) can be simplified as

$$y(t) = \sum_{k=1}^{K} A_k b_k s_k(t) + n(t) \qquad \text{for} \quad t \in [0, T_b] \tag{2.10}$$

Next we consider DS-CDMA system with frequency-selective fading channel. The received noise-free signal for user k is given by

$$\begin{aligned} y_k(t) = x_k(t) * g_k(t) &= \left[\sum_{i=-\infty}^{+\infty} A_k^i b_k^i s_k(t - iT_b - \tau_k) \right] * g_k(t) \\ &= \sum_{i=-\infty}^{+\infty} A_k^i b_k^i h_k(t - iT_b - \tau_k) \end{aligned} \tag{2.11}$$

where '$*$' denotes linear convolution, $g_k(t)$ is the impulse response of the communication channel of user k, which, according to (2.1), can be expressed as

$$g_k(t) = \sum_{m=1}^{M_k} \alpha_{km} \exp(-j\theta_{km})\ \delta(t - \tau_{km}) \tag{2.12}$$

$h_k(t)$ is called *effective signature waveform* of user k, which refers to the signature waveform observed at receiver. Note that $h_k(t)$ is usually different from the signature

waveform, $s_k(t)$, assigned at receiver. Following (2.11) and (2.12), $h_k(t)$ is expressed as

$$\begin{aligned} h_k(t) &= s_k(t) * g_k(t) \\ &= \sum_{i=1}^{N} \sum_{m=1}^{M_k} c_k(i)\alpha_{km} \exp(-j\theta_{km}) p_{T_c}(t-(i-1)T_c - \tau_{km}) \end{aligned} \tag{2.13}$$

By taking all user signals and the channel noise into account, the signal observed at receiver can be expressed as

$$y(t) = \sum_{k=1}^{K} y_k(t) + n(t) \tag{2.14}$$

where $n(t)$ is a complex-valued AWGN process with zero-mean and variance σ^2. A signal diagram for DS-CDMA systems is presented in Fig. 2.3.

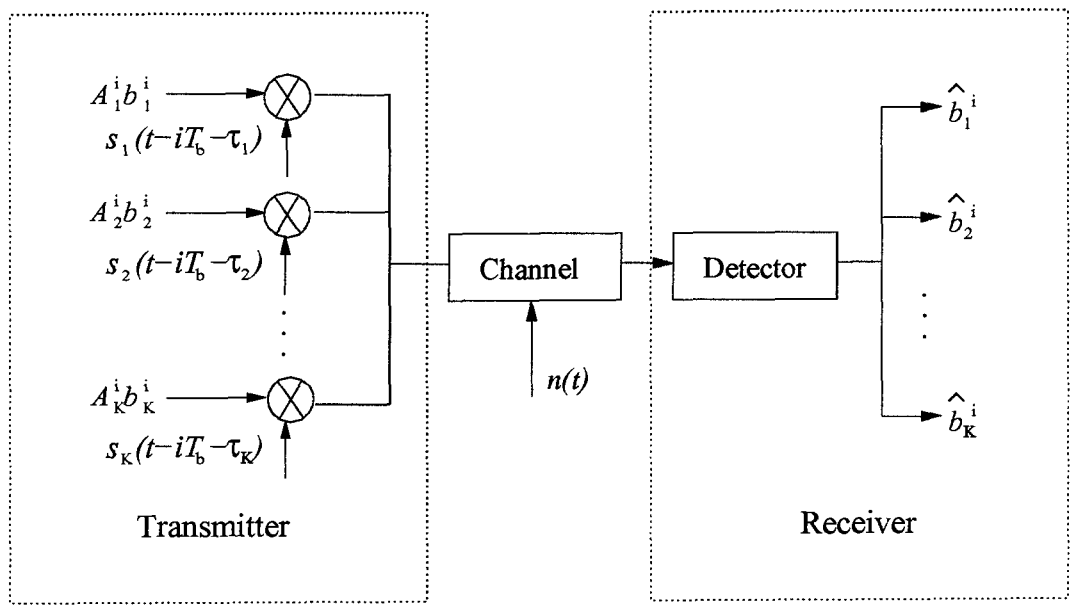

Figure 2.3. *Signal model for DS-CDMA systems.*

2.3.2 Conventional Detection

In DS-CDMA systems, conventional detection is carried out by filtering the received signal $y(t)$ through a matched filter (MF) bank which consists of K filters, each

matched to a specific signature waveform. The filters' output is sampled at the end of each symbol period. The signals obtained represent the transmitted information symbols and will be referred to as *soft-detected* signals. If antipodal signals are transmitted, then binary values 1 or -1 are generated according to the signs of the soft-detected signals. The binary signals so obtained will be referred to as *hard-detected* information bits. Note that the outputs of the MF bank possess *sufficient statistics* for making an optimal detection [17].

A conventional detector for an asynchronous DS-CDMA system over AWGN channel is illustrated in Fig. 2.4. As can be seen, the ith soft-detected signal of user k that is generated by the MF bank is given by

$$\begin{aligned} y_k^i &= \int_{iT_b+\tau_k}^{(i+1)T_b+\tau_k} y(t)s_k(t-iT_b-\tau_k)\,dt \\ &= \sum_j \left[A_j^i b_j^{i-1}(\mathbf{R}[1])_{kj} + A_j^i b_j^i(\mathbf{R}[0])_{kj} + A_j^i b_j^{i+1}(\mathbf{R}[-1])_{kj}\right] + n_k^i \end{aligned} \tag{2.15}$$

where

$$n_k^i = \int_{iT_b+\tau_k}^{(i+1)T_b+\tau_k} n(t)s_k(t-iT_b-\tau_k)\,dt \tag{2.16}$$

In (2.15), $\mathbf{R}[-1]$, $\mathbf{R}[0]$, and $\mathbf{R}[1] \in \mathcal{C}^{K\times K}$ are crosscorrelation matrices for asynchronous DS-CDMA systems with the (k,j)th element defined by

$$\mathbf{R}_{kj}[n] = \int_{-\infty}^{\infty} s_k(t-\tau_k)s_j(t+nT_b-\tau_j)\,dt \quad \text{for } n \in \{-1,\ 0,\ 1\} \tag{2.17}$$

From (2.17) it is easy to see that $\mathbf{R}[-1] = \mathbf{R}^T[1]$. The binary value produced by a conventional detector for the ith information symbol of user k is given by

$$\hat{b}_k^i = \text{sign}(y_k^i) \tag{2.18}$$

The MF outputs in (2.15) can be written in matrix form as

$$\mathbf{y}^i = \mathbf{R}[-1]\mathbf{A}[i+1]\mathbf{b}^{i+1} + \mathbf{R}[0]\mathbf{A}[i]\mathbf{b}^i + \mathbf{R}[1]\mathbf{A}[i-1]\mathbf{b}^{i-1} + \mathbf{n}^i \tag{2.19}$$

where $\mathbf{y}^i = [y_1^i\ y_2^i\ \cdots\ y_K^i]^T \in \mathcal{C}^{K\times 1}$, $\mathbf{b}^i = [b_1^i\ b_2^i\ \cdots\ b_K^i]^T \in \mathcal{C}^{K\times 1}$, $\mathbf{A}[i] = \text{diag}\{A_1^i,\ A_2^i,\ \ldots,\ A_K^i\} \in \mathcal{C}^{K\times K}$, and $\mathbf{n}^i = [n_1^i\ n_2^i\ \cdots\ n_K^i]^T \in \mathcal{C}^{K\times 1}$ is a zero-mean Gaussian process characterized by the crosscorrelation matrix

$$E[\mathbf{n}^i\mathbf{n}^{jT}] = \begin{cases} \sigma^2\mathbf{R}[i-j] & \text{for } |i-j| \le 1 \\ \mathbf{0} & \text{otherwise} \end{cases} \tag{2.20}$$

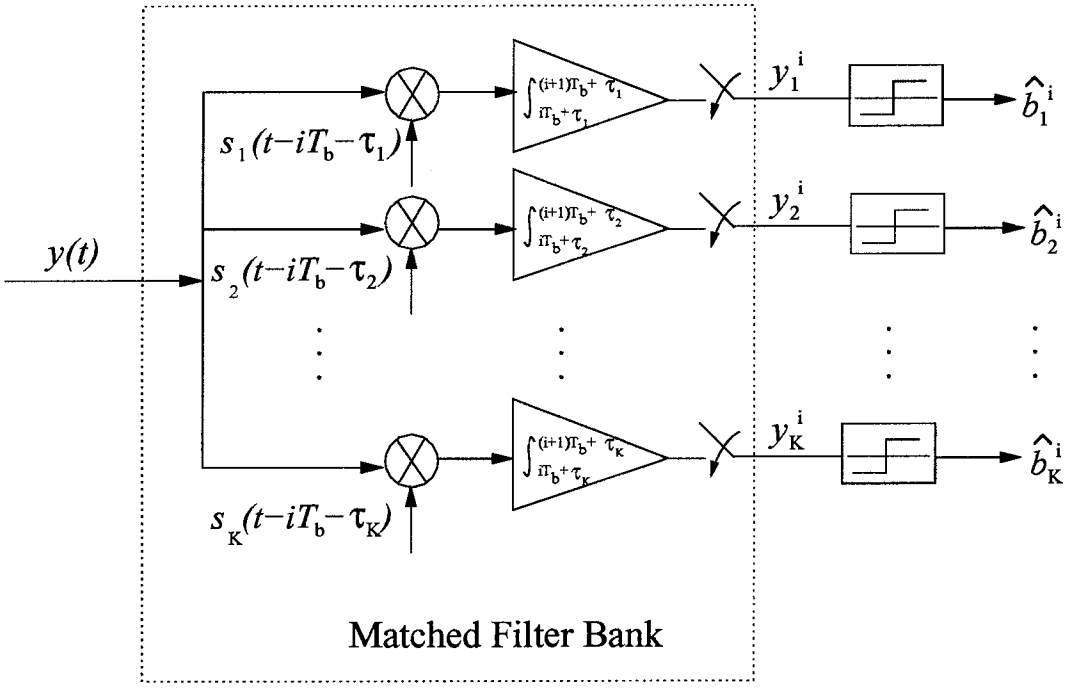

Figure 2.4. *Conventional detector for asynchronous DS-CDMA systems over AWGN channels.*

For synchronous DS-CDMA systems, the demodulation of a conventional detector relies only on the received signal of the current symbol period. Thus, (2.19) can be simplified to

$$\mathbf{y} = \mathbf{RAb} + \mathbf{n} \tag{2.21}$$

where $\mathbf{R}_{kj} = \rho_{kj} = \int_0^{T_b} s_k(t)s_j(t)\ dt$ denotes the synchronous crosscorrelation of the jth and kth signature waveforms, $\mathbf{b} = [b_1\ b_1\ \cdots\ b_K]^T$ is a vector whose elements

are the information bits of the K users, and $\mathbf{n} = [n_1\ n_2\ \cdots\ n_K]^T$ is the zero-mean Gaussian process for a synchronous system whose crosscorrelation matrix is $E[\mathbf{n}\mathbf{n}^T] = \sigma^2\mathbf{R}$.

From the above analysis, we see that a conventional detector follows the same detection strategy as that used for a single-user communication system. That is, each branch of the MF bank detects the desired user signal by completely ignoring the existence of interference. In other words, the information of other user signals is not exploited to help improve the performance. Obviously, the success of a conventional detector relies heavily on the crosscorrelations between the signature waveforms $s_1(t), \ldots, s_K(t)$. When the signature waveforms at the receiver are orthogonal to each other, multiuser interference (MUI) present in the received signal can be removed completely by using a MF bank. In such a case, the performance of a conventional detector is the same as that of a MF demodulator for a single-user communication system.

If the signature waveforms are not orthogonal to each other or the transmission is not synchronous, then MUI cannot be eliminated by the MF bank completely. Thus, the accuracy of the soft-detected signals of a conventional detector will be affected by the interference of other users. In this case, the so-called *near-far* problem (i.e., weak power signals are immersed by strong power signals) is very likely to arise in DS-CDMA systems, which may cause severe performance degradation. To alleviate the near-far problem associated with conventional detectors, several effective methods have been developed that include power control methods and multiple antenna methods.

Power control methods are widely used in current DS-CDMA systems. In these methods, the transmission power of mobiles is adjusted such that the received signal power of all users are approximately at the same level to avoid severe MUI. In *Interim Standard 95*, two power control approaches are adopted for reverse link DS-CDMA systems. In the first approach, the signal transmission power of mobiles is adjusted

based on the received signal power level without involving the operation of the base station. This power control approach is called open-loop power control approach. The other power control approach is called closed-loop power control approach where the base station is much more involved relative to the first approach.

In multiple antenna methods, an antenna array consisting of several antenna elements is designed with two objectives in mind, namely, to separate signals of different users based on the DOA information and to provide spatial diversity to combat deep channel fading.

It is known that when the elements of an antenna array are located sufficiently close to each other (e.g., less than the wavelength of the radio signal), the beam pattern of the antenna array can be controlled by adjusting the beamforming combination parameters. In mobile communication systems, the DOAs of different user signals are usually different when mobile users are located in different areas. Thus the beam pattern of an antenna array can be adjusted such that the peaks and nulls of the beam pattern are toward the signals of the desired user and interfering users, respectively. By doing so, the MUI in the received signal can be effectively suppressed, which helps improve the demodulation performance of the conventional detector. Moreover, the variation of DOAs of mobile users can be tracked by using adaptive beamforming algorithms and thus this method is useful when mobile users are moving.

In some cases, it is required that adjacent elements of the antenna array be sufficiently separated (e.g., more than several wavelengths of radio signal). In such cases, the propagation channels for the different antenna elements are relatively independent of each other. Consequently, channel fading does not have the same effect on each element of the antenna array and the probability that a mobile user will suffer deep fading can be considerably reduced. Evidently, the demodulation performance of a conventional detector equipped with such an antenna array can be improved. The structure of a conventional detector for DS-CDMA systems using an antenna array is illustrated in Fig. 2.5.

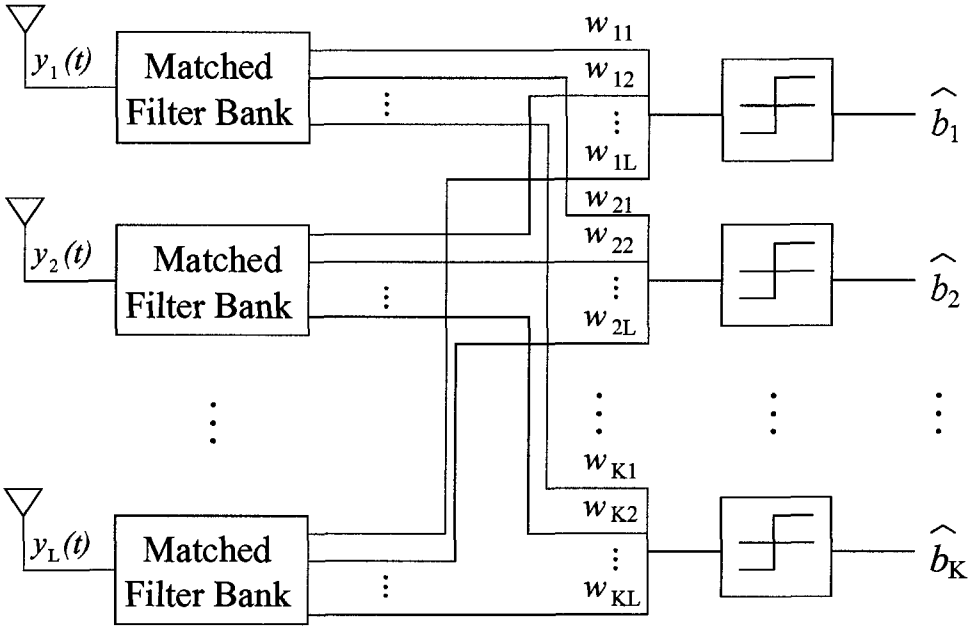

Figure 2.5. *Conventional detector for DS-CDMA system using an L-element antenna array.*

In frequency-selective fading channels, the received signal is composed of several replicas of the transmitted signal traveling along with different propagation paths and arriving at receiver with different delays. These replicas provide several essentially independent observations of the transmitted signal at the receiver. Evidently, it is very unlikely that all replicas suffer deep channel fading.

The RAKE receiver was designed to exploit the time diversity offered by multipath propagation [16]. An M-branch RAKE receiver for DS-CDMA systems is depicted in Fig. 2.6 where $c_{k,m}$ is given by $c_{k,m} = \alpha_{km}\exp(-j\theta_{km})$. It can be seen from Fig. 2.6 that the outputs generated by the RAKE receiver are given by

$$\begin{aligned} y_k(n) &= \mathrm{Re}\left[\int_{\tau_k+nT_b}^{\tau_k+(n+1)T_b} y(t)v_m^*(t)dt\right] \\ &= \mathrm{Re}\left[\sum_{m=1}^{M}\int_{\tau_k+nT_b}^{\tau_k+(n+1)T_b} y(t)c_{km}^*(t)s_k^*(t-\tau_{km})dt\right] \end{aligned} \tag{2.22}$$

where

$$y(t) = \sum_{i=-\infty}^{i=\infty} \sum_{k=1}^{K} \sum_{m=1}^{M} A_k^i b_k^i \alpha_{km} \exp(-j\theta_{km}) s_k(t - \tau_{km}) + n(t) \tag{2.23}$$

denotes the received signal.

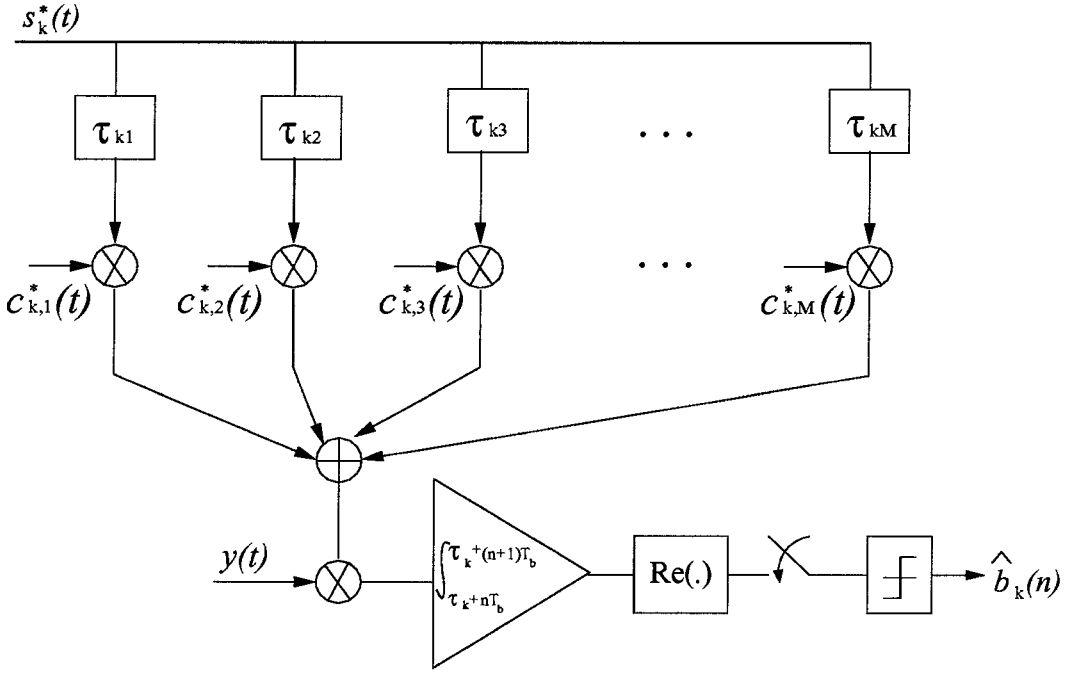

Figure 2.6. *An M-branch RAKE receiver for DS-CDMA systems over frequency-selective fading channels.*

Note that the autocorrelation and crosscorrelation of the signature waveforms may be increased due to the uncertainty of propagation delay during transmission. To maintain small autocorrelation and crosscorrelation of the delayed signature waveforms, pseudo-random signature sequences are preferred in order to generate noise-like signature waveforms for DS-CDMA systems. Like the conventional detector, the RAKE receiver also requires power control to combat the near-far problem [16].

2.4 Multiuser Detection

It is known that when the transmission channel is shared by a large number of equal-power users, the MUI at the outputs of a conventional detector can be approximated as a Gaussian random variable according to the central limit theorem. Since an MF demodulator is known to offer optimal demodulation performance for a single-user communication system over an AWGN channel, it has been assumed that a conventional detector using a bank of MFs would offer near optimal demodulation performance in a multiuser communication system. This argument, unfortunately, is now considered to be incorrect because it implicitly assumes that the detection of one user signal relies on the output of the associated MF only. As will be shown, although the outputs of the MF bank in a multiuser communication system provide sufficient information for detecting all the user signals, the output of a single MF does not provide sufficient information for detecting the signal of the associated user [17].

The objective of multiuser detection is to identify the transmitted information from the received signal waveform $y(t)$. It has been shown in [17] and many references therein that the performance of DS-CDMA systems can be significantly improved if the signals of all the users are utilized to identify the transmitted information bits. This can be done by inserting immediately after the MF bank of a conventional detector a processor that implements multiuser detection algorithms. A generic multiuser detector of this type for a synchronous DS-CDMA system is shown in Fig. 2.7.

On comparing the structure of the multiuser detector in Fig. 2.7 with that of the conventional detector in Fig. 2.5, the sign operations in Fig. 2.5 are replaced by multiuser detection algorithms in Fig. 2.7. In what follows, we examine several linear and nonlinear detectors. This will help establish the necessary background for multiuser detection and offer a basis on which several new multiuser detection methods and detectors can be developed.

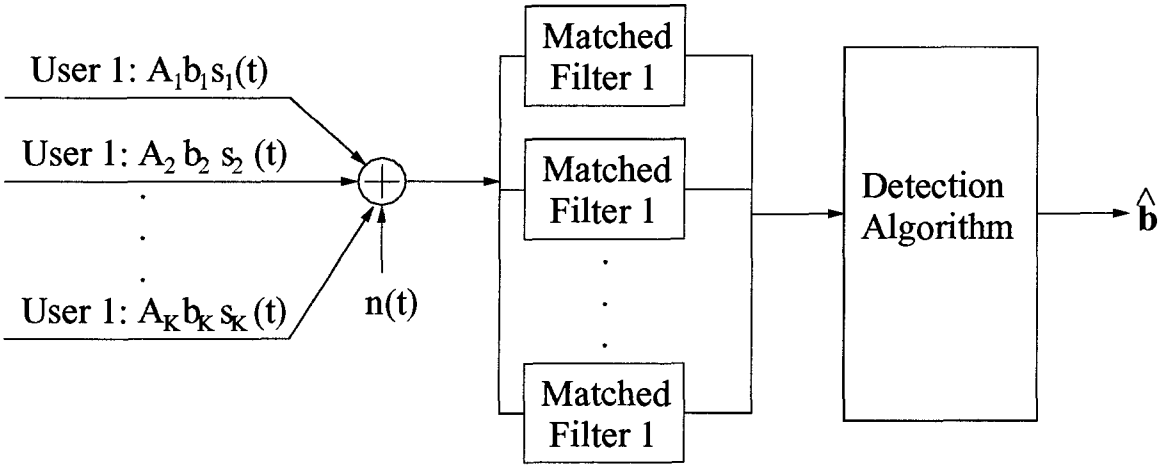

Figure 2.7. *Multiuser detector for synchronous DS-CDMA systems.*

2.4.1 Maximum Likelihood Multiuser Detection

ML detection involves maximizing the *joint a posteriori probability* by selecting the information-bearing waveform that is closest to the observed waveform in terms of Euclidean distance [17]. ML detection has been shown to offer optimal performance and is often used as a baseline for comparison of other multiuser detectors for DS-CDMA systems [17].

In asynchronous DS-CDMA systems, due to the interleaving of user signals, the demodulation relies not only on the current symbol period of the received signal, but also on the previous and subsequent symbol periods. Since this requirement has to be satisfied for detecting each symbol, ML detection for asynchronous DS-CDMA systems requires observation of the entire frame of the received signal. Assuming that the signal in each frame contains P symbols and using (2.19), ML detection can be carried out by solving the optimization problem

$$\text{minimize} \quad \mathbf{x}_a^T \mathcal{H} \mathbf{x}_a + \mathbf{x}_a^T \mathcal{P} \tag{2.24a}$$

$$\text{subject to:} \quad (\mathbf{x}_a)_i \in \{1, -1\} \quad \text{for } i = 1, 2, \ldots, PK \tag{2.24b}$$

where $\mathcal{H} = \mathcal{A}\mathcal{R}\mathcal{A}$, $\mathcal{P} = -2\mathcal{A}\mathbf{y}_P$, and $\mathbf{y}_P = [(\mathbf{y}^1)^T (\mathbf{y}^2)^T \cdots (\mathbf{y}^P)^T]^T$ is the MF outputs

of the entire frame signal, $\mathcal{A} = \text{diag}\{A[1], \ldots, A[P]\}$ is the extended amplitude matrix, $(\mathbf{x}_a)_i$ is the ith component of $\mathbf{x}_a$, and $\mathcal{R}$ denotes the extended crosscorrelation matrix defined by

$$\mathcal{R} = \begin{bmatrix} \mathbf{R}[0] & \mathbf{R}^T[1] & \mathbf{0} & \cdots & \mathbf{0} & \mathbf{0} \\ \mathbf{R}[1] & \mathbf{R}[0] & \mathbf{R}^T[1] & \cdots & \mathbf{0} & \mathbf{0} \\ \vdots & \vdots & \vdots & \vdots & \vdots & \vdots \\ \mathbf{0} & \mathbf{0} & \mathbf{0} & \cdots & \mathbf{R}[1] & \mathbf{R}[0] \end{bmatrix} \tag{2.24c}$$

Since the constraints in (2.24b) are binary, the problem in (2.24) is a combinatorial optimization problem whose solution requires computational complexity that grows exponentially with the number of variables.

An algorithm or a hardware device is termed as an ML detector if it can be used to resolve the transmitted information bits via solving the problem in (2.24). Apparently there are many implementation algorithms available for solving the problem in (2.24), however, all these algorithms offer the same performance regardless of their specific implementation details. In addition, it has been shown in [17] that the computational complexity of all algorithms used for solving the problem in (2.24) grows exponentially with the number of variables. In other words, the computational complexity of all ML detectors grows exponentially with the number of users.

For synchronous systems, we have $\tau_1 = \tau_2 = \cdots = \tau_k$ in (2.15). In such a case, the demodulation relies only on the user signals received in the current symbol period. Hence, the ML detection problem in (2.24) can be simplified to

$$\text{minimize} \quad \mathbf{x}^T\mathbf{H}\mathbf{x} + \mathbf{x}^T\mathbf{p} \tag{2.25a}$$

$$\text{subject to:} \quad x_i \in \{1, -1\} \quad \text{for } i = 1, 2, \ldots, K \tag{2.25b}$$

where x_i denotes the ith entry of $\mathbf{x}$, $\mathbf{H} = \mathbf{ARA}$, and $\mathbf{p} = -2\mathbf{Ay}$. This problem has a similar structure as that of the ML detection problem in (2.24) except that the number of variables is significantly reduced.

The computational complexity of ML detection for asynchronous DS-CDMA systems can be considerably reduced by using the *Viterbi algorithm* which was originally proposed for the decoding of convolutional codes [27]. By using this algorithm, the problem in (2.24) can be divided into several subproblems each involving fewer variables than the original problem. This approach is called the *forward dynamic programming approach* [17]. Using the Viterbi algorithm, the computational complexity for solving the problem in (2.24) is comparable with that required for the problem in (2.25). It is important to note that ML detection requires information about the signature waveform and the received amplitude of all user signals. In addition, in DS-CDMA systems over frequency-selective fading channel, complete information on the channel impulse responses of all users is required for ML detection.

2.4.2 Linear Multiuser Detectors

In attempts to reduce the computational complexity required by ML detection, several linear multiuser detection approaches that offer good demodulation performance relative to conventional detector but with much reduced computational complexity relative to ML detection have been proposed. In these schemes, a linear transformation is applied between the outputs of the MF and the decision making devices. Once the linear transformation is determined, it can be used until the system parameters such as signature waveforms, noise level, or the amplitudes are significantly changed. Because the signature waveforms of all users are usually known at the base station, linear multiuser detectors are especially useful in forward link DS-CDMA systems.

Linear multiuser detectors can be derived based on two types of signal models. The first model is symbol-rate based and it is represented by (2.19) for asynchronous and by (2.21) for synchronous systems. The second model is chip-rate based where a chip-waveform MF (also called *chip MF*) is used at the front end of the receiver followed by a sampler, both operated at chip rate. In the latter case, linear detectors can be implemented by applying linear transformations to the outputs of the chip

MFs directly. For a synchronous DS-CDMA system over an AWGN channel, the output of the chip-rate sampler can be written as

$$\mathbf{r} = \mathbf{SAb} + \mathbf{n}_c \tag{2.26}$$

where $\mathbf{r}$ denotes the discrete-time signal generated by the chip-rate sampler at the receiver, $\mathbf{S} = [\mathbf{s}_1\ \mathbf{s}_2\ \cdots\ \mathbf{s}_K]$ with $\mathbf{s}_k$ being the signature code for user K, and $\mathbf{n}_c$ is a vector of white Gaussian noise variables with zero-mean and covariance matrix $\mathrm{E}(\mathbf{n}_c\mathbf{n}_c^T) = \sigma^2\mathbf{I}$.

It is easy to see that (2.21) and (2.26) are related by $\mathbf{y} = \mathbf{S}^T\mathbf{r}$, which implies that conventional detectors can be implemented based on the chip-rate MF followed by the linear transformation. Following this idea, linear multiuser detectors can be implemented in a *decentralized* form where the matrix $\mathbf{S}$ used for a conventional detector is replaced by a specific linear transformation.

2.4.2.1 Decorrelating Detector

In a decorrelating detector, the information bits are detected based on the transformed outputs given by [28, 30]

$$\hat{\mathbf{b}}_d = \mathrm{sign}(\mathbf{R}^{-1}\mathbf{y}) = \mathrm{sign}(\mathbf{Ab} + \mathbf{R}^{-1}\mathbf{n}) \tag{2.27}$$

Note that each component of $\tilde{\mathbf{b}}_d$ is composed of the decoupled user signal plus a noise term. In other words, the MUI present in the received signal is completely removed by the transformation $\mathbf{R}^{-1}$. In fact, it can be shown that this linear transformation projects the received signal onto the signal space orthogonal to the signatures of all other users. For this reason, a decorrelating detector achieves optimal near-far resistance [28].

The performance of a decorrelating detector is much better relative to that of a conventional detector when the noise level is not significant. In addition, since the amplitude information of all users is not required in (2.27), the system complexity

of the decorrelating detector is reduced relative to that of an ML detector. One disadvantage associated with the decorrelating detector is that the enhanced noise term in (2.27) may significantly degrade the performance when the SNR of the channel is very low.

Next we examine the optimization aspects of the decorrelating detector. By neglecting the constraints in (2.25b), the combinatorial optimization problem in (2.25) becomes an unconstrained quadratic minimization problem given by

$$\text{minimize} \quad \mathbf{x}^T\mathbf{H}\mathbf{x} + \mathbf{x}^T\mathbf{p} \tag{2.28}$$

where vector $\mathbf{x}$ can assume real continuous values. Since matrix $\mathbf{H}$ is positive definite, the objective function in (2.28) is globally convex, and the problem in (2.28) has a closed-form solution given by

$$\mathbf{x}_d = -\frac{1}{2}\mathbf{H}^{-1}\mathbf{p} = \mathbf{A}^{-1}\mathbf{R}^{-1}\mathbf{y} \tag{2.29}$$

It is easy to show that the information bits determined based on (2.29) are exactly the same as those in (2.27). This implies that decorrelating detector can be implemented by solving the unconstrained optimization problem in (2.28) which is obtained from the combinatorial problem in (2.25) by removing the constraints.

In the optimization literature, a problem obtained by removing certain constraints from a constrained optimization problem or replacing them with less restrictive ones is termed a *relaxation* of the original problem. In general, the solution of a relaxation problem can be suboptimal with respect to the solution of the original problem at best. Depending on which constraints are removed or how they are replaced, different relaxations lead to different suboptimal solutions.

Using the chip-rate signal model in (2.26), the decorrelating detector can be achieved as

$$\begin{aligned}\hat{\mathbf{b}} &= \text{sign}\left(\mathbf{R}^{-1}\mathbf{y}\right) = \text{sign}\left[(\mathbf{S}^T\mathbf{S})^{-1}\mathbf{S}^T\mathbf{r}\right] \\ &= \text{sign}\left(\mathbf{A}\mathbf{b} + \mathbf{S}^\dagger\mathbf{n}_c\right)\end{aligned} \tag{2.30}$$

where $\mathbf{S}^{\dagger} = (\mathbf{S}^T\mathbf{S})^{-1}\mathbf{S}^T$ denotes the pseudo-inverse of matrix $\mathbf{S}$. From (2.30) we see that the linear transformation used in the decentralized implementation of the decorrelating detector is $\mathbf{S}^{\dagger}$.

2.4.2.2 MMSE Detector

The transformation used in MMSE (LMMSE) detection is determined by minimizing the minimum-square-error (MSE) between the known binary information bits and the transformed outputs [32, 33], i.e.,

$$\text{minimize} \quad \mathrm{E}[||\mathbf{b} - \mathbf{M}\mathbf{y}||^2] \tag{2.31}$$

It can be shown that the matrix that solves the above minimization problem also achieves the maximum signal-to-interference-plus-noise ratio (SINR) [33]. The closed-form solution of this problem is given by

$$\mathbf{M} = (\mathbf{R} + \sigma^2 \cdot \mathbf{A}^{-2})^{-1} \tag{2.32}$$

Hence, the information bits determined by the LMMSE detector are given by

$$\hat{\mathbf{b}}_m = \text{sign}\left[(\mathbf{R} + \sigma^2 \cdot \mathbf{A}^{-2})^{-1}\mathbf{y}\right] \tag{2.33}$$

In contrast to the decorrelating detector where only the effect of MUI is considered, the LMMSE detector seeks to satisfy the requirement of MUI suppression without significantly enhancing the noise term. In fact, when the channel noise is negligible ($\sigma^2 \to 0$), the linear transformation $\mathbf{M}$ becomes asymptotically the same as that used for decorrelating detection. When the channel noise is very strong, however, the linear transformation degenerates to the identity matrix so that the information bits determined by the LMMSE detector are the same as those determined by a conventional detector.

MMSE detection can be implemented in a decentralized form with a linear transformation matrix given by

$$\mathbf{M}_d = \mathbf{M}\mathbf{S} = (\mathbf{R} + \sigma^2 \cdot \mathbf{A}^{-2})^{-1}\mathbf{S} \tag{2.34}$$

It can be shown that the kth row of $\mathbf{M}_d$ is the solution of the following minimization problem

$$\text{minimize} \quad \mathrm{E}[||b_k - \mathbf{m}_k^T \mathbf{r}||^2] \tag{2.35}$$

The above problem can be solved by using adaptation algorithms if a training sequence is available at the receiver [34]. Adaptive MMSE multiuser detector has been studied in [36, 37, 38]. The implementation of an adaptive MMSE detector is carried out in two time periods: the first one is called *training period* where the detection vector is obtained with the help of training sequence, and the second one is called *detection period* where the detection vector is kept invariant to determine transmitted information bits. When system conditions such as signature waveforms or channel conditions are changed, the training period is performed again to track the variations.

Since the implementation of an adaptive MMSE detector does not require any information except training sequences, the required system complexity is lower than that for the decorrelating and LMMSE detector. A disadvantage of the adaptive MMSE detector is that the transmission efficiency or the system capacity is reduced by the use of training sequences. The capacity reduction becomes more severe when channel conditions are changing rapidly. To improve the transmission efficiency, some fast tracking adaptation algorithms such as the recursive-least-square (RLS) algorithm may be useful at the cost of more computation.

Next we compare the LMMSE detection with ML detection. Notice that the combinatorial problem in (2.25) is equivalent to

$$\text{minimize} \quad \mathbf{x}^T \mathbf{H} \mathbf{x} + \mathbf{x}^T \mathbf{p} + \alpha \cdot K \tag{2.36a}$$

$$\text{subject to:} \quad x_i \in \{1, -1\} \quad \text{for } i = 1, 2, \ldots, K \tag{2.36b}$$

where α is a positive scalar. Since the constraints in (2.36b) imply that $\mathbf{x}^T \mathbf{x} = K$,

the problem in (2.36) is equivalent to

$$\text{minimize} \quad \mathbf{x}^T\mathbf{H}\mathbf{x} + \mathbf{x}^T\mathbf{p} + \alpha \cdot \mathbf{x}^T\mathbf{x} \tag{2.37a}$$

$$\text{subject to:} \quad x_i \in \{1,-1\} \quad \text{for } i = 1, 2, \ldots, K \tag{2.37b}$$

By removing the constraint in (2.37b), the above combinatorial problem can be relaxed into an unconstrained optimization given by

$$\text{minimize} \quad \mathbf{x}^T (\mathbf{H} + \alpha \cdot \mathbf{I})\, \mathbf{x} + \mathbf{x}^T\mathbf{p} \tag{2.38}$$

The closed-form solution of the problem in (2.38) is given by

$$\mathbf{x}_M = -\frac{1}{2} (\mathbf{H} + \alpha \cdot \mathbf{I})^{-1} \mathbf{p} = \mathbf{A}^{-1} \left(\mathbf{R} + \alpha \cdot \mathbf{A}^{-2}\right)^{-1} \mathbf{y} \tag{2.39}$$

It is easy to show that if α is selected as the value of noise variance, i.e., $\alpha = \sigma^2$, the information bits determined based on (2.39) is the same as that determined based on (2.33).

2.4.2.3 Blind Detection

In downlink DS-CDMA systems, the receivers at mobile stations only have information about the signature waveform of the user of interest. Hence, the complete crosscorrelation matrix is not available at mobile receivers. In such a case, decorrelating and LMMSE detectors are not useful. Blind detection is a class of approaches that primarily attempt to provide multiuser detection at mobile receivers.

An early blind detector is *constrained minimal output energy* (CMOE) detector, which was developed by Honig *et al.* based on the CMOE criterion [35]. The linear transformation employed in the CMOE detector is determined by minimizing the mean energy of the transformed output under the constraint that the signal component of the desired user after the linear transformation is fixed, i.e.,

$$\text{minimize} \quad \mathrm{E}\left[||\mathbf{w}^T\mathbf{r}||^2\right] \tag{2.40a}$$

$$\text{subject to:} \quad \mathbf{w}^T\mathbf{s}_i = 1 \tag{2.40b}$$

where $\mathbf{r}$ is the output of a chip-rate MF defined in (2.26) and $\mathbf{s}_i$ denotes the signature sequence of the interested user. A study presented in [35] shows that the performance of the CMOE detector is the same as that of the LMMSE detector. An adaptive implementation of the CMOE detector without using a training sequence was proposed in [35]. Consequently, the transmission efficiency of the adaptive CMOE detector in [35] is higher than that of an adaptive MMSE detector. Compared with the conventional MF detector, the CMOE detector offers significantly improved performance without requiring extra information during implementation. Therefore, this detector has received a great deal of attention since it was proposed.

In a frequency-selective fading channel, multipath propagation often causes the effective user signatures observed at receiver to be different from the ones assigned at transmitters. Simulation results presented in [35] have shown that the performance of the CMOE detector degrades significantly in frequency-selective fading channel due to signature distortion. For this reason, the applications of the CMOE detector is limited to DS-CDMA systems over frequency-selective fading channels. One possible remedy to solve this problem is to first estimate the impulse responses of the unknown multipath channels and then to estimate the effective user signatures for CMOE detection. This idea has been pursued by several authors using subspace methods [40, 41] and constrained optimization methods [42, 43, 44]. In what follows, we will briefly review these two methods.

We first describe a discrete-time signal model for frequency-selective fading channels. At receiver, the demodulation begins by passing the received signal waveform $y(t)$ in (2.14) through a chip-rate MF which generates M samples in each chip duration. The discrete-time signal after the chip-rate MF can be expressed as

$$y(n) = \sum_{k=1}^{K} y_k(n) + n_c(n) \tag{2.41}$$

where $y(n) = y(t)|_{t=nT_b/M}$, $y_k(n) = y_k(t)|_{t=nT_b/M}$, and $n_c(n) = n(t)|_{t=nT_b/M}$ denote the discrete-time versions of $y(t)$, $y_k(t)$, and $n(t)$ in (2.14), respectively. Defining

$g_k(n) = g_k(t)|_{t=nT_b/M}$ and $h_k(n) = h_k(t)|_{t=nT_b/M}$ as the discrete-time counterparts of $g_k(t)$ and $h_k(t)$ in (2.12) and (2.13), we have

$$y_k(n) = \sum_{i=-\infty}^{\infty} A_k^i b_k^i h_k(n - d_k M - iMN) \tag{2.42}$$

$$h_k(n) = \sum_{m=-\infty}^{\infty} s_k(m) g_k(n - mM) \tag{2.43}$$

Without loss of generality, it is assumed that (i) the impulse responses of the multipath channel for all users are of finite duration with lengths no greater than q; (ii) the first user is the desired user to which the receiver is synchronized; and (iii) $d_k > 0$ for $k = 2, 3, \ldots, K$. In the special case where $M = 1$ (one sample per chip duration), $h_k(n)$ in (2.43) becomes the linear convolution of $s_k(n)$ and $g_k(n)$. By collecting $y(iN+1)$, $y(iN+2)$, $\cdots$, and $y(iN+N+q-1)$ into a vector $\mathbf{y}(i)$, it can be shown that

$$\mathbf{y}(i) = \mathbf{S}_1 \mathbf{g}_1 A_1^i b_1^i + \mathbf{H}\tilde{\mathbf{A}}\tilde{\mathbf{b}}(i) + \mathbf{n}_c(i) \tag{2.44a}$$

$$= \mathbf{h}_{1,0} A_1^i b_1^i + \mathbf{H}\tilde{\mathbf{A}}\tilde{\mathbf{b}}(i) + \mathbf{n}_c(i) \tag{2.44b}$$

where $\mathbf{S}_1$ is a Toeplitz matrix given by

$$\mathbf{S}_1 = \begin{bmatrix} s_1(1) & & \mathbf{0} \\ \vdots & \ddots & \\ & & s_1(1) \\ s_1(N) & & \\ & \ddots & \vdots \\ \mathbf{0} & & s_1(N) \end{bmatrix} \tag{2.45}$$

The first term at the right-hand side of (2.44a) represents the signal of the desired user of the current symbol period with $\mathbf{g}_1 = [g_1(1)\ g_1(2)\ \cdots\ g_1(q)]^T$ and $\mathbf{h}_{1,0} = \mathbf{S}_1 \mathbf{g}_1$ being the channel impulse response and effective signature of user one, respectively. The second term in (2.44a) represents all interference which includes the signal of the desired user of the preceding and following symbol periods and the signal of the interference users. $\mathbf{H}$ and $\tilde{\mathbf{b}}(i)$ can be written more explicitly as

$[\mathbf{h}_{1,-1}\ \mathbf{h}_{1,1}\ \mathbf{h}_{2,-1}\ \mathbf{h}_{2,0}\ \mathbf{h}_{2,1}\ \cdots\ \mathbf{h}_{K,-1}\ \mathbf{h}_{K,0}\ \mathbf{h}_{K,1}]$ and $[b_1^{i-1}\ b_1^{i+1}\ b_2^{i-1}\ b_2^{i}\ b_2^{i+1}\ \cdots\ b_K^{i-1}\ b_K^{i}\ b_K^{i+1}]^T$, respectively, where

$$\mathbf{h}_{1,-1} = [h_1(N+1)\ \cdots\ h_1(N+q-1)\ 0\ \cdots\ 0]^T$$

$$\mathbf{h}_{1,1} = [0\ \cdots\ 0\ h_1(1)\ \cdots\ h_1(q-1)]^T$$

$$\mathbf{h}_{k,-1} = [h_k(N+1-d_k)\ \cdots\ h_k(N+q-1)\ 0\ \cdots\ 0]^T$$

$$\mathbf{h}_{k,0} = [0\ \cdots\ 0\ h_k(1)\ \cdots\ h_k(N+q-1-d_k)]^T$$

$$\mathbf{h}_{k,1} = \begin{cases} [0\ \ 0\ \ \cdots\ \ 0]^T & \text{for} \quad d_k > q-1 \\ [0\ \ \cdots\ \ 0\ \ h_k(1)\ \cdots\ h_k(q-d_k-1)]^T & \text{otherwise} \end{cases}$$

for $k = 2, \ldots, K$. $\tilde{\mathbf{A}}$ is a matrix of amplitudes corresponding to the information bits in $\tilde{\mathbf{b}}(i)$. The last term in (2.44), $\mathbf{n}_c(i)$, is a vector of zero-mean white Gaussian noise variables with variance σ^2

The objective of the following two methods is to estimate the channel impulse response $\mathbf{g}_1$ for the first user from $\mathbf{y}(i)$ without the knowledge of interfering user signals. Then the effective signature $\mathbf{h}_{1,0}$ can be computed for the CMOE detector in (2.40).

Subspace Methods

Several subspace methods [40, 41] have been proposed for the estimation of the channel impulse response $\mathbf{g}_1$ and the corresponding detection vector $\mathbf{w}_1$ using the eigen-decomposition (ED) of the correlation matrix $\mathbf{R}$ which is defined as

$$\mathbf{R} = \mathrm{E}[\mathbf{y}(i)\mathbf{y}^H(i)] \tag{2.46}$$

The ED of matrix $\mathbf{R}$ can be expressed as

$$\mathbf{R} = [\mathbf{U}_s\mathbf{U}_n] \begin{bmatrix} \mathbf{\Lambda}_s & \mathbf{0} \\ \mathbf{0} & \mathbf{0} \end{bmatrix} \begin{bmatrix} \mathbf{U}_s^H \\ \mathbf{U}_n^H \end{bmatrix} + \sigma^2\mathbf{I} \tag{2.47}$$

where $[\mathbf{U}_s\mathbf{U}_n]$ is a unitary matrix, the columns of $\mathbf{U}_s$ and $\mathbf{U}_n$ generate the signal and noise subspaces, respectively, and $\mathbf{\Lambda}_s = \mathrm{diag}\{\lambda_1, \ldots, \lambda_\xi\}$ with ξ being the dimension

of the signal space. Because the signature vector of the first user, $\mathbf{h}_{1,}$, is in the signal subspace which is orthogonal to the noise subspace, we have

$$\mathbf{U}_n^H \mathbf{h}_{1,0} = \mathbf{U}_n^H \mathbf{S}_1 \mathbf{g}_1 = \mathbf{0} \tag{2.48}$$

By rewriting (2.47) as

$$\mathbf{R} = [\mathbf{U}_s \mathbf{U}_n] \begin{bmatrix} \mathbf{\Lambda}_s + \sigma^2 \mathbf{I}_\xi & \mathbf{0} \\ \mathbf{0} & \sigma^2 \mathbf{I}_{N-\xi} \end{bmatrix} \begin{bmatrix} \mathbf{U}_s^H \\ \mathbf{U}_n^H \end{bmatrix} \tag{2.49}$$

we observe that the eigenvectors in $\mathbf{U}_n$ are associated with the *least eigenvalues* which equal the noise variance σ^2.

In practice, matrix $\mathbf{R}$ is not available but can be approximated by its *moving average* estimation based on the J most recent observations as

$$\hat{\mathbf{R}} = \frac{1}{J} \sum_{j=i-J+1}^{i} \mathbf{y}(j)\mathbf{y}^H(j), \tag{2.50}$$

and equation (2.48) becomes

$$\hat{\mathbf{U}}_n^H \mathbf{S}_1 \mathbf{g}_1 = \mathbf{0} \tag{2.51}$$

where $\hat{\mathbf{U}}_n$ is the counterpart of $\mathbf{U}_n$ obtained by the decomposition of $\hat{\mathbf{R}}$. Because of the approximation error introduced in (2.50), it is very likely that a nonzero vector $\mathbf{g}_1$ satisfying (2.51) does not exist [41]. A remedy for this problem is to compute an approximate solution of (2.51) by solving the following optimization problem

$$\text{minimize} \quad \mathbf{g}_1^H \mathbf{S}_1^H \hat{\mathbf{U}}_n \hat{\mathbf{U}}_n^H \mathbf{S}_1 \mathbf{g}_1 \tag{2.52a}$$

$$\text{subject to:} \quad ||\mathbf{g}_1|| = 1 \tag{2.52b}$$

The solution $\mathbf{g}_1^*$ of the problem in (2.52) is the eigenvector corresponding to the least eigenvalue of $\mathbf{S}_1^H \hat{\mathbf{U}}_n \hat{\mathbf{U}}_n^H \mathbf{S}_1$ [41]. Once $\mathbf{g}_1^*$ is obtained, the detection vector for the CMOE detector can be obtained in closed-form as

$$\mathbf{w}_1 = \hat{\mathbf{R}}^{-1} \mathbf{S}_1 (\mathbf{S}_1^H \hat{\mathbf{R}}^{-1} \mathbf{S}_1)^{-1} \mathbf{g}_1^* \tag{2.53}$$

Constrained Optimization Method

In the constrained optimization method proposed in [42], the impulse response $\mathbf{g}_1$ of the multipath channel and the detection vector for the CMOE detector $\mathbf{w}_1$ are obtained as the solution of the constrained minimax problem

$$\underset{\mathbf{g}_1}{\text{maximize}} \; \underset{\mathbf{w}_1}{\text{minimize}} \quad \mathbf{w}_1^H \mathbf{R} \mathbf{w}_1 \tag{2.54a}$$

$$\text{subject to: } \mathbf{S}_1^H \mathbf{w}_1 = \mathbf{g}_1 \tag{2.54b}$$

$$||\mathbf{g}_1||^2 = 1 \tag{2.54c}$$

where $\mathbf{R}$ is the data correlation matrix defined in (2.46). In (2.54), the energy of the transformed output is minimized in terms of $\mathbf{w}_1$ and maximized in terms of $\mathbf{g}_1$, respectively. The minimization problem can be solved by using the Lagrange multiplier method to obtain

$$\mathbf{w}_1^*(\mathbf{g}_1) = \mathbf{R}^{-1}\mathbf{S}_1(\mathbf{S}_1^H \mathbf{R}^{-1}\mathbf{S}_1)^{-1}\mathbf{g}_1 \tag{2.55}$$

where $\mathbf{w}_1^*$ depends on $\mathbf{g}_1$. Using (2.55), it can be shown that the problem in (2.54) is equivalent to

$$\underset{\mathbf{g}_1}{\text{maximize}} \; \mathbf{g}_1^H (\mathbf{S}_1^H \mathbf{R}^{-1}\mathbf{S}_1)^{-1}\mathbf{g}_1 \tag{2.56a}$$

$$\text{subject to: } ||\mathbf{g}_1||^2 = 1 \tag{2.56b}$$

The solution $\mathbf{g}_1$ of the problem in (2.56) is the eigenvector of $\mathbf{S}_1^H \mathbf{R}^{-1}\mathbf{S}_1$ corresponding to the least eigenvalue. Hence, the problem in (2.56) is equivalent to

$$\underset{\mathbf{g}_1}{\text{minimize}} \; \mathbf{g}_1^H \mathbf{S}_1^H \hat{\mathbf{R}}^{-1}\mathbf{S}_1\mathbf{g}_1 \tag{2.57b}$$

$$\text{subject to: } ||\mathbf{g}_1||^2 = 1 \tag{2.57c}$$

where matrix $\mathbf{R}^{-1}$ has been replaced by $\hat{\mathbf{R}}^{-1}$ defined in (2.50). Once the solution of the problem in (2.57) is obtained, the detection vector for the CMOE detector can be computed using (2.53). Adaptive implementations of the constrained optimization method have been proposed in [44].

2.4.3 Nonlinear Multiuser Detectors

Besides the linear multiuser detectors described above, nonlinear methods are also very popular for multiuser detection. Early nonlinear detectors are decision-aided methods in which final or tentative decisions on the bits of interfering users are employed to help improve the demodulation of the information bit of interest. Popular nonlinear multiuser detectors include multistage detectors [55, 56, 85], successive interference cancellation (SIC) detectors [45, 46, 51, 52], parallel interference cancellation (PIC) detectors [53, 54], and decision-feedback detectors [57, 58]. Compared with linear multiuser detectors, decision-aided nonlinear detectors are often computationally less involved and suitable for DS-CDMA systems using long signature codes. However, the performance of decision-aided detectors depends largely on the accuracy of initial decisions.

During the past five years, several nonlinear multiuser detectors have been developed by relaxing the ML detection problem into various optimization problems that can be solved more efficiently. The detectors so obtained are referred to as *suboptimal ML* detectors since they offer suboptimal performance only relative to Verdù's ML detection method. Well-known suboptimal ML detectors include generalized MMSE (GMMSE) [59, 60], bound-constraint (BC) [59, 60, 62], and semidefinite programming relaxation (SDPR) detectors [62, 63, 64, 84].

2.4.3.1 Generalized MMSE Detector

The binary constraints associated with the ML detection problem in (2.25b) imply that $\mathbf{x}^T\mathbf{x} = K$, which refers to the sphere of a $K - dimensional$ ball centered at the origin with radius $\sqrt{K}$. If we extend the feasible region to the entire ball, then the problem in (2.25) is relaxed into the problem

$$\text{minimize} \quad \mathbf{x}^T\mathbf{H}\mathbf{x} + \mathbf{x}^T\mathbf{p} \tag{2.58a}$$

$$\text{subject to}: \quad \mathbf{x}^T\mathbf{x} \leq K \tag{2.58b}$$

Note that the problem in (2.58) is to minimize a convex objective function over a convex region and, therefore, it is a convex programming problem that has a unique global solution. The dual problem of (2.58) is given by

$$\text{maximize} \quad -\frac{1}{4}\mathbf{p}^T(\mathbf{H}+\lambda\cdot\mathbf{I})^{-1}\mathbf{p}-\lambda\cdot K \tag{2.59a}$$

$$\text{subject to:} \quad \lambda \geq 0 \tag{2.59b}$$

where λ is the *Lagrange multiplier* associated with the constraint in (2.58b) and $\mathbf{I}$ denotes the identity matrix. Since the variable of the problem in (2.59) is a scalar, the solution of this problem can be obtained very efficiently by using gradient-based algorithms. If we denote the solution of (2.59) as λ^*, then the solution of the problem in (2.58) is given by

$$\mathbf{x}_G^* = (\mathbf{H}+\lambda^*\mathbf{I})^{-1}\mathbf{A}\mathbf{y} \tag{2.60}$$

A system that can resolve the information bits by solving the optimization problem in (2.58) is referred to as a *generalized MMSE* (GMMSE) detector. It can be shown that when λ^* assumes the value of σ^2, the GMMSE detector becomes the LMMSE detector. It has been found that the GMMSE detector offers comparable demodulation performance relative to the LMMSE detector but requires a larger amount of computation. However, since σ^2 is not involved in (2.60), the GMMSE detector does not require the estimation of channel noise for detecion. On the other hand, it can be shown that when λ^* assumes the values of 0 or a sufficient large positive scalar, the GMMSE detector becomes the decorrelating or conventional matched-filter (MF) detector, respectively. In other words, the decorrelating detector, the LMMSE detector, and the conventional MF detector can be viewed as special cases of the GMMSE detector.

2.4.3.2 Bound-Constrained Detector

The constraints in (2.25b) imply that $-1 \leq x_i \leq 1$ for $i = 1,\ 2,\ \ldots,\ K$. Hence the ML detection problem in (2.25) can be relaxed into the bound-constrained optimiza-

tion problem

$$\text{minimize} \quad \mathbf{x}^T\mathbf{H}\mathbf{x} + \mathbf{x}^T\mathbf{p} \tag{2.61a}$$

$$\text{subject to:} \quad -1 \leq x_i \leq 1 \quad \text{for} \quad i = 1, 2, \ldots, K \tag{2.61b}$$

The feasible region defined by (2.61b) is the unit hypercube centered at the origin. Since the constraints in (2.61b) are linear, the problem in (2.61) is a convex quadratic programming (CQP) problem, which can be solved by using many efficient QP algorithms described in [94, 95, 96]. It has been pointed out in [59, 60] that this problem can be solved much more efficiently by using the nonlinear *Gaussian-Seidel* and *Jacobi* algorithms which can be implemented in an interference cancellation framework.

It is easy to see that the optimization problem in (2.58) can be obtained by relaxing the optimization problem in (2.61). Therefore, the BC detector is expected to offer superior performance relative to that of the GMMSE detector. The dual problem associated with the problem in (2.61) is given by

$$\text{maximize} \quad -\frac{1}{4}\mathbf{p}^T[\mathbf{H} + \text{diag}(\boldsymbol{\lambda})]^{-1}\mathbf{p} - \mathbf{e}^T\boldsymbol{\lambda} \tag{2.62a}$$

$$\text{subject to:} \quad \boldsymbol{\lambda} \geq 0 \tag{2.62b}$$

where $\mathbf{e} = [1\ 1\ \cdots\ 1]^T$, $\boldsymbol{\lambda} = [\lambda_1\ \lambda_2\ \cdots\ \lambda_K]^T$ with λ_i denoting the Lagrange multiplier associated with the ith constraint in (2.61b), and $\text{diag}(\boldsymbol{\lambda})$ is the diagonal matrix with λ_i being the ith diagonal component. Note that the solutions of the problems in (2.61) and (2.62) can be related to each other by

$$\mathbf{x}^* = -\frac{1}{2}[\mathbf{H} + \text{diag}(\boldsymbol{\lambda}^*)]^{-1}\mathbf{p} \tag{2.63}$$

2.5 Conclusion

The characteristics, classification, and basic models of mobile communication channels have been examined and several signal models for DS-CDMA systems, conventional detectors, as well as the RAKE receiver have been described. The chapter has also

reviewed several important multiuser detectors for DS-CDMA systems over AWGN and frequency-selective fading channels.

Chapter 3

New Suboptimal ML Detectors Based on Semidefinite Programming Relaxation

3.1 Introduction

Recent research on multiuser detection has shown that suboptimal nultiuser detection can be achieved by converting the combinatorial problem associated with maximum likelihood (ML) detection into other types of optimization problems. Compared with the original ML detection problem, these new optimization problems involve continuous feasible regions and can be solved by algorithms whose computational complexity is of polynomial order with respect to the number of users. Since detectors so obtained offer suboptimal performance relative to ML detectors, these detectors are referred to as *suboptimal ML detectors*. An early suboptimal ML detector is the decorrelating detector proposed in [28] where the binary constraints of the ML detection problem are completely removed in order to convert the combinatorial optimization problem into an unconstrained optimization problem. Other suboptimal detectors were proposed in the past several years [59, 60].

In this chapter, a semidefinite-programming (SDP) based suboptimal ML detector for DS-CDMA systems is proposed. It is shown that the maximization associated with

the ML detection problem can be carried out by 'relaxing' the associated combinatorial programming problem into an SDP problem where both the objective function and constraint functions are convex functions of continuous variables. This leads to a suboptimal ML detector whose computational complexity is of polynomial order with respect to the number of users. This will be referred to as the *primal SDP relaxation-based detector.* Computer simulations are presented which demonstrate that the proposed detector offers near-optimal performance for both synchronous and asynchronous DS-CDMA systems as well as a significantly reduced computational complexity compared with that associated with the ML detection method proposed in [20]. Comparisons with some other known detectors, such as the conventional matched filter (MF), decorrelating, and linear MMSE (LMMSE) detectors, are also presented.

Next, we propose an efficient dual algorithm to solve the SDP problem in three steps. First, the primal SDP problem is converted into a dual problem based on the concept of duality. Then the dual SDP problem is solved using the projective method [61] which leads to improved efficiency due to the reduced number of variables. Then, the solution of the primal SDP problem is expressed in terms of the solution of the dual SDP problem based on the Karush-Kuhn-Tucker (KKT) conditions and the central path concept. The dual algorithm obtained leads to a new detector which will be referred to as the *dual SDP relaxation-based detector.* Computer simulations are presented which demonstrate that the proposed dual algorithm solves the SDP problem efficiently without impairing the demodulation performance. Note that the signal model used can be found in Sec. 2.4.1.

The chapter is organized as follows. In Sec. 3.2, the primal SDP relaxation-based algorithm is developed. In Sec. 3.3, the dual SDP relaxation-based algorithm is deduced. Computer simulation results are presented in Sec. 3.4, and the main conclusions are summarized in Sec. 3.5.

3.2 New Multiuser Detector Based on SDP Relaxation

In this section, the SDP relaxation approach is first described and then applied to multiuser detection for both synchronous and asynchronous DS-CDMA systems. The optimality issue of the proposed detector is also addressed.

3.2.1 Semidefinite Programming

SDP is a class of mathematical methods for the solution of optimization problems where the objective function is linear and the constraints are linear matrix inequalities. A typical SDP problem formulation is given by

$$\text{minimize} \quad \mathbf{c}^T\mathbf{x} \tag{3.1a}$$

$$\text{subject to:} \quad \mathbf{F}(\mathbf{x}) = \mathbf{F}_0 + \sum_{i=1}^{n} x_i\mathbf{F}_i \succeq \mathbf{0} \tag{3.1b}$$

where $\mathbf{x} = [x_1 \ x_2 \ \cdots \ x_n]^T$ denotes the variable vector, $\mathbf{c} \in R^{n\times 1}$, $\mathbf{F}_i \in R^{m\times m}$ for $0 \leq i \leq n$ are symmetric matrices and (3.1b) is a linear matrix inequality (LMI). The notation $\mathbf{F}(\mathbf{x}) \succeq \mathbf{0}$ denotes that matrix $\mathbf{F}(\mathbf{x})$ is positive semidefinite.

Many important analysis and design problems in engineering can be formulated as SDP problems [71], and efficient interior-point optimization algorithms and software for SDP have been developed in the past several years [72]-[74].

3.2.2 SDP Relaxation of MAX-CUT Problem

The MAX-CUT problem is a well-known combinatorial problem in graph theory. It can be formulated as [75]

$$\text{maximize} \quad \frac{1}{2}\sum_{i<j}\sum w_{ij}(1 - x_ix_j) \tag{3.2a}$$

$$\text{subject to}: \quad x_i \in \{1, -1\} \quad \text{for } 1 \leq i \leq n \tag{3.2b}$$

where w_{ij} are the weights associated with a graph. The constraints in (3.2b) can be expressed as $x_i^2 = 1$ for $1 \leq i \leq n$. If $\mathbf{W} = \{w_{ij}\}$ is a symmetric matrix with $w_{ii} = 0$ for $1 \leq i \leq n$, then the objective function in (3.2a) can be expressed as

$$\begin{aligned}\frac{1}{2}\sum_{i<j}\sum w_{ij}(1 - x_i x_j) &= \frac{1}{4}\sum\sum w_{ij} - \frac{1}{4}\mathbf{x}^T\mathbf{W}\mathbf{x} \\ &= \frac{1}{4}\sum\sum w_{ij} - \frac{1}{4}\mathrm{tr}(\mathbf{W}\mathbf{X}) \end{aligned} \tag{3.3}$$

where $\mathrm{tr}(\cdot)$ denotes the trace of the matrix and $\mathbf{X} = \mathbf{x}\mathbf{x}^T$ with $\mathbf{x} = [x_1\ x_2\ \cdots\ x_n]^T$. Therefore, the optimization problem in (3.2) can be converted into

$$\text{minimize} \quad \mathrm{tr}(\mathbf{W}\mathbf{X}) \tag{3.4a}$$

$$\text{subject to:} \quad \mathbf{X} = \mathbf{x}\mathbf{x}^T \tag{3.4b}$$

$$x_{ii} = 1 \quad \text{for } 1 \leq i \leq n \tag{3.4c}$$

where x_{ii} denotes the ith diagonal element of $\mathbf{X}$. Since the set of matrices

$$\{\mathbf{X} : \mathbf{X} = \mathbf{x}\mathbf{x}^T \text{ with } x_{ii} = 1 \text{ for } 1 \leq i \leq n\} \tag{3.5}$$

can also be represented by

$$\{\mathbf{X} : \mathbf{X} \succeq \mathbf{0};\ \mathrm{rank}(\mathbf{X}) = 1; x_{ii} = 1,\ \text{for } 1 \leq i \leq n\}, \tag{3.6}$$

the problem in (3.4) is equivalent to

$$\text{minimize} \quad \mathrm{tr}(\mathbf{W}\mathbf{X}) \tag{3.7a}$$

$$\text{subject to :} \quad \mathbf{X} \succeq \mathbf{0} \tag{3.7b}$$

$$x_{ii} = 1 \quad \text{for } 1 \leq i \leq n \tag{3.7c}$$

$$\mathrm{rank}(\mathbf{X}) = 1 \tag{3.7d}$$

In [75], Geomans and Williamson proposed a relaxation of the above problem by removing the rank constraint in (3.7d) which leads to

$$\text{minimize} \quad \mathrm{tr}(\mathbf{W}\mathbf{X}) \tag{3.8a}$$

$$\text{subject to :} \quad \mathbf{X} \succeq \mathbf{0} \tag{3.8b}$$

$$x_{ii} = 1 \quad \text{for } 1 \leq i \leq n \tag{3.8c}$$

Note that the objective function in (3.8a) is a linear function of $\mathbf{X}$ and the constraints in (3.8b) and (3.8c) can be combined into an LMI as

$$\sum_{i>j}\sum x_{ij}\mathbf{F}_{ij} + \mathbf{I} \succeq \mathbf{0} \tag{3.9}$$

where, for each (i,j) with $i > j$, $\mathbf{F}_{ij}$ is a symmetric matrix with its (i,j)th and (j,i)th entries being ones and all the remaining entries being zeros. Therefore, the problem in (3.8) fits into the formulation in (3.1) and, therefore, is an SDP problem. For this reason, the problem in (3.8) is known as an *SDP relaxation* of the combinatorial problem in (3.4) and, equivalently, of the problem in (3.7).

If we denote the minimum value of the objective function in problems (3.4) and (3.8) as μ^* and ν^*, respectively, then since the feasible region of the problem in (3.4) is a subset of the feasible region in problem in (3.8), we have $\nu^* \leq \mu^*$. Furthermore, it has been shown in [76] that if the weights w_{ij} are all nonnegative, then $\nu^* \geq 0.87856\mu^*$. In other words, we have

$$0.87856 \cdot \mu^* \leq \nu^* \leq \mu^* \tag{3.10}$$

This indicates that the solution of the SDP problem in (3.8) is, in general, a good approximation of the solution of the problem in (3.4). It is the good quality of the approximation in conjunction with reduced computational complexity of SDP that makes the Geomans-Williamson SDP relaxation an attractive optimization tool for combinatorial minimization problems. As a matter of fact, the Geomans-Williamson SDP relaxation has found many applications in graph optimization, network management, and scheduling [71, 74] since it was proposed in [75]. In what follows, we propose a new multiuser detector based on SDP relaxation.

3.2.3 Primal SDP-Relaxation Based Detector

We first apply the SDPR relaxation approach in multiuser detection for synchronous systems and then for asynchronous systems. For this purposes, we define two matrices

$$\hat{\mathbf{X}} = \begin{bmatrix} \mathbf{x}\mathbf{x}^T & \mathbf{x} \\ \mathbf{x}^T & 1 \end{bmatrix} \quad \text{and} \quad \mathbf{C} = \begin{bmatrix} \mathbf{H} & \mathbf{p}/2 \\ \mathbf{p}^T/2 & 1 \end{bmatrix} \tag{3.11}$$

By noting that $\text{tr}(\mathbf{AB}) = \text{tr}(\mathbf{BA})$, the objective function of the ML detection problem in (2.25a) can be expressed as

$$\mathbf{x}^T\mathbf{H}\mathbf{x} + \mathbf{x}^T\mathbf{p} = \text{tr}(\mathbf{C}\hat{\mathbf{X}}) \tag{3.12}$$

Using an argument similar to that in Sec. 3.2.2, the constraints in (2.25b) can be converted into

$$\hat{\mathbf{X}} \succeq 0, \quad \hat{x}_{ii} = 1 \quad \text{for } 1 \leq i \leq K \tag{3.13a}$$

$$\text{rank } (\hat{\mathbf{X}}) = 1 \tag{3.13b}$$

where $\hat{x}_{ii}$ denotes the ith diagonal element of $\hat{\mathbf{X}}$. By removing the rank constraint in (3.13b), we obtain an SDP relaxation of the ML detection problem in (2.25) as

$$\text{minimize } \text{tr}(\mathbf{C}\hat{\mathbf{X}}) \tag{3.14a}$$

$$\text{subject to: } \hat{\mathbf{X}} \succeq \mathbf{0} \tag{3.14b}$$

$$\hat{x}_{ii} = 1 \quad \text{for } i = 1, 2, \cdots, K+1 \tag{3.14c}$$

An algorithm or hardware system used for resolving the transmitted information bits by solving the problem in (3.14) is a suboptimal ML detector since its performance is suboptimal with respect to that of an ML detector based on Verdù's approach. Since the problem in (3.14) is obtained by using the SDP relaxation (SDPR) approach, the suboptimal ML detector so obtained will be referred to as an SDPR detector hereafter.

For asynchronous systems, we apply the SDP relaxation approach to the ML detection problem in (2.24) in the same way, which leads to

$$\text{minimize} \quad \text{tr}(\mathbf{C}_a\hat{\mathbf{X}}_a) \tag{3.15a}$$

$$\text{subject to:} \quad \hat{\mathbf{X}}_a \succeq \mathbf{0} \tag{3.15b}$$

$$\hat{x}_{aii} = 1 \quad \text{for} \quad i = 1, 2, \ldots, PK+1 \tag{3.15c}$$

where

$$\hat{\mathbf{X}}_a = \begin{bmatrix} \mathbf{x}_a\mathbf{x}_a^T & \mathbf{x}_a \\ \mathbf{x}_a^T & 1 \end{bmatrix}, \quad \mathbf{C}_a = \begin{bmatrix} \mathcal{H} & \mathcal{P}/2 \\ \mathcal{P}^T/2 & 1 \end{bmatrix}, \tag{3.16}$$

and $\hat{x}_{aii}$ denotes the ith diagonal element of $\hat{\mathbf{X}}_a$. Note that although the SDP problems in (3.14) and (3.15) have identical structure, the sizes of these problems in terms of the number of variables involved are significantly different: the problem in (3.14) has $K(K+1)/2$ variables whereas that in (3.15) has $PK(PK+1)/2$ variables.

Since $\mathcal{H}$ in (3.16) is a band-limited matrix, the solution of the problem in (3.15) can be approximated by using *dynamic programming* (DP) approaches [17]. Through one of these approaches, the problem in (3.15) can be divided into a number of sub-problems each of which involves a significantly reduced number of variables relative to the problem in (3.15). By doing so, the amount of computation required for solving the problem in (3.15) can be significantly reduced.

3.2.4 Binary Solution

The variables in the optimization problem in (2.24) and (2.25) assume only values of 1 or -1 whereas the variable $\mathbf{X}$ in the SDP problem (3.14) assumes continuous values. In what follows, we describe two approaches that can be used to generate a binary solution for the problems in (2.25) based on the solution $\hat{\mathbf{X}}$ of the SDP problem in (3.14). Note that the same methods can be applied to generate a binary solution for (2.25) based on the solution of (3.15).

Let the solution of (3.14) be denoted as $\hat{\mathbf{X}}^*$. It follows from (3.11) that $\hat{\mathbf{X}}^*$ is a $(K+1) \times (K+1)$ symmetric matrix of the form

$$\hat{\mathbf{X}}^* = \begin{bmatrix} \mathbf{X}^* & \mathbf{x}^* \\ \mathbf{x}^{*T} & 1 \end{bmatrix} \tag{3.17}$$

with

$$(\hat{x}^*)_{ii} = 1 \quad \text{for} \quad i = 1,\ 2,\ \ldots,\ K. \tag{3.18}$$

In view of the structure of (3.17), the first approach is simply to apply operator $\text{sgn}(\cdot)$ to $\mathbf{x}^*$ in (3.17), i.e.,

$$\hat{\mathbf{b}} = \text{sgn}\left[\hat{\mathbf{X}}^*(1:K, K+1)\right] \tag{3.19}$$

where $\hat{\mathbf{X}}^*(1:K, K+1)$ denotes the vector formed by using the first K entries in the last column of $\hat{\mathbf{X}}^*$.

At the cost of more computations, a better binary solution can be obtained using the eigen-decomposition of matrix $\hat{\mathbf{X}}^*$, i.e.,

$$\hat{\mathbf{X}}^* = \mathbf{U}\mathbf{S}\mathbf{U}^T \tag{3.20}$$

where $\mathbf{U}$ is an orthogonal matrix and $\mathbf{S}$ is a diagonal matrix with the eigenvalues of $\hat{\mathbf{X}}^*$ on its diagonal in decreasing order [77, 78]. It is well known that an optimal rank-one approximation of $\hat{\mathbf{X}}^*$ in the 2-norm sense is given by $\lambda_1 \mathbf{u}_1 \mathbf{u}_1^T$, where λ_1 is the largest eigenvalue of $\hat{\mathbf{X}}^*$ and $\mathbf{u}_1$ is the eigenvector associated with λ_1 [77]. If we denote the vector formed by using the first K entries of $\mathbf{u}_1$ as $\tilde{\mathbf{u}}$, and the last entry of $\mathbf{u}_1$ as u_{K+1}, i.e.,

$$\mathbf{u}_1 = \begin{bmatrix} \tilde{\mathbf{u}} \\ u_{K+1} \end{bmatrix} \tag{3.21}$$

then the optimal rank-one approximation of $\hat{\mathbf{X}}^*$ can be written as

$$\begin{aligned}\hat{\mathbf{X}}^* &\approx \lambda_1 \mathbf{u}_1 \mathbf{u}_1^T \\ &= \lambda_1 \begin{bmatrix} \tilde{\mathbf{u}}\tilde{\mathbf{u}}^T & u_{K+1}\tilde{\mathbf{u}} \\ u_{K+1}\tilde{\mathbf{u}}^T & u_{K+1}^2 \end{bmatrix} \\ &= \lambda_1 u_{K+1}^2 \begin{bmatrix} \tilde{\mathbf{x}}_1\tilde{\mathbf{x}}_1^T & \tilde{\mathbf{x}}_1 \\ \tilde{\mathbf{x}}_1^T & 1 \end{bmatrix} \end{aligned} \tag{3.22}$$

where $\tilde{\mathbf{x}}_1 = \tilde{\mathbf{u}}/u_{K+1}$. Since $\lambda_1 > 0$, upon comparing (3.22) with (3.17) we see that vector $\tilde{\mathbf{x}}_1$ is a reasonable approximation of $\mathbf{x}^*$. Therefore, a binary solution of the problem in (2.25) can be generated as

$$\hat{\mathbf{b}} = \begin{cases} \text{sgn}[\mathbf{u}_1(1:K)] & \text{if} \quad \mathbf{u}_1(K+1) > 0 \\ -\text{sgn}[\mathbf{u}_1(1:K)] & \text{if} \quad \mathbf{u}_1(K+1) < 0 \end{cases} \tag{3.23}$$

Note that many efficient and reliable algorithms are available in the literature for computing the eigenvector associated with the largest eigenvalue of $\hat{\mathbf{X}}^*$ [77] -[80].

An algorithm based on the above approach is said to be a *primal algorithm* since it solves the problem at hand directly as opposed to the algorithm proposed in Sec. 3.3 which solves the so-called dual version of the problem. A multiuser detector based on the primal algorithm described will be referred to as the primal SDPR (PSDPR) detector.

3.2.5 Optimality of Solution

Because of the use of relaxation, the PSDPR detector is, in theory, *suboptimal.* As mentioned in Sec. 3.2.2, the SDP relaxation of the MAX-CUT problem yields a good suboptimal solution. However, there are two important differences between the SDP problems in (3.8) and (3.14): the diagonal entries of $\mathbf{W}$ in (3.8) are all zero while those of $\mathbf{C}$ in (3.14) are all strictly positive; and the off-diagonal entries in $\mathbf{W}$ are non-negative whereas matrix $\mathbf{C}$ may assume negative off-diagonal entries. Consequently,

the bounds in (3.8) do not hold in general for the SDP problem in (3.14). As will be demonstrated by our simulations, however, the demodulation performance achieved in SDPR detector is comparable with that offered by the ML detector.

3.3 Dual SDP-Relaxation Based Detector

Although interior-point algorithms [72, 74] can be applied to the SDP problem at hand and their computational complexity increases in a non-exponential manner with respect to the number of users, numerical difficulties may arise in solving the SDP problem because of the large number of variables involved even for the detection of a moderate number of users. For example, if $K = 20$, the dimension of vector $\mathbf{x}$ in (3.14) is 20 and the number of variables in $\hat{\mathbf{X}}$ becomes $K(K+1)/2 = 210$; and for an asynchronous system with $K = 20$ and $P = 4$, the SDP problem in (3.15) involves 3240 variables.

In this section, we present a new and more efficient algorithm that can be used to obtain a solution of the SDP problem at hand. The proposed method entails two steps, as follows: First, the so-called dual of the SDP problem at hand is solved [72, 79] and, second, the solution obtained for the dual problem is converted into the solution of the primal SDP problem.

The SDP relaxation problem in (3.14) can be expressed as

$$\text{minimize} \quad \text{tr}(\mathbf{C}\hat{\mathbf{X}}) \tag{3.24a}$$

$$\text{subject to:} \quad \hat{\mathbf{X}} \succeq \mathbf{0} \tag{3.24b}$$

$$\text{tr}(\mathbf{A}_i\hat{\mathbf{X}}) = 1 \quad \text{for } i = 1, \ \ldots, K+1 \tag{3.24c}$$

where matrix $\mathbf{A}_i$ is a diagonal matrix whose diagonal entries are all zeros except the ith entry which is one. It follows from [74, 81] that the dual of the problem in (3.24)

is given by

$$\text{minimize} \quad -\mathbf{b}^T\mathbf{y} \tag{3.25a}$$

$$\text{subject to: } \mathbf{S} = \mathbf{C} - \sum_{i=1}^{K+1} y_i \mathbf{A}_i \tag{3.25b}$$

$$\mathbf{S} \succeq \mathbf{0} \tag{3.25c}$$

where $\mathbf{y} = [y_1 \ \cdots \ y_{K+1}]^T$ and $\mathbf{b} = [1 \ \cdots \ 1]^T \in \mathcal{C}^{(K+1)\times 1}$. Note that the dual problem in (3.25) involves only $K+1$ variables and it can be solved efficiently by using interior-point algorithms such as the projective method proposed by Nemirovskii and Gahinet [61]. This method has been implemented in the MATLAB *LMI* toolbox and has been applied for the solution of a variety of SDP problems [73].

In order to obtain the solution of the primal SDP problem in (3.24), the KKT conditions for the solutions of the problems in (3.24) and (3.25) need to be examined. The KKT conditions state that $\{\hat{\mathbf{X}}^*, \ \mathbf{y}^*\}$ solves the problems in (3.24) and (3.25) if and only if they satisfy the conditions

$$\sum_{i=1}^{K+1} y_i^* \mathbf{A}_i + \mathbf{S}^* = \mathbf{C} \tag{3.26a}$$

$$\text{tr}(\mathbf{A}_i \hat{\mathbf{X}}^*) = 1 \quad \text{for } i = 1, \ \ldots \ , K+1 \tag{3.26b}$$

$$\mathbf{S}^* \hat{\mathbf{X}}^* = \mathbf{0} \tag{3.26c}$$

$$\hat{\mathbf{X}}^* \succeq \mathbf{0} \ \text{ and } \ \mathbf{S}^* \succeq \mathbf{0} \tag{3.26d}$$

From (3.26a), we have

$$\mathbf{S}^* = \mathbf{C} - \sum_{i=1}^{K+1} y_i^* \mathbf{A}_i \tag{3.27}$$

Since the solution $\mathbf{y}^*$ is typically obtained by using an *iterative* algorithm (such as the projective algorithm proposed by Nemirovskii and Gahinet), $\mathbf{y}^*$ can be a good approximate solution of (3.26) at best, which means that $\mathbf{y}^*$ is in the *interior* of the feasible region. Consequently, matrix $\mathbf{S}^*$ remains *positive definite*. Therefore, the set $\{\mathbf{y}^*, \ \mathbf{S}^*, \ \hat{\mathbf{X}}^*\}$ can be regarded as a point in the feasible region that is sufficiently

close to the limiting point of the central path for the problems in (3.24) and (3.25). Recall that the central path is defined as a parameterized set $\{\mathbf{y}(\tau),\ \mathbf{S}(\tau),\ \hat{\mathbf{X}}(\tau)$ for $\tau > 0\}$ that satisfies the modified KKT conditions [74]

$$\sum_{i=1}^{K+1} y_i(\tau)\mathbf{A}_i + \mathbf{S}(\tau) = \mathbf{C} \tag{3.28a}$$

$$\mathrm{tr}(\mathbf{A}_i\hat{\mathbf{X}}(\tau)) = 1 \quad \text{for } i = 1,\ \ldots\ K+1 \tag{3.28b}$$

$$\mathbf{S}(\tau)\hat{\mathbf{X}}(\tau) = \tau\mathbf{I} \tag{3.28c}$$

$$\hat{\mathbf{X}}(\tau) \succeq \mathbf{0} \ \text{ and } \ \mathbf{S}(\tau) \succeq \mathbf{0} \tag{3.28d}$$

The relation between equations (3.27) and (3.28) becomes apparent as one realizes that the entire central path defined by (3.28) lies in the interior of the feasible region and as $\tau \to 0$, the path converges to a solution set $\{\mathbf{y}^*,\ \mathbf{S}^*,\ \hat{\mathbf{X}}^*\}$ that satisfies (3.26). From (3.28c), it follows that

$$\hat{\mathbf{X}}(\tau) = \tau\mathbf{S}^{-1}(\tau) \tag{3.29}$$

which suggests an approximate solution for the problem in (3.26) as

$$\hat{\mathbf{X}} = \tau(\mathbf{S}^*)^{-1} \tag{3.30}$$

In (3.30), τ is a sufficiently small constant such that $\tau > 0$ and $\mathbf{S}^*$ is given by (3.27). In order for matrix $\hat{\mathbf{X}}$ in (3.30) to satisfy the equality constraints in (3.24c), $\hat{\mathbf{X}}$ needs to be slightly modified by using a scaling matrix $\mathbf{\Pi}$, i.e.,

$$\hat{\mathbf{X}}^* = \mathbf{\Pi}(\mathbf{S}^*)^{-1}\mathbf{\Pi} \tag{3.31a}$$

where

$$\mathbf{\Pi} = \mathrm{diag}\{\xi_1^{1/2} \ \cdots \ \xi_{K+1}^{1/2}\} \tag{3.31b}$$

and ξ_i is the ith diagonal entry of $(\mathbf{S}^*)^{-1}$. In (3.31a), we have pre- and post-multiplied $(\mathbf{S}^*)^{-1}$ by $\mathbf{\Pi}$ to ensure that matrix $\hat{\mathbf{X}}^*$ remains *symmetric* and *positive definite*. It is

worth noting that by imposing the equality constraints in (3.24c) on $\hat{\mathbf{X}}$, the parameter τ in (3.30) is incorporated in the scaling matrix $\mathbf{\Pi}$.

Based on above discussions, an approximate solution $\hat{\mathbf{X}}$ of the SDP problem in (3.24) can be computed through the following steps:

(i) Form matrix $\mathbf{C}$ using (3.11).

(ii) Solve the dual SDP problem in (3.25) and denote its solution as $\mathbf{y}^*$.

(iii) Compute $\mathbf{S}^*$ using (3.27).

(iv) Compute $\hat{\mathbf{X}}^*$ using (3.31).

(v) Compute $\hat{\mathbf{b}}$ using (3.19) or (3.23).

Two remarks can be made pertaining to the computational complexity of the proposed algorithm and the accuracy of the solution obtained. To a large extent the computational complexity of our algorithm is determined by steps (ii) and (iv) where a $(K+1)$-variable SDP problem is solved and a $(K+1)\times(K+1)$ positive definite matrix is inverted, respectively. Compared to the computations required to directly solve the $K(K+1)/2$-variable SDP problem in (3.24), the new method reduces the computational complexity by a considerable amount. Concerning the accuracy of the solution, we note that it is the binary solution that determines the performance of the multiuser detector. Since the binary solution is the result of the sign operation (see (3.19) and (3.23)), the approximation introduced in (3.31) is expected to have a negligible effect on the accuracy of the solution. An implementation of the above algorithm will be referred to as the dual SDP relaxation (DSDPR) detector hereafter.

The use of semidefinite programming was also explored recently in [62] and [64]. In both articles, it has been shown that when the number of users or the crosscorrelations of signature waveforms is increased in DS-CDMA systems, the MUI present in the received signal can be significant, which leads to observable degradation in the performance of the detector based on the primal SDP relaxation. In such a case, although PSDPR detectors can still offer much better demodulation performance relative to other suboptimal detectors, their performance is not as good as that of an

ML detector.

3.4 Simulation Results

Computer simulations were carried out to evaluate the performance of the proposed SDPR detectors in terms of bit-error rate (BER) and computational complexity, and to compare them with the conventional MF, decorrelating, and LMMSE detectors as well as with a detector based on Verdù's ML detection method which will be referred to hereafter as the ML detector. In this detector, detection is achieved by calculating the objective function in (2.25a) 2^K times and selecting the combination of the information bits that yields the lowest value of the objective function.

The PSDPR and DSDPR detectors were implemented using the MATLAB LMI control toolbox [73]. Since the ultimate goal of multiuser detection is to estimate the *binary-valued* information vector $\mathbf{b}$, a fairly large convergence tolerance $\varepsilon = 10^{-2}$ was used in order to keep the number of iterations, and hence the computational complexity, low. In addition, an upper bound $K_u = 5$ was imposed on the number of iterations. In our simulations, 10^5 runs were performed to evaluate the average BER performance for each of PSDPR, DSDPR, conventional MF, decorrelating, LMMSE, and ML detectors.

In the first simulation, a six-user synchronous system with AWGN channel using 15-chip Gold sequences for signatures was considered. The received signal powers of the six users were set to 5, 3, 1.8, 0.6, 0.3, and 0.2. The last user with power 0.2 was designated as the desired one. The average BERs versus SNR for the PSDPR, DSDPR, decorrelating, LMMSE, and ML detectors are plotted in Fig. 3.1.

The second simulation concerned an eight-user synchronous system in a frequency-flat Rayleigh fading channel. The user signatures were the same as those in the first simulation and the received signal power of the eight users were set to 5, 3, 1.8, 1, 0.6, 0.3, 0.2 and 0.1. The fourth user, the one with unity power, was designated as the

desired user. The coherent time of the fading channel was set to ten times the symbol period. The signal-to-noise ratio (SNR) was assumed to be known for the LMMSE detector. The average BERs versus SNR for the PSDPR, DSDPR, decorrelating, LMMSE, and ML detectors are plotted in Fig. 3.2.

The third simulation was carried out to examine the near-far resistance of PSDPR and DSDPR detectors for a six-user synchronous system with AWGN channel using the same user signatures as before. The SNR of the desired user signal was fixed to 8 dB higher than channel noise. The SNR of the five interference user signals were identical and the SNR varied from 0 to 14 dB during the transmission. The average BERs versus SNR for the PSDPR, DSDPR, conventional MF, decorrelating, LMMSE, and ML detectors are plotted in Fig. 3.3.

From these simulations, it is observed that in synchronous systems the demodulation performance of PSDPR and DSDPR detectors is consistently very close to that of the ML detector and is superior relative to that of decorrelating and LMMSE detectors.

For asynchronous systems, the amount of computation required by the ML detector becomes prohibitive even for a very moderate number of users K and frame size P. The PSDPR detector requires significantly less computation than the ML detector but for a large number of runs, this detector would also require a prohibitive amount of computation. For these reasons, the fourth simulation evaluated the performance of only the DSDPR, conventional MF, decorrelating, and LMMSE detectors for a four-user equal-power asynchronous system with AWGN channel where the frame size is $P = 3$. The signal model used for the simulation of asynchronous DS-CDMA systems follows the definition in (2.24) where the crosscorrelation matrices $\mathbf{R}[0]$ and

$\mathbf{R}[1]$ in (2.24c) were set to

$$\mathbf{R}[1] = \begin{bmatrix} 1 & 0.2 & 0.2 & 0.2 \\ 0.2 & 1 & 0.2 & 0.2 \\ 0.2 & 0.2 & 1 & 0.2 \\ 0.2 & 0.2 & 0.2 & 1 \end{bmatrix} \quad \mathbf{R}[0] = \begin{bmatrix} -0.2 & -0.2 & -0.2 & -0.2 \\ -0.2 & -0.2 & -0.2 & -0.2 \\ -0.2 & -0.2 & -0.2 & -0.2 \\ -0.2 & -0.2 & -0.2 & -0.2 \end{bmatrix} \tag{3.32}$$

The average BER versus SNR for the DSDPR, conventional MF, decorrelating, and LMMSE detectors are plotted in Fig. 3.4. For comparison purpose, Fig. 3.4 also includes the approximate bound of the error probability for the ML detector (solid line). As is expected, the DSDPR detector outperforms all linear detectors simulated and offers very close BER performance as that of the ML detector.

Although it can be observed in Figs. (3.1)-(3.3) that the DSDPR detector offers slightly better performance relative to the PSDPR detector, the same conclusion might not be extended successfully to the general case. In fact, a complete study on the performance of the PSDPR and DSDPR algorithms is still not available at this stage. The conjecture on the phenomena appeared in the above figures is very likely due to more sereve numerical difficulities in solving the PSDP problem since more number of variables is involved in the problem.

The computational complexity of the various detectors was evaluated in terms of the CPU time[1] as measured by the MATLAB LMI Control toolbox used for the optimization [72]. The logarithm of the CPU time for the PSDPR, DSDPR, and ML detectors is plotted versus the number of active users in Fig. 3.5. The number of active users for the ML detectors was restricted to the range 10 to 17 to avoid the extremely high computational effort involved but, for the sake of comparison, the curve was extrapolated as shown in Fig. 3.5 assuming that the trend established for the range 10 to 17 users continues for larger numbers of users.

[1]All simulations in this thesis was conducted on Sun Blade workstations using MATLAB 6.5. In what follows, the CPU time of each algorithm presented in the thesis was obtained by using MATLAB commands 'cputime', 'tic', and 'toc'.

As can be observed in Fig. 3.5, the SDPR detectors are obviously much more efficient than the ML detector when the number of active users is larger, and the DSDPR detector is much more efficient than the PSDPR detector. Specifically, the PSDPR detector requires 8.6% and 0.05% the computational effort required by the ML detector for 15 and 25 users, respectively. On the other hand, the DSDPR detector requires 10.43% and 7.86% the computational effort required by the PSDPR detector again for 15 and 25 users, respectively.

Based on the simulation results obtained, the computational complexity of three detectors can be quantified in terms of the approximate CPU time which is given by

$$\mathcal{C}_{ML} \approx 4.5 \times 10^{-4}\ 2^{K} \tag{3.33a}$$

$$\mathcal{C}_{PSDPR} \approx 4.2 \times 10^{-5}\ K^{3.9} \tag{3.33b}$$

$$\mathcal{C}_{DSDPR} \approx 2.6 \times 10^{-5}\ K^{3.3} \tag{3.33c}$$

where K is the number of active users. In effect, the computational complexity of the ML detector increases exponentially with the number of users whereas that of the SDPR detectors is of polynomial order. It should be mentioned here that the computational effort pertaining to the DSDPR detector can be further reduced by taking the special structure of matrix $\mathbf{A}_i$ into consideration but this possibility has not been explored so far.

3.5 Conclusions

SDP relaxation based multiuser detectors have been proposed. It has been shown that by neglecting the rank constraint on the positive semidefinite matrix, the combinatorial problem associated with ML detection can be relaxed into an SDP problem. The solution of the primal SDP problem can also be obtained by solving its dual SDP problem in which the number of variables involved is reduced by an order of magnitude. Computer simulations have demonstrated that the demodulation performance

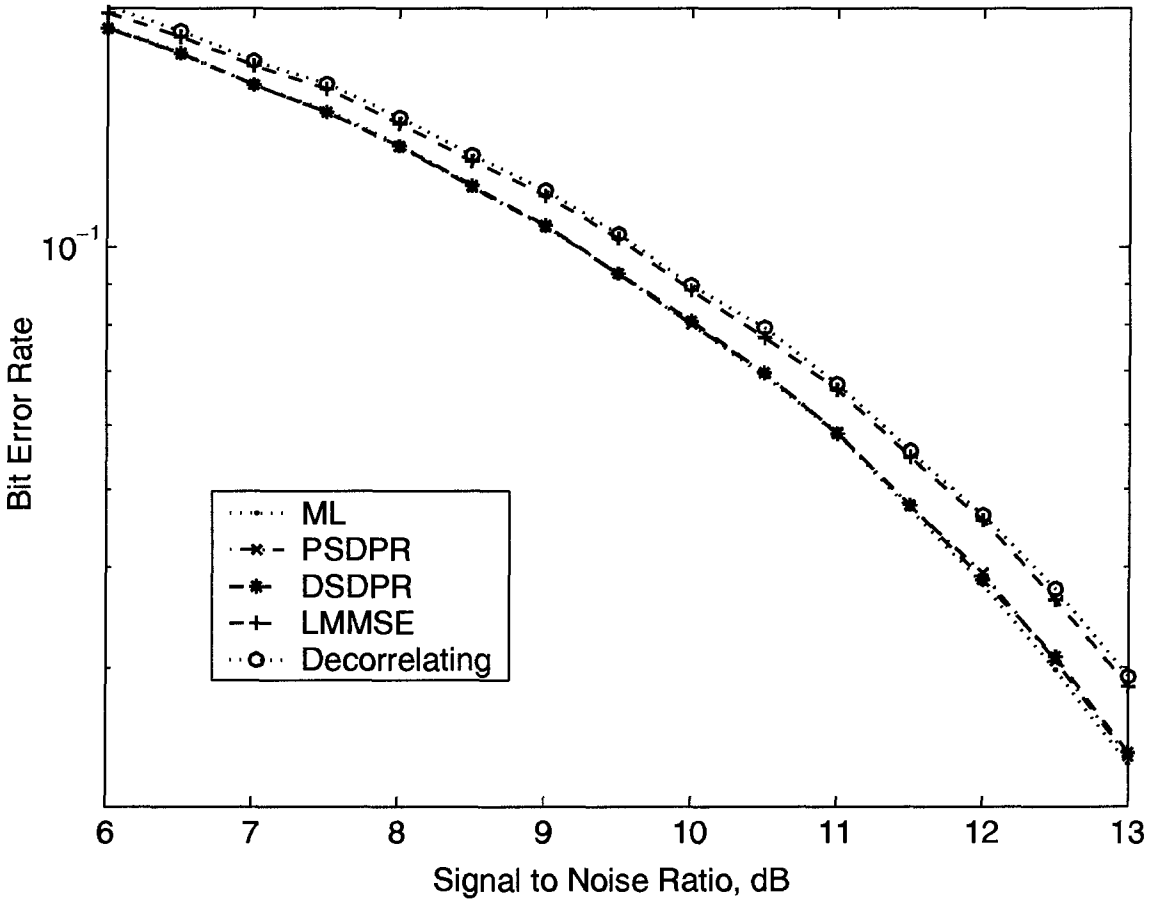

Figure 3.1. *BER versus SNR for a six-user synchronous DS-CDMA system over AWGN channel.*

of the SDPR detectors is near-optimal, and is significantly better than those of other suboptimal multiuser detectors such as the decorrelating and MMSE detectors. However, the computational complexity required by the SDPR detectors is of polynomial order with respect to the number of users by contrast with that required by the ML detector which grows exponentially as the number of users is increased. A comparison of SDPR detectors has shown that the DSDPR detector is much more efficient than the PSDPR detector owing to the large reduction in the variables involved. The simulation results have shown that the improvements in efficiency are brought about without degrading the demodulation performance relative to that achieved with the

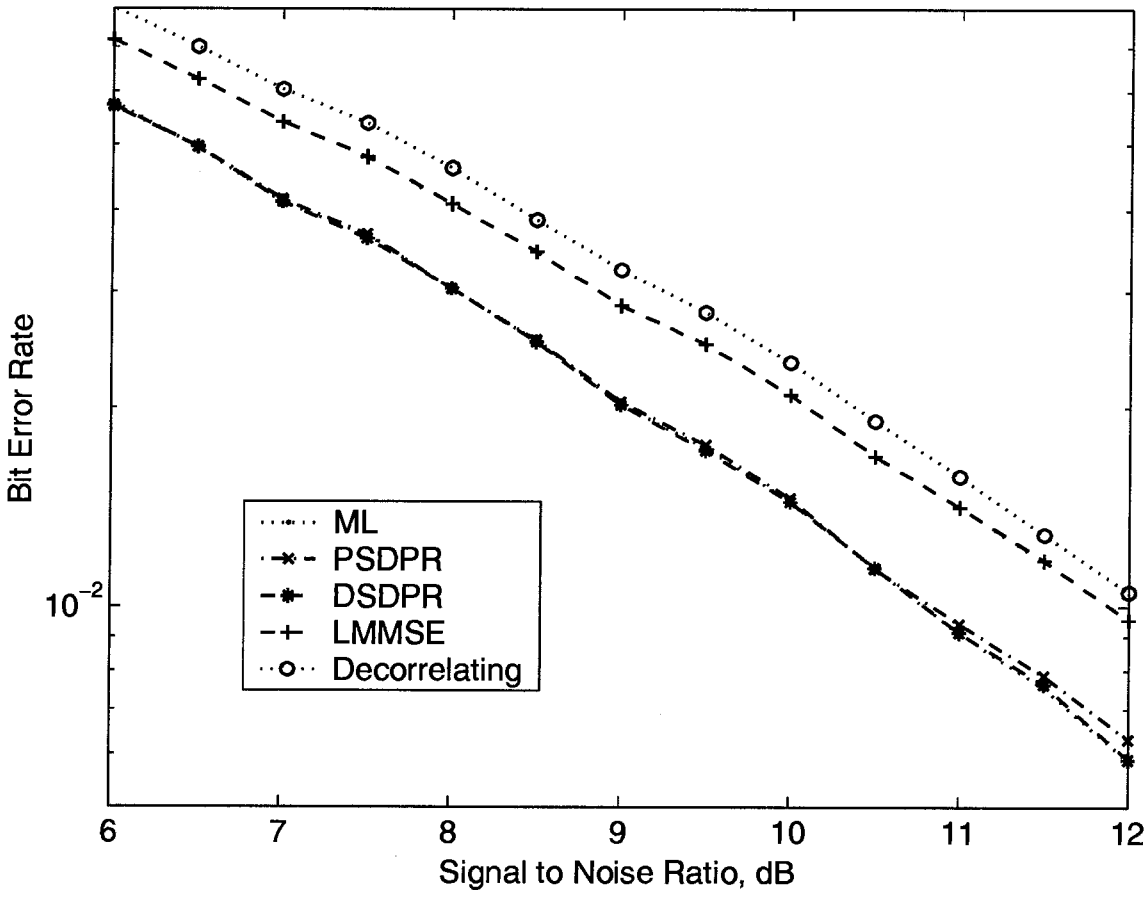

Figure 3.2. *BER versus SNR for an eight-user synchronous DS-CDMA system over flat Rayleigh fading channel.*

ML detector.

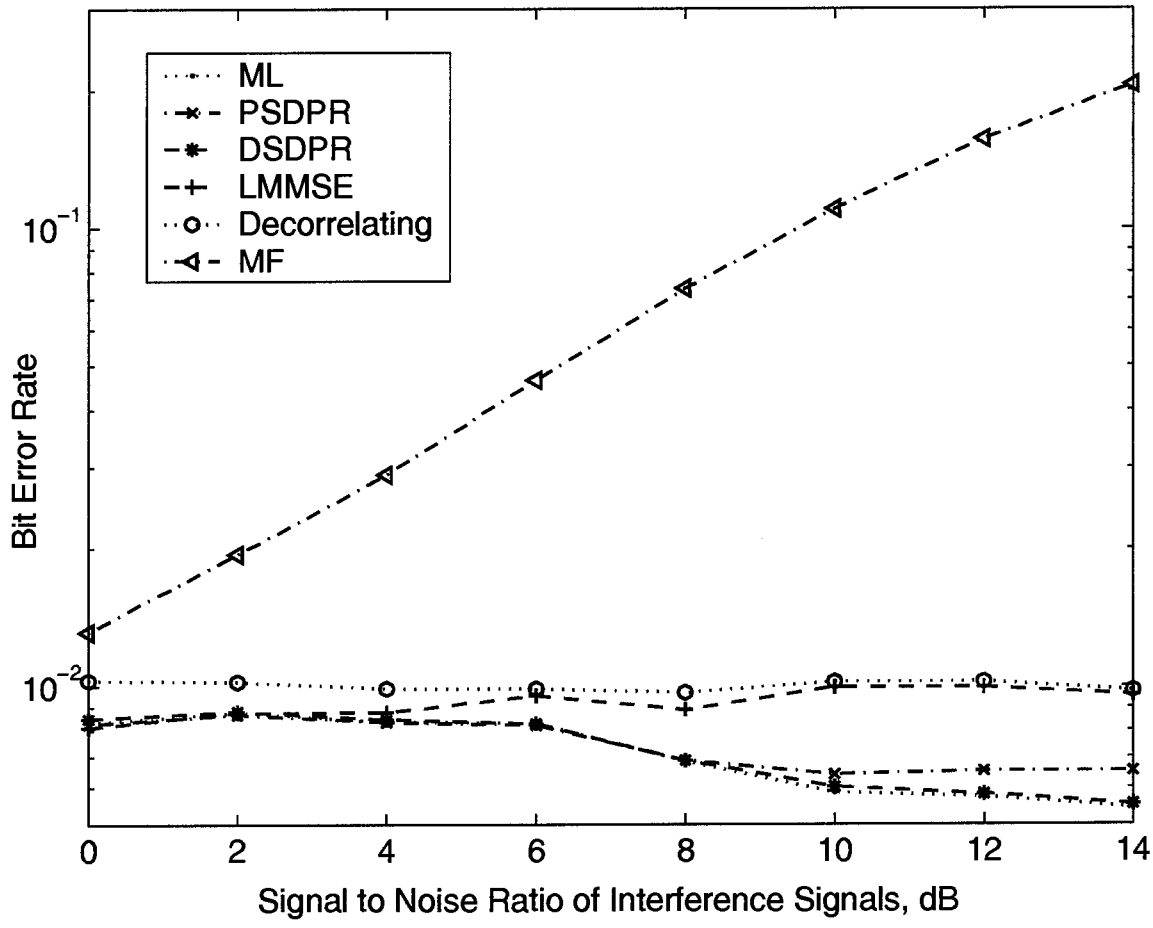

Figure 3.3. *Near-far performance in a six-user synchronous DS-CDMA system over AWGN channel.*

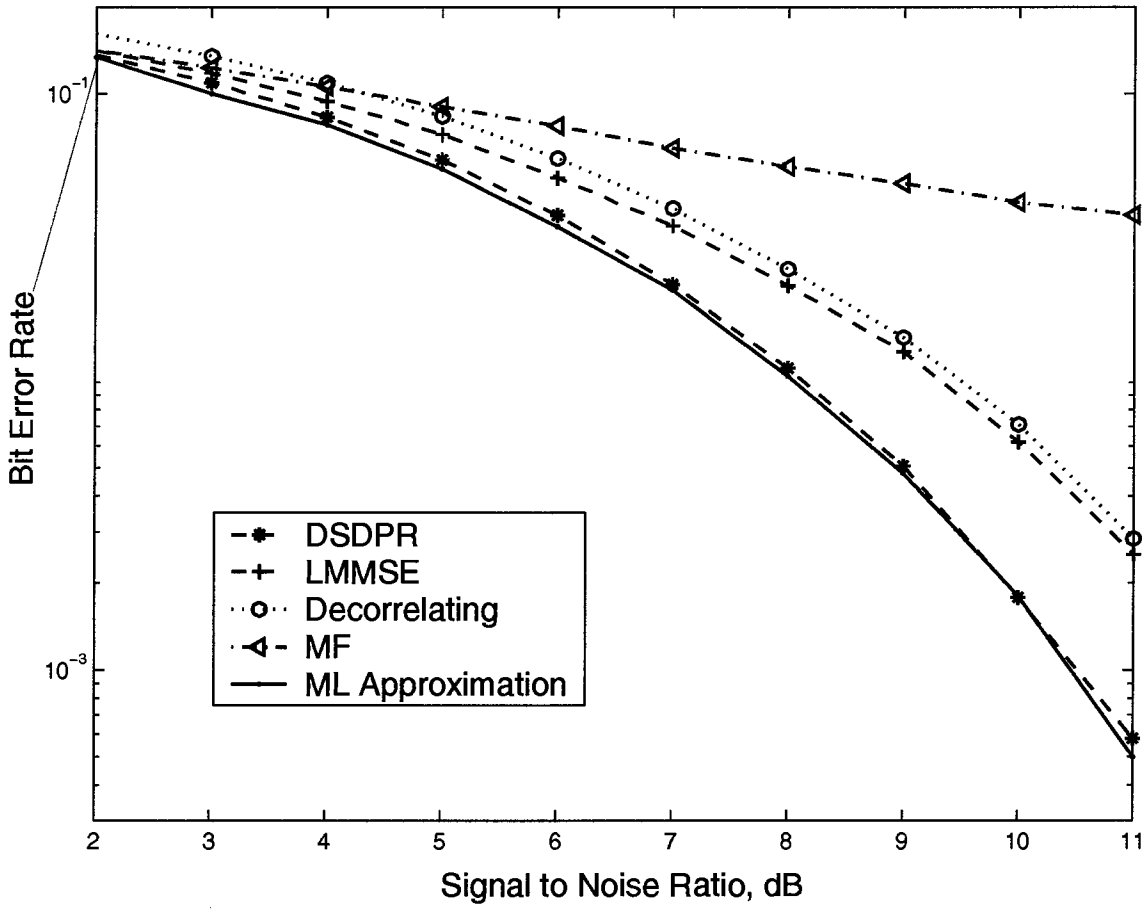

Figure 3.4. *BER versus SNR for a four-user asynchronous DS-CDMA system over AWGN channel.*

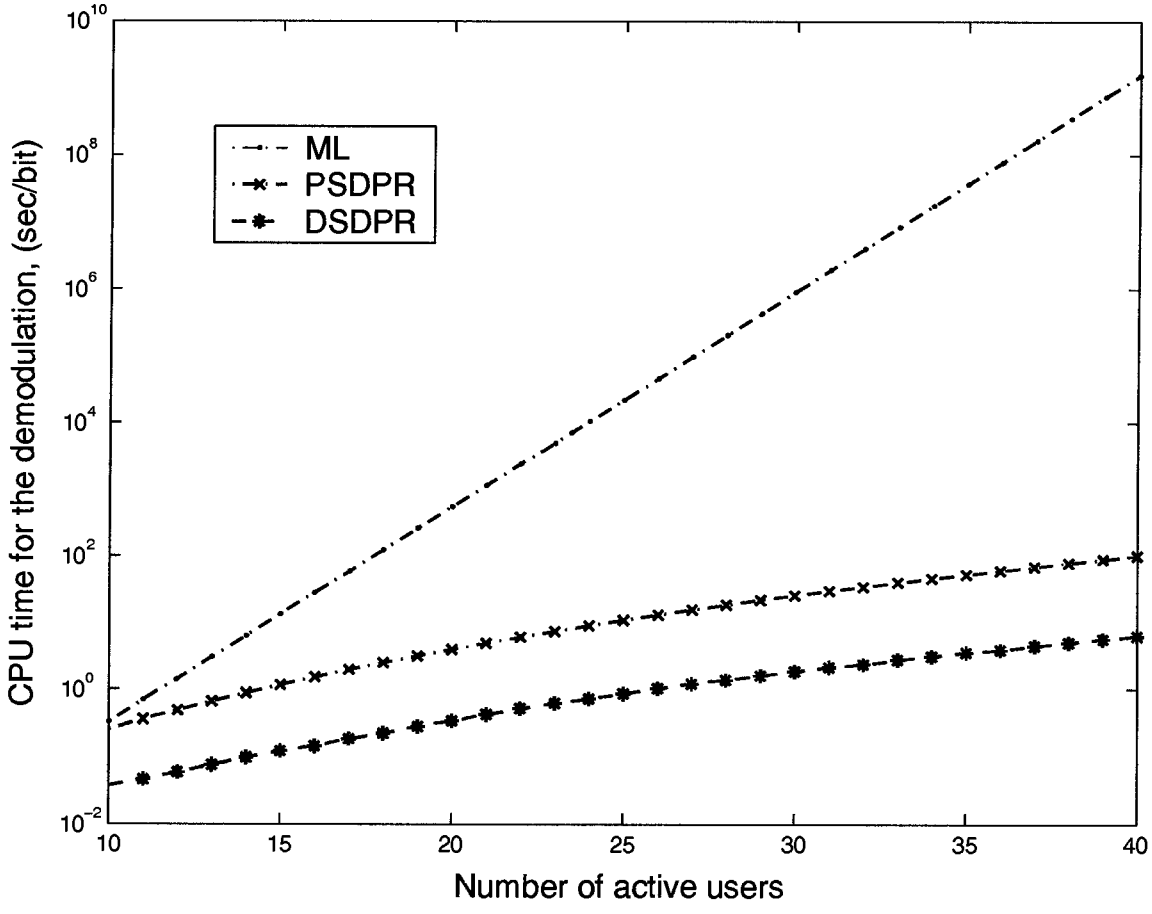

Figure 3.5. *Computational complexity of the demodulation for ML, PSDPR, DSDPR detectors.*

Chapter 4

Multiuser Detector Based on Recursive Convex Programming

4.1 Introduction

The semidefinite programming relaxation-based (SDPR) detectors proposed in Chapter 3 are obtained by relaxing the ML detection problem to other types of optimization problems that can be solved with reduced computational complexity. Other detectors of this category include the decorrelating, bound-constrained (BC), GMMSE, and linear MMSE (LMMSE) detectors (see Sec. 2.4 for more information). In these detectors, the ML detection or a modified ML detection problem is relaxed to an unconstrained, a convex quadratic programming (CQP), a convex programming (CP), or an unconstrained optimization problem, respectively [28, 59, 60]. Since it has been shown in [62] that the optimization problems associated with decorrelating, LMMSE, GMMSE, and BC detecotrs can be obtained by relaxing the SDP problem associated with the SDPR detector, it is expected that the SDPR detector offers better detection performance than these detectors.

Although the computational complexity of SDPR detectors can be reduced by using a dual algorithm, as was shown in Chapter 3, the amount of computation required in the DSDPR detector is significantly greater than that required in the decorrelating, LMMSE, GMMSE, and BC detectors, and many other suboptimal detectors

[17]. It has been shown in [62, 64] that when multiuser interference (MUI) present in DS-CDMA systems is significant, the performance of SDPR detectors degrades significantly relative to that associated with the ML detector. To overcome this problem, other types of suboptimal ML detectors with lower computational complexity and better performance should be explored.

In this chapter, a new suboptimal ML detector for DS-CDMA systems based on a *recursive convex programming* (RCP) approach is proposed. In this detector, the combinatorial problem associated with ML detection is relaxed into a convex programming (CP) problem and then a recursive approach is applied to obtain an approximate solution for the ML detection problem. Computer simulations are presented which demonstrate that this new detector offers a BER performance which is superior relative to that in many other suboptimal ML detectors. Specifically, for DS-CDMA system with strong MUI, the new detector offers better performance relative to SDPR detectors and, in addition, it requires significantly less computation than SDPR and ML detectors. Our attention is focused on synchronous DS-CDMA systems whose signal model can be found in Sec. 2.4.1.

The chapter is organized as follows. The application of CP relaxation for the ML detection problem and the proposed detector are discussed in Secs. 4.2 and 4.3, respectively. Implementation issues are investigated in Sec. 4.4. In Sec. 4.5, the proposed detector is compared with other detectors with respect to BER performance and computational complexity. Conclusions are drawn in Sec. 4.6.

4.2 Convex Relaxation of ML Detection

Recall that the relaxation for a GMMSE detector and a BC detector is carried out by expanding the discrete feasible set defined in the ML detection problem in (2.25b)

to the continuous and convex feasible regions

$$\{\mathbf{x} : \mathbf{x}^T\mathbf{x} \leq K\} \quad \text{for GMMSE detector} \tag{4.1}$$

$$\{\mathbf{x} : -1 \leq x_i \leq 1, \quad i = 1, 2, \ldots, K\} \quad \text{for BC detector} \tag{4.2}$$

With this in mind, we will examine the possibility of relaxing the ML detection problem in (2.25) into

$$\text{minimize} \quad \mathbf{x}^T\mathbf{H}\mathbf{x} + \mathbf{x}^T\mathbf{p} \tag{4.3a}$$

$$\text{subject to} : c(\mathbf{x}) \leq 0 \tag{4.3b}$$

where the feasible region, denoted as $\mathcal{R}_p$, depends on a scalar parameter $p > 0$ and is given by

$$c(\mathbf{x}, p) = |x_1|^p + |x_2|^p + \cdots + |x_K|^p - K \leq 0 \tag{4.4}$$

In what follows, the optimization problem

$$\text{minimize} \quad \mathbf{x}^T\mathbf{H}\mathbf{x} + \mathbf{x}^T\mathbf{p} \tag{4.5a}$$

$$\text{subject to} : |x_1|^p + |x_2|^p + \cdots + |x_K|^p - K \leq 0 \tag{4.5b}$$

is referred to as Problem $\mathcal{U}_p$. The following two propositions describe some properities of the feasible region defined by (4.5b).

Proposition 4.1: The feasible region defined in $\mathcal{R}_p$ includes all feasible points of the ML detection problem in (2.25). In addition, $\mathcal{R}_p$ is convex for $p \geq 1$.

Proof. By substituting in (4.5) the coordinates of each feasible point of the problem in (2.25), it is easy to verify that $c(\mathbf{x}, p) = 0$ holds for any scalar $p > 0$. Hence, all feasible points of the problem in (2.25) are on the boundary of $\mathcal{R}_p$. In other words, $\mathcal{R}_p$ includes all feasible points of the problem in (2.25).

To examine the convexity of the feasible region, note that the constraint in (4.5) can be expressed as

$$||\mathbf{x}||_p \leq K^{1/p} \tag{4.6}$$

If points $\mathbf{x}_1$ and $\mathbf{x}_2$ satisfy the constraint in (4.6), then according to the well-known *Brunn-Minkowski inequality* [97], we have

$$||\lambda\mathbf{x}_1 + (1-\lambda)\mathbf{x}_2||_p \leq \lambda||\mathbf{x}_1||_p + (1-\lambda)||\mathbf{x}_2||_p \leq K^{1/p} \tag{4.7}$$

for $0 \leq \lambda \leq 1$ and $p \geq 1$. This implies that $\mathbf{x}^* = \lambda\mathbf{x}_1 + (1-\lambda)\mathbf{x}_2$ also satisfies (4.6). Hence, the feasible region is convex for $p \geq 1$.

Proposition 4.1 implies that (a) for any fixed scalar $p > 1$, the problem in (4.5) can be regarded as a relaxation of the problem in (2.25), and (b) that it is a convex programming problem that has a unique global soltion. Note that if K in (4.5) is reduced, then all feasible points of the problem in (2.25) will be located outside $\mathcal{R}_p$ and, therefore, K is the smallest scalar required for the validity of the proposition.

Proposition 4.2: If $\mathcal{R}_m$ and $\mathcal{R}_n$ are the feasible regions defined by $c(\mathbf{x}, m) \leq 0$ and $c(\mathbf{x}, n) \leq 0$, respectively, and $m \geq n \geq 1$, then $\mathcal{R}_m \subseteq \mathcal{R}_n$. See Appendix A for the proof.

Several observations can be made based on Proposition 4.2:

Observation 1: If $m \geq n \geq 1$, the relaxation applied to problem $\mathcal{U}_m$ is tighter than the relaxation made in problem $\mathcal{U}_n$. Therefore, it is expected that the performance of a detector based on problem $\mathcal{U}_m$ would be superior to that of a detector based on problem $\mathcal{U}_n$.

Observation 2: The tightest CP relaxation problem that can be obtained from (4.5) is given by

$$\mathcal{U}_\infty = \lim_{p \to +\infty} \mathcal{U}_p \tag{4.8}$$

Hence, the performance of a detector based on problem $\mathcal{U}_\infty$ is superior to that of a detector based on any other CP relaxation problem generated by (4.5).

Observation 3: The decorrelating detector, GMMSE detector, or BC detector can be considered as a special case of the CP detector where p assumes the values of 0, 2, and ∞, respectively. Hence, as will be supported by our computer simulations,

the performance of the GMMSE detector is expected to be better then that of the decorrelating detector, and worse than that of the BC detector.

To see the equivalence of the BC detector and the detector based on problem $\mathcal{U}_\infty$, we write

$$c(\mathbf{x}, \infty) = \lim_{p\to\infty} c(\mathbf{x}, p) = \lim_{p\to\infty} [(||\mathbf{x}||_p)^p - K] \tag{4.9}$$

Hence, the feasible region defined by $c(\mathbf{x}, \infty) \leq 0$ can be expressed as

$$\left\{\mathbf{x} : ||\mathbf{x}||_\infty \leq \lim_{p\to\infty}(K^{1/p}) = 1\right\} \tag{4.10}$$

Note that the feasible region defined by (4.10) is equivalent to that defined by

$$\{\mathbf{x} : -1 \leq x_i \leq 1 \quad \text{for} \quad i = 1,\ 2,\ \ldots,\ K\} \tag{4.11}$$

which is the same as the feasible region defined in (4.2). The feasible regions defined by (2.25b) and $\mathcal{R}_p$ for $K = 2$, $p = 1, 2, 3$, and 20 are illustrated in Fig. (4.1)

4.3 Recursive CP-based Multiuser Detection

Although the performance of a $\mathcal{U}_p$-based detector can be improved by increasing the value of p, the improvement is limited by that of a $\mathcal{U}_\infty$-based detector, which is considered to offer inferior performance to that of an SDPR detector. In this section, a recursive approach is developed for the CP relaxation to improve the performance.

In the proposed approach, decisions are made only for those information bits that can be detected with high accuracy in each iteration. These bits are fixed in subsequent iterations, which leads to a CP problem of reduced size for the undetected information bits. This process is continued until the detection of all information bits is completed. In what follows, we first describe a recursive approach to ML detection and on the basis of these principles, we then introduce the recursive approach for CP relaxation-based detection.

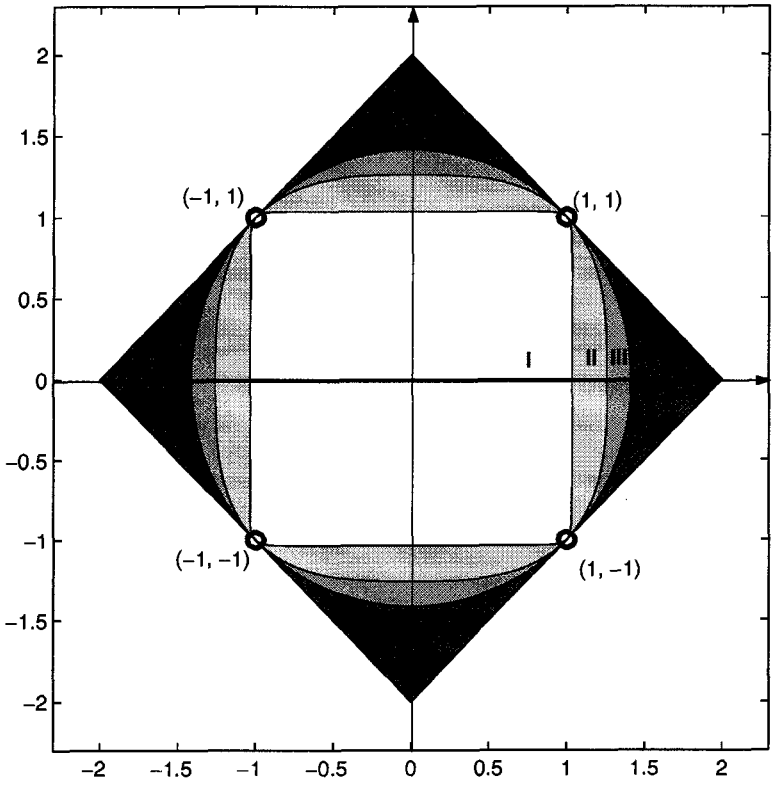

Figure 4.1. *Feasible regions defined by (4.1b) (labeled with small circles) and by (4.13b) for $p = 20$ (denoted as I), $p = 3$ (I+II), $p = 2$ (I+II+III) and $p = 1$ (I+II+III+IV).*

4.3.1 Recursive ML Approach for Multiuser Detection

Denote the set of indices associated with the information bits that have been detected before the jth iteration as Ω_j and let $\bar{b}_i$ for $i \in \Omega_j$ be the value of the ith information bit detected. By using the recursive approach, the combinatorial optimization problem in (2.25) can be modified into

$$\text{minimize} \quad \mathbf{x}^T\mathbf{H}\mathbf{x} + \mathbf{x}^T\mathbf{p} \tag{4.12a}$$

$$\text{subject to:} \quad x_i \in \{1, -1\} \quad \text{for} \quad i \notin \Omega_j \tag{4.12b}$$

$$x_i = \bar{b}_i \quad \text{for} \quad i \in \Omega_j \tag{4.12c}$$

Once the solution of the minimization problem is obtained, Ω_j is updated to Ω_{j+1} by including the indices of the information bits that are detected in the jth iteration, and a similar problem can be formulated for the rest of the information bits.

Obviously, this approach attempts to get an approximate solution for ML detection with the help of information bits obtained in previous iterations. This approach is similar to that used in decision-aided multiuser detectors such as multistage detectors, interference cancellation detectors, and decision-feedback detectors (see [17] for more details). To see the relationship between the recursive approach and these decision-aided detectors, the problem in (4.12) will now be expressed in a different but equivalent form.

Proposition 4.3: The problem in (4.12) is equivalent to

$$\text{minimize} \quad \mathbf{x}_j^T \mathbf{A}_j \mathbf{S}_j^T \mathbf{S}_j \mathbf{A}_j \mathbf{x}_j - 2\mathbf{x}_j^T \mathbf{A}_j \mathbf{S}_j^T (\mathbf{r} - \bar{\mathbf{S}}_j \bar{\mathbf{A}}_j \bar{\mathbf{b}}_j) \tag{4.13a}$$

$$\text{subject to}: \quad x_i \in \{1, -1\} \quad \text{for} \quad i \notin \Omega_j \tag{4.13b}$$

where $\mathbf{x}_j = \{x_i, i \notin \Omega_j\}$ denotes the variable vector obtained by removing the components of $\mathbf{x}$ whose indices are in Ω_j, $\bar{\mathbf{b}}_j = \{\bar{b}_i, i \in \Omega_j\}$ denotes the vector of binary bits that have been determined *before* the jth iteration, $\mathbf{r}$ is defined in (2.26), $\mathbf{A}_j$ and $\bar{\mathbf{A}}_j$ are submatrices of $\mathbf{A}$ obtained by removing the columns and rows of $\mathbf{A}$ whose indices are in Ω_j and not in Ω_j, respectively, $\mathbf{S}_j$ and $\bar{\mathbf{S}}_j$ are submatrices of $\mathbf{S}$ obtained by removing the columns of $\mathbf{S}$ whose indices are in Ω_j and not in Ω_j, respectively.

Proof. By substituting (4.12c) into (4.12a), the objective function in (4.12a) can be expressed as

$$\mathbf{x}^T \mathbf{H} \mathbf{x} + \mathbf{x}^T \mathbf{p} = \mathbf{x}_j^T \mathbf{H}_j \mathbf{x}_j + \mathbf{x}_j^T (\mathbf{p}_j + 2\tilde{\mathbf{H}}_j \bar{\mathbf{b}}_j) + const \tag{4.14}$$

where $\mathbf{p}_j$ is obtained by removing the components of $\mathbf{p}$ whose indices are in Ω_j, $\mathbf{H}_j$ and $\tilde{\mathbf{H}}_j$ denote submatrices of $\mathbf{H}$ where $\mathbf{H}_j$ is obtained by removing the rows and columns of $\mathbf{H}$ whose indices are in Ω_j, and $\tilde{\mathbf{H}}_j$ is obtained by removing the rows of $\mathbf{H}$ whose indices are in Ω_j and columns of $\mathbf{H}$ whose indices are not in Ω_j. The term

const in (4.14) is a constant associated with (4.12a), which depends on all quantities that are not related to $\mathbf{x}_j$. Note that $\mathbf{H}_j$, $\tilde{\mathbf{H}}_j$, and $\mathbf{p}_j$ can be expressed as

$$\mathbf{H}_j = \mathbf{A}_j \mathbf{S}_j^T \mathbf{S}_j \mathbf{A}_j \tag{4.15a}$$

$$\tilde{\mathbf{H}}_j = \mathbf{A}_j \mathbf{S}_j^T \bar{\mathbf{S}}_j \bar{\mathbf{A}}_j \tag{4.15b}$$

$$\mathbf{p}_j = -2\mathbf{A}_j \mathbf{S}_j^T \mathbf{r} \tag{4.15c}$$

Substituting (4.15) into (4.14), the objective function in (4.12a) can be expressed as

$$\mathbf{x}^T \mathbf{H} \mathbf{x} + \mathbf{x}^T \mathbf{p} = \mathbf{x}_j^T \mathbf{A}_j \mathbf{S}_j^T \mathbf{S}_j \mathbf{A}_j \mathbf{x}_j - 2\mathbf{x}_j^T \mathbf{A}_j \mathbf{S}_j^T \mathbf{r}_j + const \tag{4.16}$$

where $\mathbf{r}_j = \mathbf{r} - \bar{\mathbf{S}}_j \bar{\mathbf{A}}_j \bar{\mathbf{b}}_j$. Obviously, the problem in (4.12) without the constant term is equivalent to the problem in (4.13).

It can be seen from Proposition 4.3 that, in each iteration, the recursive ML approach involves two steps. First, the MUI corresponding to the determined information bits is expressed as $\bar{\mathbf{S}}_j \bar{\mathbf{A}}_j \bar{\mathbf{b}}_j$ and then subtracted from the observed signal $\mathbf{r}$. Second, an ML detection problem is formulated to facilitate the detection of the rest of the information bits. Obviously, if the decisions in $\bar{\mathbf{b}}_j$ are correct, then the MUI of these bits can be represented accurately, which helps reduce the interference observed in $\mathbf{r}_j$ and thus improve the performance in detecting the other information bits. However, if the decisions are incorrect, then the interference in $\mathbf{r}_j$ will be doubled and this may lead to a significant performance degradation.

4.3.2 RCP-Based Multiuser Detection

Due to the binary constraints in (4.12b), the problem in (4.12) is also a combinatorial problem involving fewer variables than the original ML detection problem in (2.25). In this section, we consider relaxing this problem into a CP problem. On comparing the problems in (2.25), (4.3), and (4.12), the problem in (4.12) can be relaxed into

the problem

$$\text{minimize} \quad \mathbf{x}^T\mathbf{H}\mathbf{x} + \mathbf{x}^T\mathbf{p} \tag{4.17a}$$

$$\text{subject to:} \quad c_j(\mathbf{x}, p) \leq 0 \tag{4.17b}$$

$$x_i = \bar{b}_i \quad \text{for} \quad i \in \Omega_j \tag{4.17c}$$

According to Proposition 4.3, this problem can be expressed as

$$\text{minimize} \quad \mathbf{x}_j^T\mathbf{H}_j\mathbf{x}_j + \mathbf{x}_j^T(\mathbf{p}_j + 2\tilde{\mathbf{H}}_j\bar{\mathbf{b}}_j) \tag{4.18a}$$

$$\text{subject to:} \quad c_j(\mathbf{x}_j, p) \leq 0 \tag{4.18b}$$

where $\mathbf{x}_j$ and $\mathbf{b}_j$ are defined in (4.14), $\mathbf{H}_j$, $\tilde{\mathbf{H}}_j$, and $\mathbf{p}_j$ are defined in (4.15), and $c_j(\mathbf{x}_j, p)$ is defined by

$$c_j(\mathbf{x}_j, p) = \sum_{i \notin \Omega_j} |x_{ji}|^p - k_j \tag{4.19}$$

where x_{ji} is the ith component of $\mathbf{x}_j$ and k_j is the number of variables which belong to the complementary set of Ω_j.

Once the problem in (4.18) is solved, some information bits can be determined through a thresholding process as follows: if the magnitude of a solution component is greater than a prescribed threshold, then a decision for this information bit is made according to the sign of the component; otherwise, the information bit remains to be detected in subsequent iterations.

The RCP detector can be implemented by the algorithm described in Table 4.1 where $\max(|\mathbf{x}_j^*|)$ in Step 2 denotes the greatest magnitude of the components of $\mathbf{x}_j^*$ and x_{ji}^* denotes the ith component of $\mathbf{x}_j^*$.

Table 4.1. *Recursive CP Detector*

Parameters: $n_j \geq j-1$ is the number of bits detected before the jth iteration.

Ω_j is the index set of bits detected before the jth iteration.

ξ_j is the threshold used in the jth iteration.

p is the polynomial order used in defining the feasible region.

Initialization: $j=1$, $n_1=0$, $\Omega_1 = null$, $\mathbf{H}_1 = \mathbf{H}$, $\mathbf{p}_1 = \mathbf{p}$, $\bar{\mathbf{b}}_1 = \mathbf{0}$, and $\tilde{\mathbf{H}}_1 = \mathbf{0}$

Step 1: Solve the following CP problem

$$\text{minimize:} \quad \mathbf{x}_j^T \mathbf{H}_j \mathbf{x}_j + \mathbf{x}_j^T (\mathbf{p}_j + 2\tilde{\mathbf{H}}_j \bar{\mathbf{b}}_j) \qquad (4.20a)$$

$$\text{subject to:} \quad c_j(\mathbf{x}_j, p) \leq 0 \qquad (4.20b)$$

and denote the solution as $\mathbf{x}_j^*$.

Step 2: Let $\xi_j \in [0, \max(|\mathbf{x}_j^*|)]$. For $i = 1,\ 2,\ \ldots,\ K - n_j$,

if $|x_{ji}^*| \geq \xi_j$, determine $\text{sign}(x_{ji}^*)$ as the binary decision for the information bit corresponding to x_{ji}^*.

Step 3: Denote Ω_{j+1} as the index set which includes all indices of Ω_j and those of the information bits detected in Step 2. Update n_{j+1}. If $n_{j+1} = K$, stop and output $\bar{\mathbf{b}}_j$ as the vector of all the information bits detected.

Step 4: Update $\bar{\mathbf{b}}_{j+1}$ according to (4.13), $\mathbf{H}_{j+1}$, $\tilde{\mathbf{H}}_{j+1}$, $\mathbf{p}_{j+1}$ according to (4.15) and $c_{j+1}(\mathbf{x}_{j+1}, p)$ according to (4.19). Set $j = j+1$ and repeat from Step 1.

The threshold ξ_j in Step 2 is assigned a value less than $\max(|\mathbf{x}_j^*|)$ so that at least one information bit is determined in each iteration. Consequently, all bits can be detected in at most K iterations. In general, smaller threshold values reduce the number of iterations but may degrade the performance and larger threshold values tend to improve the performance but would require more iterations. As an extreme example when ξ_j for $j = 1, 2, \ldots$ are all specified as zeros, the proposed detector degenerates into the CP detector discussed in Sec. 4.2. The effect of the threshold values on the RCP detectors will be investigated through computer simulations described in Sec. 4.5.

It has been pointed out in Sec. 4.3.1 that the recursive approach applied here is similar to the interference cancellation approaches that have been used for other decision-aided detectors (see [17] and the references therein). In these decision-aided detectors, the order of cancellation and the decisions of the information bits depend largely on the amplitudes of user signals or the outputs of the matched-filter bank. Hence, the performance of these detectors is unsatisfactory especially for DS-CDMA systems with equal-power users. In the proposed detector, however, the order of cancellation and the decisions of the information bits are based on the solution of convex programming problem. It is this property that leads to the superior performance of the proposed detector relative to those of other detectors using interference cancellation approaches.

4.3.3 Relationship Between RCP Detector and SDPR Detectors

In this section, the proposed detector is first compared with the SDPR detector. Since the DSPDR detector proposed in Chapter 3 is essentially an efficient implementation algorithm of the PSDPR detector, we compare the proposed detector with the PSDPR detector.

Recall that the SDP problem associated with the PSDPR detector is given by

$$\text{minimize} \quad \text{tr}\,(\mathbf{XH}) + \mathbf{x}^T\mathbf{p} \tag{4.21a}$$

$$\text{subject to:} \quad X_{ii} = 1 \quad \text{for} \quad i = 1, 2, \ldots, K \tag{4.21b}$$

$$\mathbf{X} \succeq \mathbf{0} \tag{4.21c}$$

and the problem in (4.17) can be expressed as

$$\text{minimize} \quad \text{tr}\,(\mathbf{XH}) + \mathbf{x}^T\mathbf{p} \tag{4.22a}$$

$$\text{subject to :} \quad c_j(\mathbf{x}, p) \leq 0 \tag{4.22b}$$

$$x_i = \bar{b}_i \quad \text{for} \quad i \in \Omega_j \tag{4.22c}$$

$$\mathbf{X} = \mathbf{x}\mathbf{x}^T \tag{4.22d}$$

In (4.22), the only variable of interest is $\mathbf{x}$. For comparison purposes, the ML detection problem in (2.25) is expressed as

$$\text{minimize} \quad \text{tr}\,(\mathbf{XH}) + \mathbf{x}^T\mathbf{p} \tag{4.23a}$$

$$\text{subject to :} \quad X_{ii} = 1 \quad \text{for} \quad i = 1, 2, \ldots, K \tag{4.23b}$$

$$\mathbf{X} = \mathbf{x}\mathbf{x}^T \tag{4.23c}$$

Comparing the above three optimization problems, it can be seen that the constraint in (4.23c) is replaced by (4.21c), which leads to an SDP problem in (4.21), while in (4.22) the constraint in (4.23c) is kept but the equality constraints in (4.23b) are replaced by those in (4.22b) and (4.22c). Hence, the SDP problem in (4.21) and the RCP problem in (4.22) represent two different ways to obtain an approximate solution for the problem in (4.23). Specifically when $p \to \infty$, the problem in (4.22) can be expressed as

$$\text{minimize} \quad \text{tr}\,(\mathbf{XH}) + \mathbf{x}^T\mathbf{p} \tag{4.24a}$$

$$\text{subject to :} \quad -1 \leq x_i \leq 1 \quad \text{for} \quad i \notin \Omega_j \tag{4.24b}$$

$$x_i = \bar{b}_i \quad \text{for} \quad i \in \Omega_j \tag{4.24c}$$

$$\mathbf{X} = \mathbf{x}\mathbf{x}^T \tag{4.24d}$$

By comparing the problems in (4.23) and (4.24), it is obvious that some equality constraints in (4.23b) are replaced by determined information bits and the others are relaxed into a bounded regions.

4.4 Improved RCP Detector

The computation required by the proposed detector is used largely in solving the CP problems, and it is more intensive than that required by linear multiuser detectors. In this section, the efficiency of the RCP detector is improved by reducing the amount of computation required in solving the CP problems. The amount of computation is critically dependent on the initial point and a good initial point usually leads to a considerable reduction in computation.

If the constraint in (4.20b) is removed, the CP problem in (4.20) becomes the following unconstrained optimization problem

$$\text{minimize}: \quad \mathbf{x}_j^T \mathbf{H}_j \mathbf{x}_j + \mathbf{x}_j^T (\mathbf{p}_j + 2\tilde{\mathbf{H}}_j \bar{\mathbf{b}}_j) \tag{4.25}$$

whose solution can be computed in closed-form as

$$\mathbf{x}_j^* = -\frac{1}{2} \mathbf{H}_j^{-1} (\mathbf{p}_j + 2\tilde{\mathbf{H}}_j \bar{\mathbf{b}}_j) \tag{4.26}$$

If the solution in (4.26) happens to satisfy the condition

$$c_j(\mathbf{x}_j^*, p) \leq 0 \tag{4.27}$$

then obviously $\mathbf{x}_j^*$ is the solution for the CP problem in (4.20). Note that the amount of computation required to obtain (4.26) is comparable to that for linear detectors, which is significantly less than that for solving the CP problem in (4.20). Motivated by this observation, the proposed detection algorithm in Table 4.1 can be improved as follows.

Table 4.2. *Improved Recursive CP Detector*

Parameters: n_j is the number of bits detected before the jth iteration.

Ω_j is the index set of bits detected before the jth iteration.

ξ_j is the threshold used in the jth iteration.

p is the polynomial order used in defining the feasible region.

Initialization: $j = 1$, $n_1 = 0$, $\Omega_1 = null$, $\mathbf{H}_1 = \mathbf{H}$, $\mathbf{p}_1 = \mathbf{p}$, $\bar{\mathbf{b}}_1 = \mathbf{0}$, and $\tilde{\mathbf{H}}_1 = \mathbf{0}$.

Step 1: Compute $\mathbf{x}_j^{\dagger} = -0.5\mathbf{H}_j^{-1}(\mathbf{p}_j + 2\tilde{\mathbf{H}}_j\bar{\mathbf{b}}_j)$ and check the constraint in (4.27).

If the constraint in (4.27) is valid, let $\mathbf{x}_j^* = \mathbf{x}_j^{\dagger}$ and go to Step 2.

Otherwise, solve the CP problem

$$\text{minimize:} \quad \mathbf{x}_j^T\mathbf{H}_j\mathbf{x}_j + \mathbf{x}_j^T(\mathbf{p}_j + 2\tilde{\mathbf{H}}_j\bar{\mathbf{b}}_j) \qquad (4.28a)$$

$$\text{subject to:} \quad c_j(\mathbf{x}_j, p) \leq 0 \qquad (4.28b)$$

using $\mathbf{x}_j^0 = \text{sign}(\mathbf{x}_j^*)$ as the initial solution.

Step 2: Let $0 \leq \xi_j \leq \min(1, \max(|\mathbf{x}_j^*|))$. For $i = 1, 2, \ldots, K - n_j$, if $|x_{ji}^*| \geq \xi_j$, determine $\text{sign}(x_{ji}^*)$ as the binary decision for the information bit corresponding to x_{ji}^*.

Step 3: Denote Ω_{j+1} as the index set which includes all indices of Ω_j and those of the information bits detected in Step 2. Update n_{j+1}. If $n_{j+1} = K$, stop and output $\bar{\mathbf{b}}_j$ as the vector of all the information bits detected.

Step 4: Compute $\bar{\mathbf{b}}_{j+1}$ according to (4.13), $\mathbf{H}_{j+1}$, $\mathbf{p}_{j+1}$, $\tilde{\mathbf{H}}_{j+1}$ according to (4.15), and $c_{j+1}(\mathbf{x}_{j+1}, p)$ according to (4.19). Set $j = j + 1$ and repeat from Step 1.

In the first step of each iteration, $\mathbf{x}_j^*$ is first computed according to (4.26) and then the constraint in (4.27) is checked for $\mathbf{x}_j^*$. If this constraint is satisfied for $\mathbf{x}_j^*$, then obtain $\mathbf{x}_j^*$ as the solution for the CP problem in (4.28) and continue with the subsequent steps; otherwise, solve the CP problem in (4.28) by using

$$\mathbf{x}_j^0 = \text{sign}(\mathbf{x}_j^*) \tag{4.29}$$

as an initial solution. Note that the components of $\mathbf{x}_j^0$ assume only binary values and thus satisfy the constraint in (4.27). The modified RCP approach is described in Table 4.2.

The following proposition will be useful to investigate the efficiency of the improved RCP detector.

Proposition 4.4: Denote the two CP problems obtained in the jth and $(j+1)$th iterations as $\mathcal{G}_j$ and $\mathcal{G}_{j+1}$ by using the improved RCP detector described in Table 4.2, i.e.,

$$\mathcal{G}_j: \quad \begin{array}{c} \text{minimize}: \quad \mathbf{x}_j^T \mathbf{H}_j \mathbf{x}_j + \mathbf{x}_j^T \left(\mathbf{p}_j + 2\tilde{\mathbf{H}}_j \bar{\mathbf{b}}_j\right) \\ \text{subject to}: \quad c_j(\mathbf{x}_j, p) \leq 0 \end{array} \tag{4.30}$$

$$\mathcal{G}_{j+1}: \quad \begin{array}{c} \text{minimize}: \quad \mathbf{x}_{j+1}^T \mathbf{H}_{j+1} \mathbf{x}_{j+1} + \mathbf{x}_{j+1}^T \left(\mathbf{p}_{j+1} + 2\tilde{\mathbf{H}}_{j+1} \bar{\mathbf{b}}_{j+1}\right) \\ \text{subject to}: \quad c_{j+1}(\mathbf{x}_{j+1}, p) \leq 0 \end{array} \tag{4.31}$$

and let the solutions of the problems $\mathcal{G}_j$ and $\mathcal{G}_{j+1}$ be $\mathbf{x}_j^*$ and $\mathbf{x}_{j+1}^*$, respectively. If the decisions of the ith information bit b_i for $i \in \Omega_{j+1}$ are all correct, $c_j(\mathbf{x}_j^*, p) < 0$, and $\xi_j < 1$, then the probability that

$$\mathbf{x}_{j+1}^* = -0.5\mathbf{H}_{j+1}^{-1}(\mathbf{p}_{j+1} + 2\tilde{\mathbf{H}}_{j+1}\bar{\mathbf{b}}_{j+1}) \tag{4.32}$$

is bounded from below by

$$\text{P}\left(\mathbf{x}_{j+1}^* = -0.5\mathbf{H}_{j+1}^{-1}(\mathbf{p}_{j+1} + 2\tilde{\mathbf{H}}_{j+1}\bar{\mathbf{b}}_{j+1})\right) \geq \prod_{i \notin \Omega_{j+1}} \text{erf}\left(\frac{1-\xi_j}{\sqrt{2}\sigma\rho_i}\right) \tag{4.33}$$

where $\text{erf}(\cdot)$ denotes the *error function* given by

$$\text{erf}(x) = \frac{2}{\sqrt{\pi}} \int_0^x e^{-t^2}\, dt \tag{4.34}$$

and ρ_i is defined by

$$\rho_i = \sqrt{\left[\left(\mathbf{H}_{j+1} - \hat{\mathbf{H}}_j(\check{\mathbf{H}}_j)^{-1}(\hat{\mathbf{H}}_j)^T\right)^{-1} - \mathbf{H}_{j+1}^{-1}\right]_{i,i}} \tag{4.35}$$

In (4.35), $\check{\mathbf{H}}_j$ is a submatrix of $\mathbf{H}_j$ obtained by removing the rows and columns of $\mathbf{H}_j$ whose indices are not in Ω_{j+1} and $\hat{\mathbf{H}}_j$ is the submatrix of $\mathbf{H}_j$ obtained by removing the rows of $\mathbf{H}_j$ whose indices are in Ω_{j+1} and the columns of $\mathbf{H}_j$ whose indices are not in Ω_{j+1}. See Appendix B for proof.

As can be seen from (4.33) and (4.35), the lower bound of the probability for which (4.32) is valid is related to the signature waveforms, the SNR of the received signals, and the threshold used in each iteration of the proposed approach. By using the *Matrix Inverse Lemma* [34], the quality in (4.35) can be expressed as

$$(\mathbf{H}_{j+1} - \hat{\mathbf{H}}_j\check{\mathbf{H}}_j^{-1}\hat{\mathbf{H}}_j^T)^{-1} - \mathbf{H}_{j+1}^{-1} = -\mathbf{H}_{j+1}^{-1}\hat{\mathbf{H}}_j(\hat{\mathbf{H}}_j^T\mathbf{H}_{j+1}^{-1}\hat{\mathbf{H}}_j + \check{\mathbf{H}}_j^{-1})^{-1}\hat{\mathbf{H}}_j^T\mathbf{H}_{j+1}^{-1} \tag{4.36}$$

Note that $\mathbf{H}_{j+1}$, $\hat{\mathbf{H}}_j$, and $\check{\mathbf{H}}_j$ describe unnormalized crosscorrelation and autocorrelation properties of the signature waveforms. Hence, when near-orthogonal signature waveforms are used for all users and the SNR of the received signal for each user is high, it can be shown that ρ_i for $i \in \Omega_{j+1}$ in (4.35) are very close to zero. In such a case, the probability bound in (4.33) can be close to one if small thresholds ξ_j is used in each step. On the other hand, although the probability in (4.33) is obtained by assuming that no detection errors for the binary decisions, when the SNR of the received signal is high, the probability of error-free detection is close to one. Therefore, the probability lower bound in (4.33) can be used to approximate the error probability lower bound without assuming that the detected information bits b_i for $i \in \Omega_{j+1}$ are all correct.

Based on Proposition 4.4 and the above discussion, we can draw a conclusion that if the constraint of the CP problem in the jth iteration of the RCP approach is inactive, then the probability that $\mathbf{x}_{j+1}^*$ can be correctly computed using (4.32) is close to one. Consequently, the amount of computation required for solving the

CP problems in (4.28) can be reduced to that for computing (4.32). In other words, the efficiency of the RCP detector can be improved by adopting the modifications described in Table 4.2 without impairing the performance. Before ending this section, it is stressed that the approach in Table (4.2) is proposed in order to reduce the computational complexity of the RCP detector only. In other words, this approach will not affect the detection performance of the RCP detectors.

4.5 Simulation Results

Computer simulations were conducted to evaluate the performance of the improved RCP detector in terms of BER and computational complexity. Comparisons with several other suboptimal detectors as well as the ML detector defined in Sec. 3.4 were also carried out. Since the DSDPR detetor offers similar performance as that of the PSDPR detector but with less computation, the RCP detector is only compared with the DSDPR detector in our simulations. For a better comparison of the performance of the DSDPR and RCP detectors, DS-CDMA systems subject to significant MUI were considered. In the simulations, the thresholds used in the RCP detectors were assumed to be

$$\xi_j = \alpha \cdot \min\left(1, \max(|\mathbf{x}_j^*|)\right) \qquad \text{for } j = 1,\ 2, \ldots \tag{4.37}$$

where α is a positive scalar which was assigned the values 0.95, 0.80, 0.50 in the simulation.

In the first example, we considered a seven-user synchronous DS-CDMA system with AWGN channel by assuming equal signal power for all users. The crosscorrela-

tion matrix for these users is

$$\mathbf{R} = \begin{bmatrix} 1 & -0.24 & 0.33 & -0.08 & 0.10 & 0.41 & -0.39 \\ -0.24 & 1 & -0.32 & 0.27 & -0.07 & -0.30 & -0.52 \\ 0.33 & -0.32 & 1 & -0.07 & 0.07 & 0.29 & -0.12 \\ -0.08 & 0.27 & -0.07 & 1 & 0.30 & -0.45 & 0.09 \\ 0.10 & -0.07 & 0.07 & 0.30 & 1 & -0.02 & -0.04 \\ 0.41 & -0.30 & 0.29 & -0.45 & -0.02 & 1 & 0.07 \\ -0.39 & -0.52 & -0.12 & 0.09 & -0.04 & 0.07 & 1 \end{bmatrix} \tag{4.38}$$

The BERs averaged for seven users (over 10^5 runs) with $p = 2$ (denoted as RCP-2), $p = 10$ (denoted as RCP-10), and $p \to \infty$ (denoted as RCP-∞) are plotted in Figs. 4.2-4.4. For comparison purposes, the averaged BERs of the ML, DSDPR, GMMSE, BC, LMMSE, and SIC detectors are also plotted. As can be observed from Figs. 4.2 to 4.4, the average BERs of the RCP-2, RCP-10, and RCP-∞ detectors are very close to each other, and very close to that of the ML detector. This indicates that the performance of the RCP detector is insensitive to the value of p. In addition, it can be observed that the reduction of α only introduced slight degradation in the BER performance when α is above 0.5. Figs. 4.2 to 4.4 also show that the average BERs in the RCP detectors are superior relative to that in the DSDPR, GMMSE, BC, LMMSE, and SIC detectors.

In the second example, we considered a fifteen-user synchronous DS-CDMA system with AWGN channel where the received signal power of each user was assumed to be log-normally distributed random variables with logrithmitic variance of 10. The signature sequences were 31-chip random sequences which were normalized to unit norm. The thresholds used for the RCP detector were determined in the same way as those in the first example with α assuming the values 0.95, 0.8, 0.5, 0.3. The BERs averaged for fifteen users (over 10^5 runs) of the RCP detector with $p = 2$, $p = 10$, and $p \to \infty$ are plotted in Figs. 4.5 to 4.8. Note that the BER of the ML detector is not plotted in these figures since its evaluation would involve extremely large amount

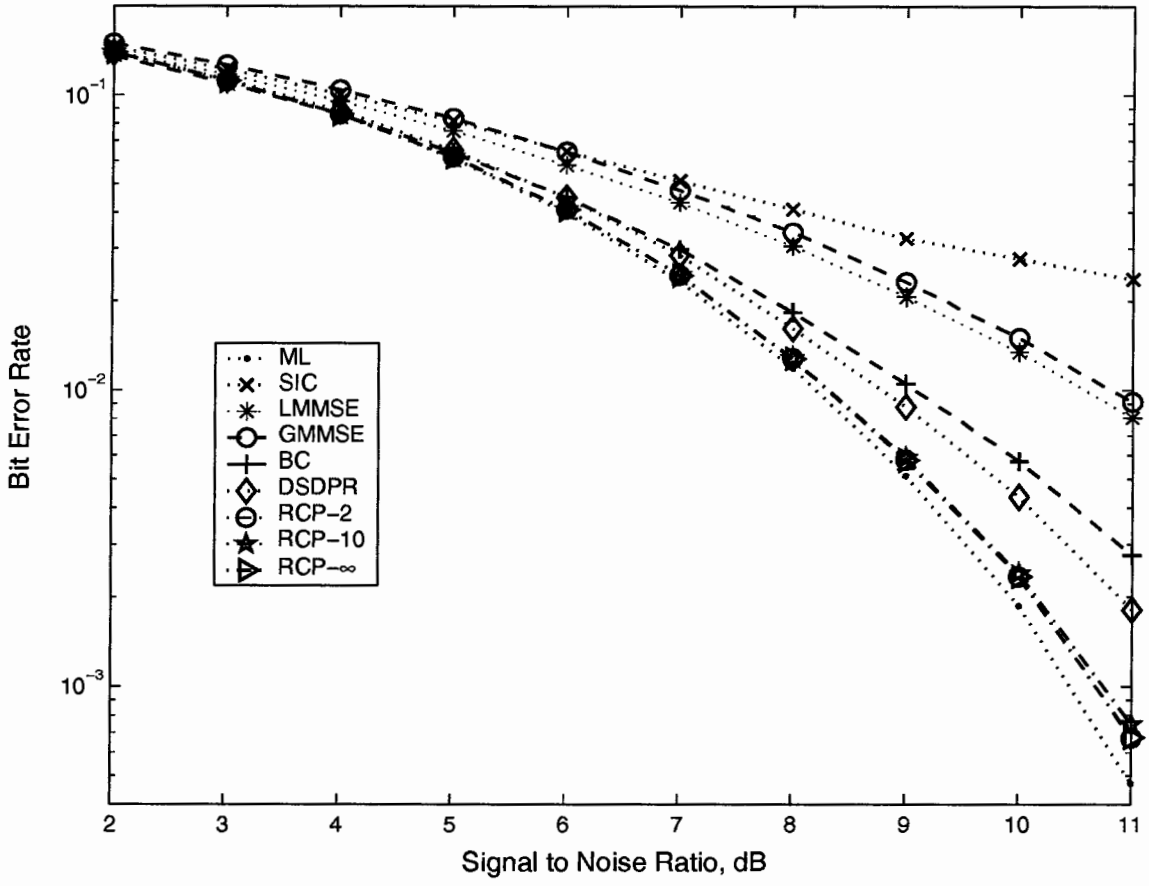

Figure 4.2. *BERs of the seven-user system for* $\alpha = 0.95$.

of computation. As can be seen in Figs. 4.5 to 4.8, the BER performance offered by the RCP detector is superior relative to that offered by the other suboptimal detectors. In addition, the BER performance of the RCP detector is insensitive to p but is slightly sensitive to α.

The computational complexity of the ML, the DSDPR, and the RCP detectors by using the improved algorithms in Table 4.2 were evaluated in terms of the CPU time for different numbers of users. The results obtained are plotted in Fig. 4.9. As can be seen, the computational complexity of the RCP detector is significantly lower than those of the ML and SDPR detectors when the number of users is large.

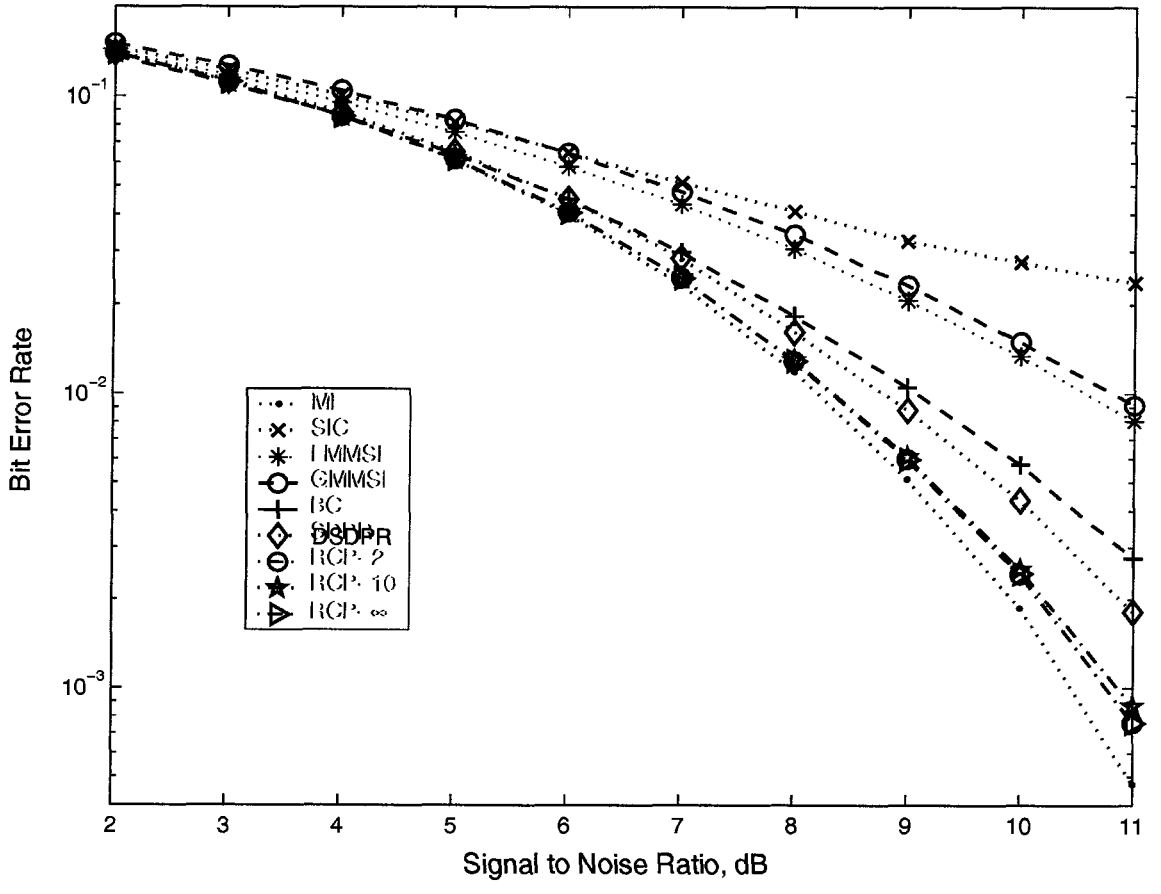

Figure 4.3. *BERs of the seven-user system for* $\alpha = 0.80$.

4.6 Conclusions

A new RCP-based detector has been proposed. In this detector, the combinatorial problem associated with the ML detector is relaxed into a convex programming problem which is then implemented in terms of a recursive approach. An efficient implementation of the RCP detector has been developed and a theoretical analysis of its efficiency has been presented. Computer simulations show that the RCP detector offers near-optimal performance and is superior to many existing suboptimal detectors. On the other hand, the computation complexity associated with the RCP detector is significantly lower than that for the ML and SDPR detectors.

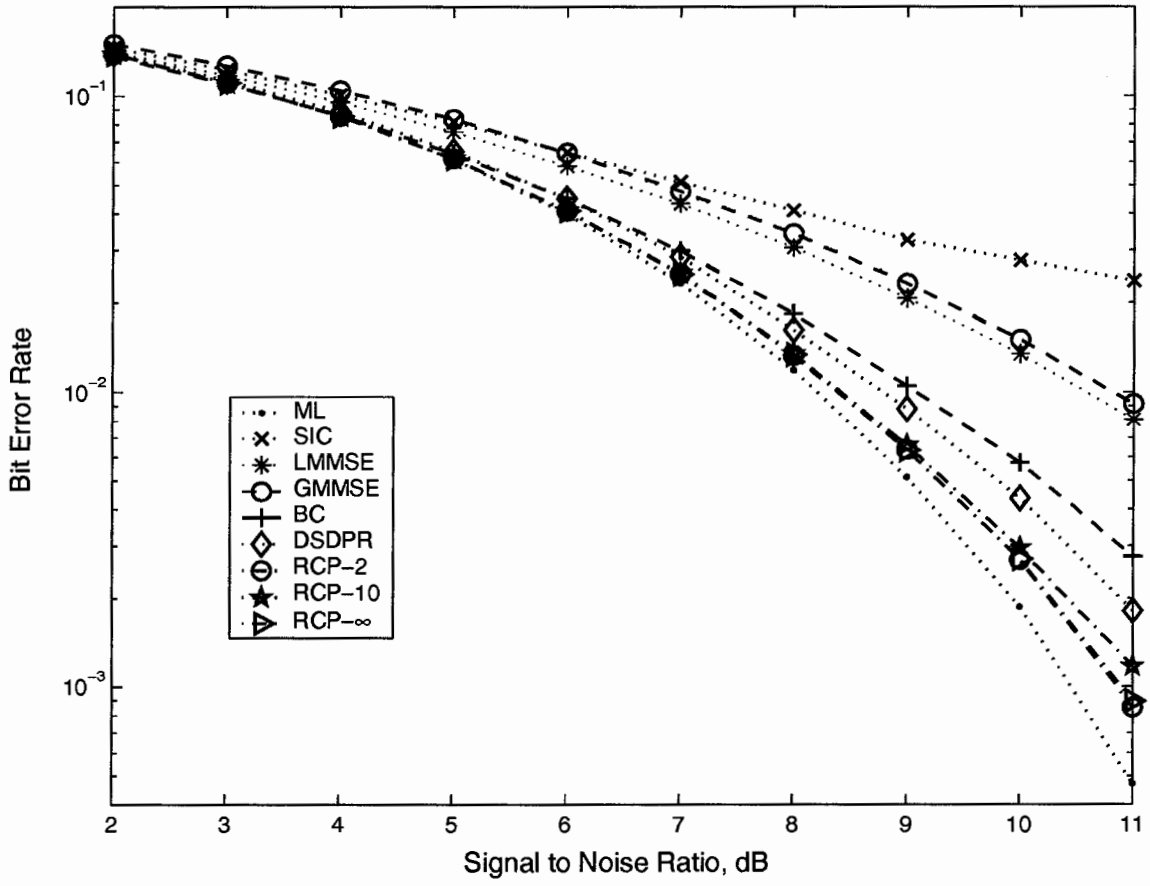

Figure 4.4. *BERs of the seven-user system for* $\alpha = 0.50$.

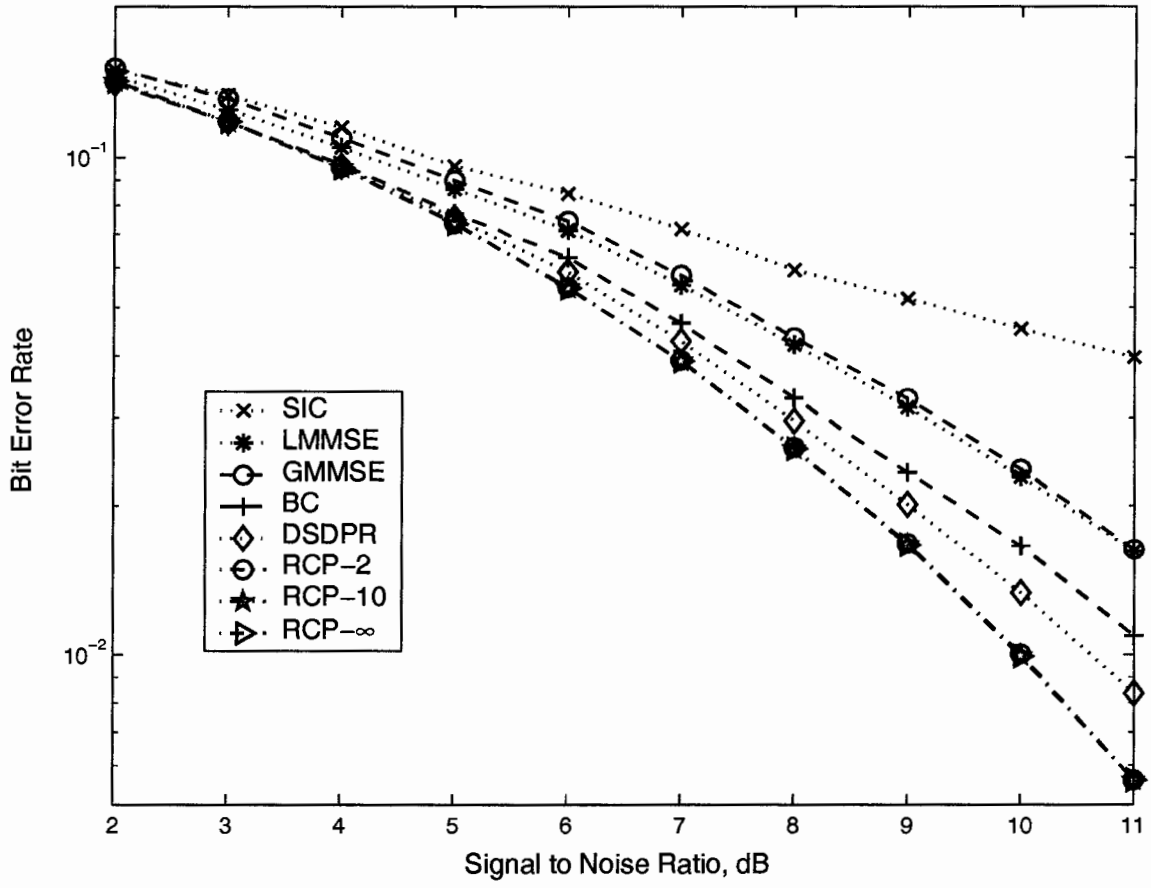

Figure 4.5. *BERs of the fifteen-user system for* $\alpha = 0.95$.

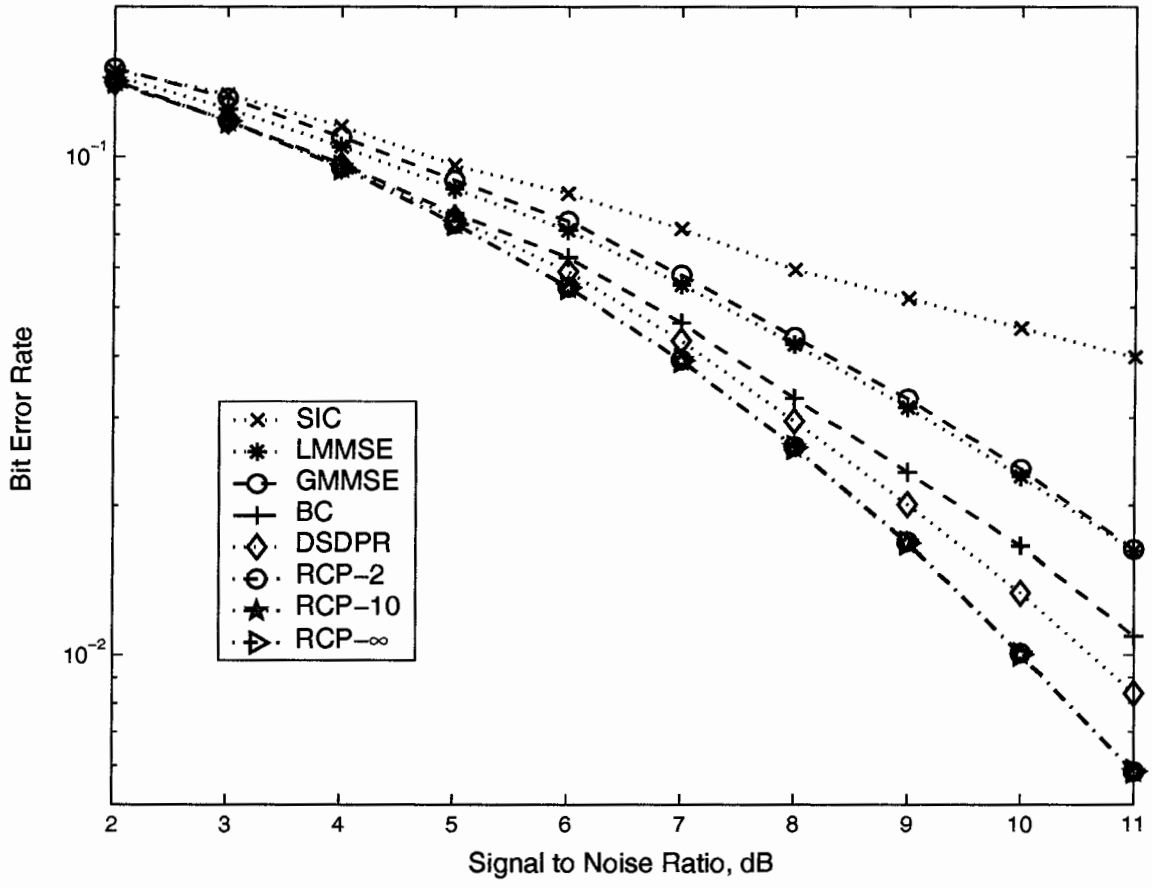

Figure 4.6. *BERs of the fifteen-user system for* $\alpha = 0.80$.

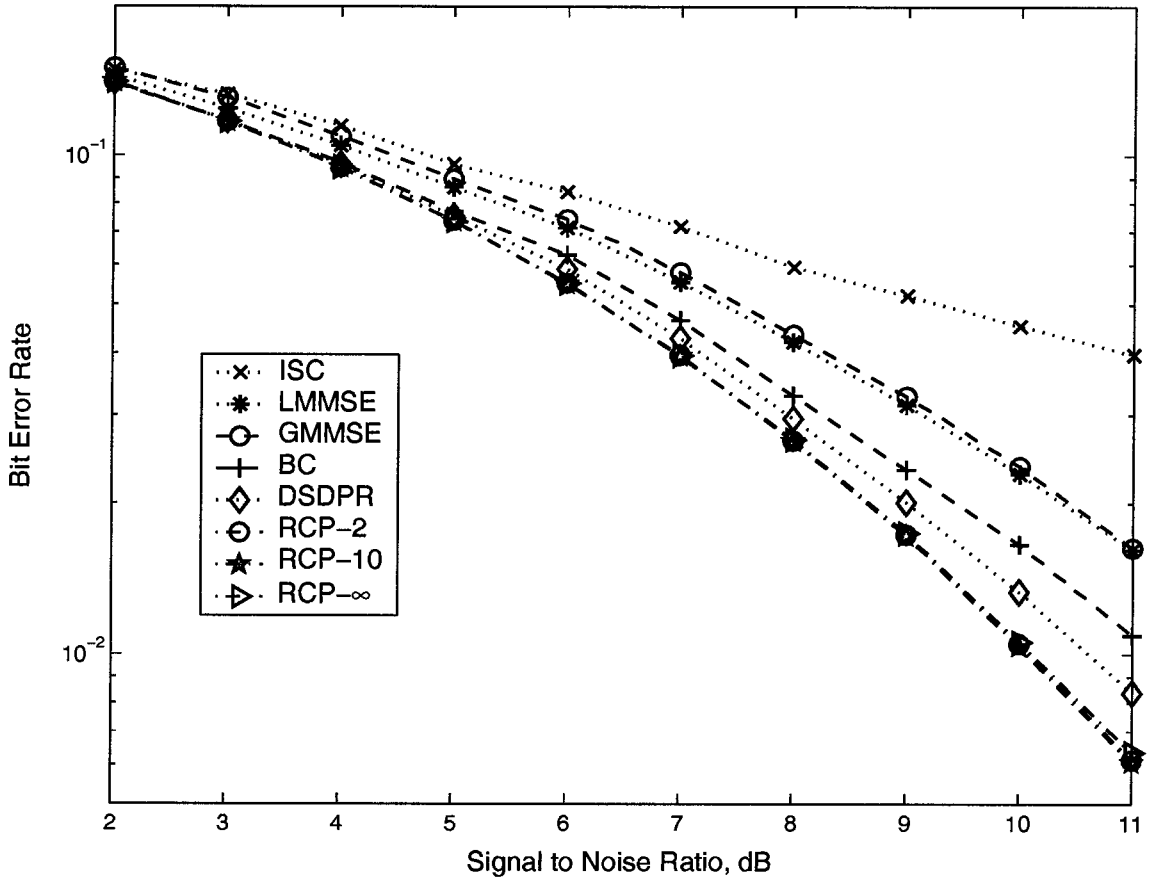

Figure 4.7. *BERs of the fifteen-user system for* $\alpha = 0.50$.

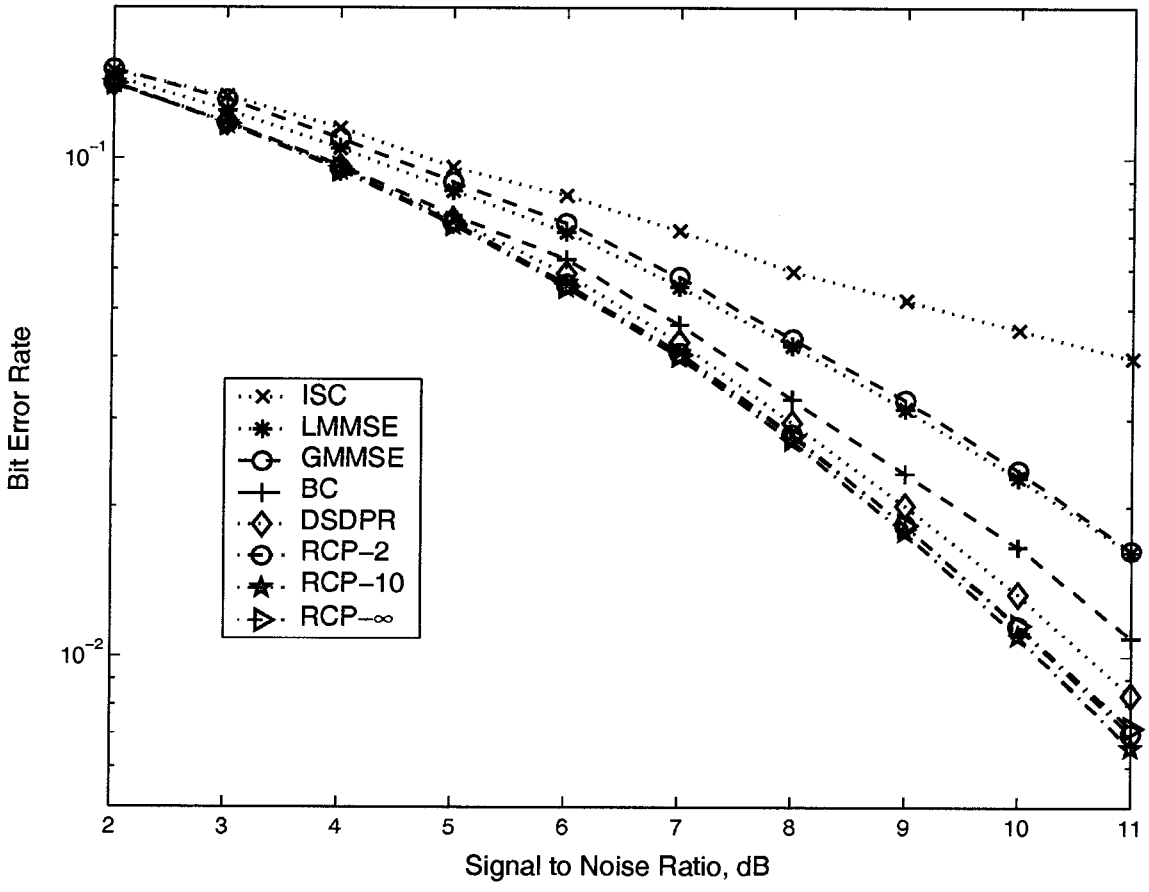

Figure 4.8. *BERs of the fifteen-user system for* $\alpha = 0.30$.

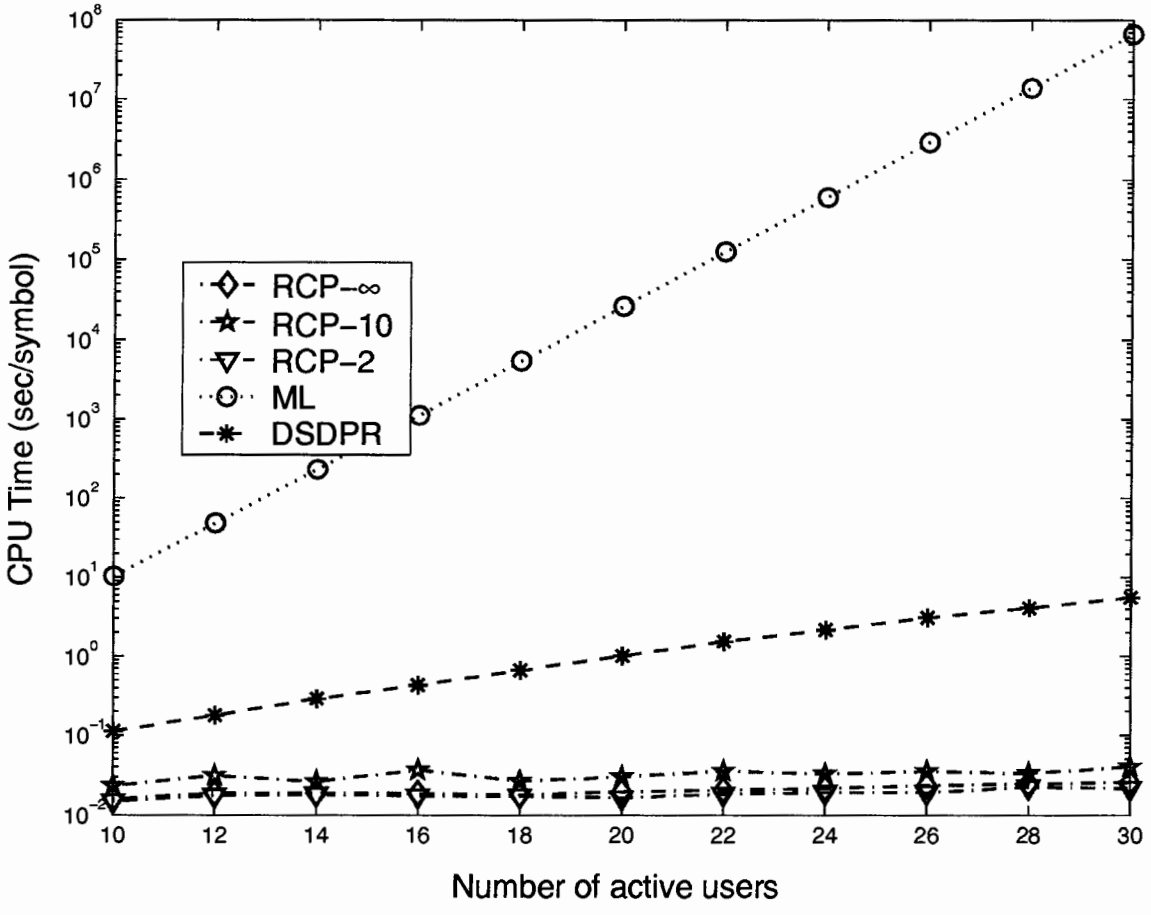

Figure 4.9. *Computational complexity of various detectors.*

Chapter 5

Subspace Estimation Based Multiuser Detector for Multipath DS-CDMA Channels

5.1 Introduction

The multiuser detectors proposed in the previous two chapters are intended for the receivers at base stations where the required information such as signature waveforms, amplitudes, and transmission delays of the signals of all users is available and the detection is performed for the signals of all users. At mobile stations, however, information pertaining to other user signals may not be available and detection is usually required only for the signal of a desired user. Hence, multiuser detectors that are suitable for base stations are not suitable for mobile receivers and alternative multiuser detectors have to be considered.

As has been shown in Chapter 2, linear detectors such as the decorrelating and MMSE detectors can be implemented in a decentralized form by implicitely exploiting the information of interference signals, and these detectors can be implemented in adaptive form through the use of training sequences [31, 32]. A notable progress in the development of decentralized multiuser detectors was made by Honig *et al.* [35] based on the observation that multiuser interference (MUI) can to a large extent

be suppressed if the energy of a linearly transformed output is minimized under the constraint that the inner product of the received signal and the signature sequence of the desired user is a constant. A detector obtained on the basis of this principle is called the *constrained minimal-output-energy* (CMOE) detector and its adaptive implementation can be achieved without the help of a training sequence. Compared with other detectors, the adaptive CMOE detector is of particular importance primarily for three reasons: first, it offers improved demodulation performance relative to the conventional matched-filter (MF) detector, second, the detection can be carried out without using extra information, and third, system capacity can be improved especially in fading channels where frequent training is required for tracking the variation of channel conditions.

In typical mobile systems, the signal bandwidth is usually larger than the conherence bandwidth. Consequently, transmitted signals often experience multipath propagation and, as a result, the effective signatures observed at the receiver are very likely to be distorted and hence may not be recognized. Simulation results presented in [35] have shown that the performance of the CMOE detector is very sensitive to distortion of the effective signatures caused by multipath propagation (or frequency-selective fading). One possible remedy for this problem is to first estimate the impulse responses of the unknown multipath channels, then to reconstruct the effective signature of the desired user, and after that perform CMOE detection by using the effective signature. This idea has been pursued by several researchers using subspace methods [40, 41] and constrained optimization methods [42, 43, 44] to estimate the channel impulse response for the desired user. As has been shown in Sec. 2.4.2.3, although subspace methods provide better estimates for the impulse response of the unknown channel than constrained optimization methods, especially in very noisy channels, they usually require more computation which could become a burden in some applications.

In this chapter, we propose a constrained optimization method based on subspace

estimation for the estimation of the channel impulse response in CDMA systems. A key difference between subspace methods and constrained optimization methods is the way the noise subspace is approximated. In the proposed method, the approximation of the noise subspace is improved by estimating the least eigenvalue of the data correlation matrix. It is demonstrated that the proposed method can achieve nearly the same performance as subspace methods [40, 41] with much reduced computational complexity. Compared with existing constrained optimization methods [42, 43, 44], our method offers a much improved performance while requiring a comparable amount of computation. The signal model used in this chapter is the same as that in Sec. 2.4.2.3.

The rest of the chapter is organized as follows. In Sec. 5.2, the relationship between subspace methods and constrained optimization methods is examined. In Sec. 5.3, a constrained optimization method is proposed for the evaluation of the channel impulse response based on a new subspace estimation technique which is then used to develop a new subspace estimation based detector (SED). Computer simulations are described in Sec. 5.4 and Sec. 5.5 summarizes the main results.

5.2 Relationship between Subspace Methods and Constrained Optimization Methods

Recall that the optimization problems involved in subspace methods and constrained optimization problem are

$$\text{minimize} \quad \mathbf{g}_1^H \mathbf{S}_1^H \hat{\mathbf{U}}_n \hat{\mathbf{U}}_n^H \mathbf{S}_1 \mathbf{g}_1 \tag{5.1a}$$

$$\text{subject to:} \quad ||\mathbf{g}_1|| = 1 \tag{5.1b}$$

and

$$\underset{\mathbf{g}_1}{\text{minimize}} \; \mathbf{g}_1^H \mathbf{S}_1^H \hat{\mathbf{R}}^{-1} \mathbf{S}_1 \mathbf{g}_1 \tag{5.2b}$$

$$\text{subject to:} \quad ||\mathbf{g}_1|| = 1 \tag{5.2c}$$

respectively where the first user is deemed to be the user of interest. The above two problems have an interesting relation. To see this, note that $\hat{\mathbf{R}}^{-1}$ in (2.50) can be expressed as [42]

$$\hat{\mathbf{R}}^{-1} = \hat{\mathbf{U}}_s \mathbf{D} \hat{\mathbf{U}}_s^H + \frac{1}{\sigma_v^2} \hat{\mathbf{U}}_n \hat{\mathbf{U}}_n^H \tag{5.3}$$

where

$$\mathbf{D} = \text{diag}\left\{ \frac{1}{\lambda_1 + \sigma_v^2}, \frac{1}{\lambda_2 + \sigma_v^2}, \cdots, \frac{1}{\lambda_\xi + \sigma_v^2} \right\} \tag{5.4}$$

This implies that

$$\sigma_v^2 \hat{\mathbf{R}}^{-1} = \hat{\mathbf{U}}_s \mathbf{M} \hat{\mathbf{U}}_s^H + \hat{\mathbf{U}}_n \hat{\mathbf{U}}_n^H \tag{5.5}$$

where

$$\mathbf{M} = \sigma_v^2 \mathbf{D} = \text{diag}\left\{ \frac{\sigma_v^2}{\lambda_1 + \sigma_v^2}, \frac{\sigma_v^2}{\lambda_2 + \sigma_v^2}, \cdots, \frac{\sigma_v^2}{\lambda_\xi + \sigma_v^2} \right\} \tag{5.6}$$

As a result,

$$\begin{aligned} \lim_{\sigma_v^2 \to 0} \sigma_v^2 \hat{\mathbf{R}}^{-1} &= \lim_{\sigma_v^2 \to 0} \sigma_v^2 \sum_{i=1}^{\xi} \frac{\hat{\mathbf{u}}_{s,i} \hat{\mathbf{u}}_{s,i}^H}{\lambda_i + \sigma_v^2} + \hat{\mathbf{U}}_n \hat{\mathbf{U}}_n^H \\ &= \hat{\mathbf{U}}_n \hat{\mathbf{U}}_n^H \end{aligned} \tag{5.7}$$

where $\hat{\mathbf{u}}_{s,i}$ is the eigenvector associated with λ_i. Consequently, (5.7) indicates that when the channel noise is insignificant (i.e., σ_v^2 is small), $\hat{\mathbf{R}}^{-1}$ would be a good approximation of $\hat{\mathbf{U}}_n \hat{\mathbf{U}}_n^H$ to within a scalar multiplier. In other words, the solutions obtained by solving the problems in (5.1) and (5.2) would be very close to each other when σ_v^2 is small. On the other hand, if σ_v^2 is large, the solution of the problem in (5.2) can only be a degraded version of that in (5.1). For this reason, constrained optimization methods can be viewed as modified subspace methods.

In an effort to improve the performance of constrained optimization methods, matrix $\hat{\mathbf{U}}_n \hat{\mathbf{U}}_n^H$ was replaced by $\hat{\mathbf{R}}^{-1} - \beta \mathbf{I}$ in [43] where β is the reciprocal of the largest eigenvalue of $\hat{\mathbf{R}}$. However, for systems with strong MAI, the value of β becomes very small which leads to a limited performance improvement.

5.3 Constrained Optimization Method Based on Subspace Estimation

It was found out in Sec. 5.2 that the quality of estimation of the channel impulse response is largely determined by the accuracy of the approximating matrix $\hat{\mathbf{U}}_n\hat{\mathbf{U}}_n^H$ used in (5.1a). In this section, we propose a new way for obtaining an approximation for this crucial matrix.

We start by subtracting a scaled identity matrix $\alpha\mathbf{I}$ from the data correlation $\mathbf{R}$, which yields

$$\mathbf{R} - \alpha\mathbf{I} = [\mathbf{U}_s\mathbf{U}_n]\begin{bmatrix} \mathbf{\Lambda}_s & \mathbf{0} \\ \mathbf{0} & \mathbf{0} \end{bmatrix}\begin{bmatrix} \mathbf{U}_s^H \\ \mathbf{U}_n^H \end{bmatrix} + (\sigma_v^2 - \alpha)\mathbf{I} \tag{5.8}$$

If $\alpha < \sigma_v^2$, then matrix $\mathbf{R} - \alpha\mathbf{I}$ remains positive definite and its inverse is given by

$$(\mathbf{R} - \alpha\mathbf{I})^{-1} = \mathbf{U}_s\mathbf{E}\mathbf{U}_s^H + \frac{1}{\sigma_v^2 - \alpha}\mathbf{U}_n\mathbf{U}_n^H \tag{5.9}$$

where

$$\mathbf{E} = \text{diag}\left\{\frac{1}{\lambda_1 + \sigma_v^2 - \alpha}, \frac{1}{\lambda_2 + \sigma_v^2 - \alpha}, \cdots, \frac{1}{\lambda_\xi + \sigma_v^2 - \alpha}\right\} \tag{5.10}$$

Upon multiplying both sides of (5.9) by $(\sigma_v^2 - \alpha)$, we obtain

$$(\sigma_v^2 - \alpha)(\mathbf{R} - \alpha\mathbf{I})^{-1} = \mathbf{U}_s\mathbf{N}\mathbf{U}_s^H + \mathbf{U}_n\mathbf{U}_n^H \tag{5.11}$$

where $\mathbf{N} = (\sigma_v^2 - \alpha)\mathbf{E}$. If we use $\alpha \to \sigma_v^{2-}$ to denote a limiting process where α approaches σ_v^2 from the left side of the real axis, then (5.11) implies that

$$\begin{aligned} \lim_{\alpha \to \sigma_v^{2-}} (\sigma_v^2 - \alpha)(\mathbf{R} - \alpha\mathbf{I})^{-1} &= \lim_{\alpha \to \sigma_v^{2-}} (\sigma_v^2 - \alpha)\sum_{i=1}^{\xi} \frac{\mathbf{u}_{s,i}\mathbf{u}_{s,i}^H}{\lambda_i + \sigma_v^2 - \alpha} + \mathbf{U}_n\mathbf{U}_n^H \\ &= \mathbf{U}_n\mathbf{U}_n^H \end{aligned} \tag{5.12}$$

Equation (5.12) shows that if we can estimate the variance of the channel noise, σ_v^2, and choose a constant α which is close to but less than σ_v^2, then the matrix $\mathbf{U}_n\mathbf{U}_n^H$

can be well approximated by $(sigma_v^2 - \alpha)(\mathbf{R} - \alpha\mathbf{I})^{-1}$ to within a scalar multiplier. Note that the introduction of parameter α in (5.12) allows one to use $(\mathbf{R} - \alpha\mathbf{I})^{-1}$ to approximate the noise subspace accurately for a wide range of noise variance values. It is because of this property that the performance of a detector based on subspace estimation is comparable with that of the subspace methods in [40, 41] even for very noisy channels. Concerning computational complexity, since σ_v^2 is the least eigenvalue of $\mathbf{R}$, which can be computed efficiently by using, for example, the inverse-power method [77], the eigenvalue decomposition of $\mathbf{R}$ can be avoided.

In practice, $\mathbf{R}$ is usually not available but can be approximated by using a *moving average* estimation based on the J most recent observations as

$$\hat{\mathbf{R}} = \frac{1}{J} \sum_{j=i-J+1}^{i} \mathbf{y}(j)\mathbf{y}^H(j), \tag{5.13}$$

This method entails computing the least eigenvalue of matrix $\hat{\mathbf{R}}$, denoted as γ_0. Then α is chosen to be close to but less than γ_0 to within a certain tolerance so as to avoid numerical difficulties in the matrix inversion. Next, matrix $(\hat{\mathbf{R}} - \alpha\mathbf{I})^{-1}$ is used in a constrained optimization method. The channel impulse response can then be estimated as the solution of the optimization problem

$$\text{minimize} \quad \mathbf{g}_1^H \mathbf{S}_1^H (\hat{\mathbf{R}} - \alpha\mathbf{I})^{-1} \mathbf{S}_1 \mathbf{g}_1 \tag{5.14a}$$

$$\text{subject to:} \quad ||\mathbf{g}_1||^2 = 1 \tag{5.14b}$$

Obviously, the solution $\hat{\mathbf{g}}_1$ in (5.14) is the eigenvector of $\mathbf{S}_1^H(\mathbf{R} - \alpha\mathbf{I})^{-1}\mathbf{S}_1$ associated with its least eigenvalue. Through an approach similar to that presented in [42], it can be shown that the channel impulse response estimate is related to the noise power and constant α in terms of the relation

$$\hat{\mathbf{g}}_1 = \frac{\mathbf{g}_1}{||\mathbf{g}_1||} - (\gamma_0 - \alpha)\mathbf{A}_0^\dagger \mathbf{A}_1 \frac{\mathbf{g}_1}{||\mathbf{g}_1||} + O[(\gamma_0 - \alpha)^2] \tag{5.15}$$

where $\dagger$ denotes the pseudo-inverse, and $\mathbf{A}_0$ and $\mathbf{A}_1$ are given by

$$\mathbf{A}_0 = \mathbf{S}_1^H \hat{\mathbf{U}}_n \hat{\mathbf{U}}_n^H \mathbf{S}_1 \tag{5.16}$$

$$\mathbf{A}_1 = \mathbf{S}_1^H \hat{\mathbf{U}}_s \hat{\mathbf{\Lambda}}_s^{-1} \hat{\mathbf{U}}_s^H \mathbf{S}_1 \tag{5.17}$$

where matrices $\hat{\mathbf{\Lambda}}_s$ and $\hat{\mathbf{U}}_s$ are the counterparts of $\mathbf{\Lambda}_s$ and $\mathbf{U}_s$ defined in (2.47), respectively. After $\mathbf{g}_1$ is obtained, the linear transformation vector for blind multiuser detector can be obtained as

$$\mathbf{w}_1 = \hat{\mathbf{R}}^{-1}\mathbf{S}_1(\mathbf{S}_1^H\hat{\mathbf{R}}^{-1}\mathbf{S}_1)^{-1}\mathbf{g}_1^* \tag{5.18}$$

A detector based on the above method referred to as the subspace estimation based detector is as follows:

i) Obtain the estimated data correlation matrix $\hat{\mathbf{R}}$ using (5.13).

ii) Compute the least eigenvalue of $\hat{\mathbf{R}}$ denoted as γ_0.

iii) Choose α close to but less than γ_0 and compute $(\hat{\mathbf{R}} - \alpha\mathbf{I})^{-1}$.

iv) Obtain $\mathbf{g}_1$ by solving the optimization problem in (5.14).

v) Form detection vector $\mathbf{w}^*$ using (5.18) and determine the transmitted information bits of the first user as

$$\hat{b} = \text{sign}\left[\text{Re}\left(\mathbf{w}_1^H\mathbf{y}\right)\right] \tag{5.19}$$

5.4 Simulations

Computer simulations were performed to examine the performance of the proposed detector with respect to the estimation of channel impulse responses, and to compare it with that of the detector using subspace method (SM) described in [40, 41] and the detector using constrained optimization methods (COM) described in [42, 43, 44]. Gold sequences of length 31 were used as spreading sequences. The impulse responses of the channels for all users were randomly generated and assumed to have a maximum order of 4. The channel estimation performance was measured in terms of the averaged mean-squared-error (MSE) of the estimated channel impulse responses and their true values.

In the first example, we considered a 10-user CDMA synchronous system where each interference user was 40 dB stronger than the desired user and the signal-to-noise

ratio varied from -20 dB to 20 dB. The constant α in (5.14a) was assumed to be $0.999\gamma_0$ where γ_0 is the lowest eigenvalue of $\hat{\mathbf{R}}$. The MSE (averaged over 10^3 runs) of the estimation of the channel impulse response is plotted in Fig. 5.1. As expected, all detectors offer almost the same performance when the SNR of the channel is very high (about 20 dB) because the noise subspace can be accurately obtained. When the SNR of the channel is low, however, the performance of the SED is close to that of the SM detector, which is much better than that of the COM detector.

In the second example, the role of parameter α in (5.14a) was investigated. The simulation environment was the same as in the first example except that each interference user was 10 dB stronger than the desired user. The parameter α assumed the values $\alpha_m = (1-10^{-0.5m})\cdot\gamma_0$ for $m = 1,\ 2,\ \ldots,\ 7$. The MSE obtained (averaged over 10^2 runs) is plotted in Fig. 5.2. It is obvious that the closer α is to 1, the lower is the MSE in the estimation. A good value of α can be determined based on information about the approximation accuracy of matrix $\hat{\mathbf{R}}$.

5.5 Conclusions

A new multiuser detector based on subspace estimation has been proposed for DS-CDMA systems with multipath fading channels. It has been shown the proposed detector offers robust performance with respect to channel estimation in both high and low SNR white Gaussian noise channels. It has been demonstrated that the performance of the proposed detector is comparable with that of some known detectors using subspace methods while requiring a much reduced computational complexity. Relative to some known detectors that use constrained optimization methods, our detectors offer a significantly improved performance while requiring a comparable amount of computation.

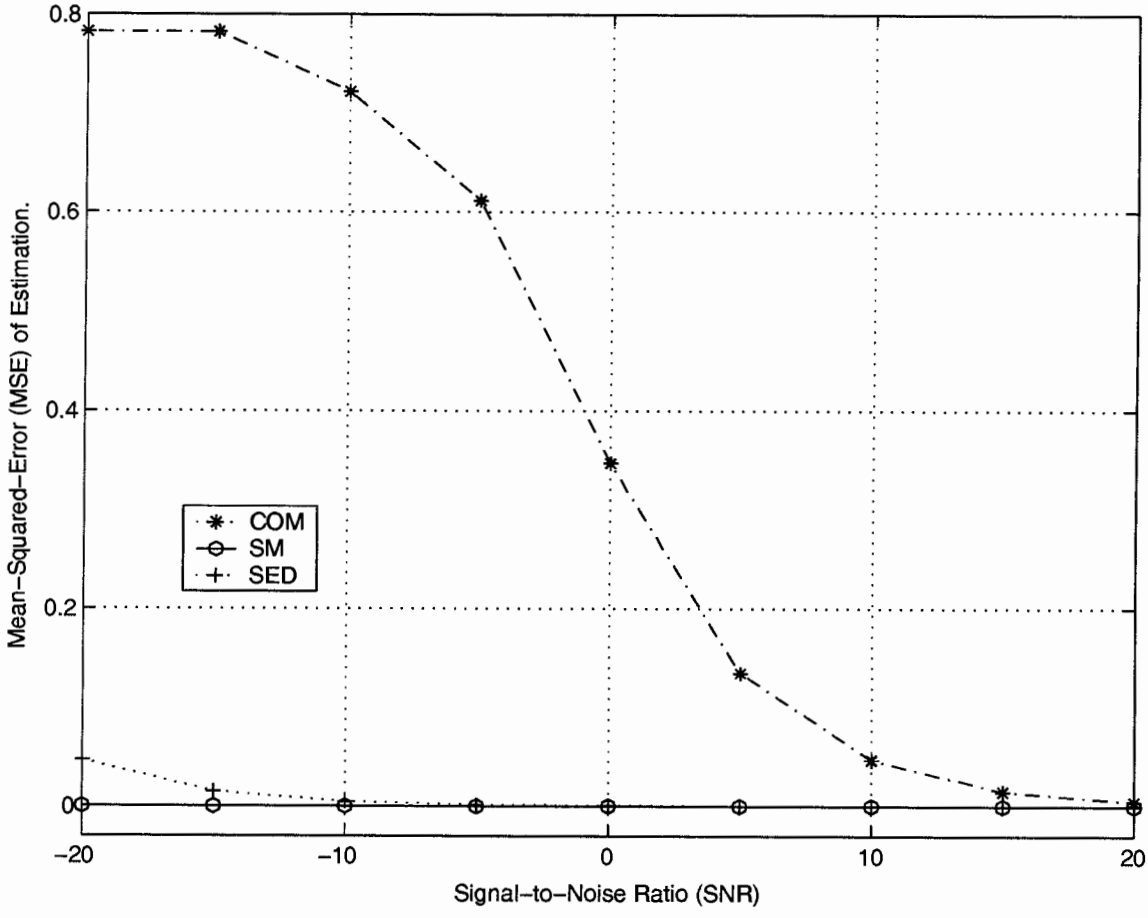

Figure 5.1. *MSE of the estimation of the channel impulse response in Example 1.*

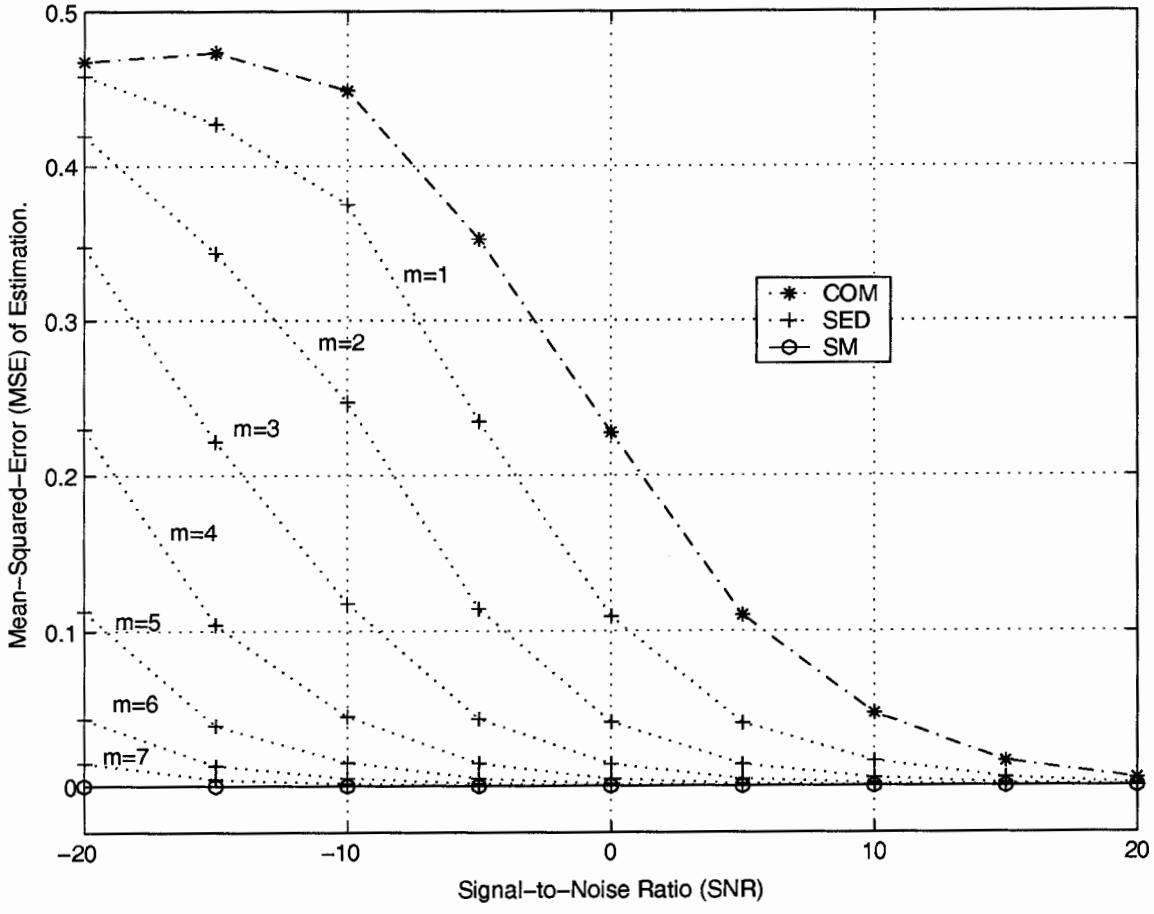

Figure 5.2. *MSE of the estimation of the channel impulse response in Example 2.*

Chapter 6

VCM Multiuser Detector for DS-CDMA Systems with Multipath Fading Channels

6.1 Introduction

The multiuser detector proposed in Chapter 5 was designed for DS-CDMA systems with multipath propagation channels where both multiuser interference (MUI) and intersymbol interference (ISI) are present in the received signal. Since the proposed detector is a linear detector, its computational complexity depends largely on the number of samples generated in one symbol duration. In order to reduce the computational complexity of the detector while not sacrificing the performance, the sampling frequency at the front end of the receiver is usually of the same order as the chip rate of the nominal signature waveform.

In a multipath propagation channel, the effective signature waveform observed at the receiver is a linear convolution of the channel impulse response and the nominal signature waveform assigned at the transmitter. If perfect sampling is assumed at the front end of the receiver, the discrete-time effective signature can also be expressed as a linear convolution of the discrete-time version of the channel impulse response and the nominal signature waveform.

According to the sampling theorem, for perfect sampling the sampling frequency has to be equal to or higher than the *Nyquist rate* of the effective signature waveform, i.e., twice the highest frequency in the nominal signature waveform and the channel impulse response. In Chapter 2 we have shown that in multipath propagation channels, the received signal is composed of several attenuated versions of the transmitted signals which arrive at the receiver at different times having been transmitted along different paths of different lengths. When the lengths of several propagation paths are very close to each other, which happens very often in wireless communications for in-door communications, wireless local access networks (WLANs), and personal access networks (PANs), the difference in the propagation time of the signals traveling along different paths will be very small. In such a case, the highest frequency in the channel impulse response is very likely to be significantly higher than the chip rate of the nominal signature waveform, which makes it very difficult for the receiver to achieve perfect sampling at the front end and low complexity detection simultaneously. If the sampling frequency is of the same order as the chip frequency of the nominal signature waveform, aliasing could arise during the sampling process and, as a result, the linear convolution relationship assumed in the detectors described in Chapter 5 breaks down. In this chapter, our attention is focused on the multiuser detection problem in DS-CDMA systems with multipath propagation channels where the discrete-time effective signatures are affected by aliasing.

The effect of aliasing on the discrete-time effective signature has three features: first, it is difficult to be timely and accurately estimated in a fast fading channel; second, it does not change until the system parameters such as the sampling frequency, channel impulse responses, or the signature sequences change; and third, it is additive. Based on these features, the discrete-time effective signature can be expressed as a linear convolution of the discrete-time versions of the nominal signature waveform and the channel impulse response plus an unknown term representing the distortion caused by aliasing. Our simulation results show that although the multiuser detectors

described in Chapter 5 are very effective in dealing with signature distortion due to multipath propagation, they are sensitive to the additive distortion caused by aliasing.

In this chapter, new multiuser detectors are proposed to deal with the multiuser detection problem in multipath DS-CDMA channels when the discrete-time signature is distorted by multipath propagation and aliasing. This detection is carried out by solving a linear constrained optimization problem whose objective function is formulated based on the vector constant modulus (VCM) criterion. Two adaptation algorithms, namely, the constrained stochastic gradient (CSG) algorithm and the recursive vector constant modulus (RVCM) algorithm, are proposed for solving the optimization problem. Computer simulations have been conducted which demonstrate that the proposed detectors can effectively suppress both MUI and ISI. More importantly, the proposed detectors show very robust performance when the discrete-time signature is distorted by aliasing at the receiver.

The chapter is organized as follows. In Sec. 6.2, a signal model for a DS-CDMA system with multipath propagation channel is briefly described. In Sec. 6.3, a VCM approach based multiuser detection method is proposed. Two adaptation algorithms for solving the optimization problem are presented in Sec. 6.4 and a performance analysis for the proposed detectors is presented in Sec. 6.5. Simulation results are described in Sec. 6.6 and Sec. 6.7 summarizes the main results.

6.2 Signal Model

We continue the signal model description in Sec. 2.4.2.3. It follows from (2.44) that when aliasing is not present at the receiver, the discrete-time signal can be expressed in matrix form as

$$\mathbf{y}(i) = A_1 b_1^i \mathbf{h}_{1,0} + \sum_{k=2}^{K} A_k b_k^i \mathbf{h}_{k,0} + \sum_{k=1}^{K} A_k b_k^{i-1} \mathbf{h}_{k,-1} + \sum_{k=1}^{K} A_k b_k^{i+1} \mathbf{h}_{k,+1} + \mathbf{n}_c(i) \quad (6.1)$$

(See (2.44) for definitions). In (6.1), the first term denotes the signal of the desired user (i.e., the first user) in the ith symbol duration, the second term denotes the interference signal of all other users in the ith symbol duration, the third and fourth terms denote the interference signal in the $(i-1)$th and $(i+1)$th symbol duration, respectively, and the last term denotes a vector of white Gaussian noise. When aliasing is present during the sampling process, $\mathbf{h}_{1,0}$ can be expressed as

$$\mathbf{h}_{1,0} = \mathbf{S}_1\mathbf{g}_1 + \mathbf{e}_1 \tag{6.2}$$

where $\mathbf{S}_1$ and $\mathbf{g}_1$ are defined in (2.45), $\mathbf{e}_1 = [e_1(1)\ e_1(2)\ \cdots\ e_1(N+M-1)]^T$ denotes the additive term to the effective signature of the first user due to aliasing distortion. For the sake of simplicity, $e_1(i)$ for $i = 1,\ \ldots,\ N+M-1$ are modeled as independent zero-mean Gaussian random variables with variance γ. Note that $\mathbf{e}_1$ does not change within the channel coherence time. In what follows, coherent multiuser detection is assumed, i.e., θ_{km} for $k = 1,\ \ldots,\ K$, $m = 1,\ \ldots,\ M$ are assumed to be known at receiver.

6.3 VCM-Based Blind Multiuser Detectors

The vector constant modulus (VCM) approach was first proposed as an extension of the constant modulus (CM) approach [47, 48] for blind channel equalization when the source data has a near-Gaussian distribution. In such a case, it is very likely that a channel equalizer using the constant modulus (CM) approach would fail to converge [49, 50]. It has been shown that a channel equalizer based on the VCM approach outperforms a channel equalizer based on the CM approach [49, 50].

A VCM-based channel equalizer can be obtained by solving the minimization problem [49, 50].

$$\text{minimize}: \quad \mathcal{J}(\mathbf{w}) = \mathrm{E}\ \left[||\mathbf{z}||^2 - \alpha^2\right]^2 \tag{6.3}$$

where $\mathbf{a} = \{a(n)\}$, $\mathbf{c} = \{c(n)\}$, $\mathbf{x} = \{x(n)\} = \mathbf{a} * \mathbf{c}$, $\mathbf{w} = [w_1\ w_2\ \cdots\ w_L]^T$, and $\mathbf{z} = \{z(n)\} = \mathbf{w} * \mathbf{x}$ denote the transmitted signal, the channel impulse response, the received signal, the equalization vector, and the equalized signal, respectively, '$*$' denotes linear convolution and $||\cdot||$ denotes the 2-norm of $(\cdot)$, $\alpha = \mathrm{E}(\mathbf{a}^4)/\mathrm{E}(\mathbf{a}^2)$ is a constant denoting the modulus of source data $\mathbf{a}$.

Let us consider the MUI and ISI suppression problem in DS-CDMA systems using the VCM approach. By reformulating the signals in the previous and subsequent symbol durations as the signals of the current symbol duration of additional equivalent users, (6.1) can be expressed as

$$\mathbf{y}(i) = \sum_{k=1}^{3K} \bar{A}_k \bar{b}_k^i \bar{\mathbf{h}}_k + \mathbf{n}_c(i) \tag{6.4}$$

In (6.4), $\bar{A}_k$ is the amplitude, $\bar{b}_k$ is the information bit, and $\bar{\mathbf{h}}_k$ is the discrete-time effective signature of the kth equivalent user. These parameters are defined in Table 6.1.

Table 6.1. *Definitions of $\bar{A}_k$, $\bar{b}_k^i$, and $\bar{\mathbf{h}}_k$ in (6.4)*

k	$k \in [1,\ K]$	$k \in [K+1,\ 2K]$	$k \in [2K+1,\ 3K]$
$\bar{A}_k$	A_k	A_{k-K}	A_{k-2K}
$\bar{b}_k^i$	b_k^i	b_{k-K}^{i-1}	b_{k-K}^{i+1}
$\bar{\mathbf{h}}_k$	$\mathbf{h}_{k,0}$	$\mathbf{h}_{k-K,-1}$	$\mathbf{h}_{k-2K,1}$

Note that after reformulation, the interference in the previous and subsequent symbol durations in (6.1) is expressed as MUI of $2K$ equivalent users in (6.4). As can be seen in Table 6.1, the signal of the desired user in the current symbol duration corresponds to the signal of the first equivalent user in (6.4). If $\mathbf{w}$ is a detection vector, we have

$$\mathbf{w} * \mathbf{y}(i) = \mathbf{w}^H[\mathbf{y}_1(i)\ \mathbf{y}_2(i)\ \cdots\ \mathbf{y}_M(i)] \tag{6.5}$$

where $\mathbf{y}_m(i) = [y(iN+m)\ y(iN+m+1)\ \cdots\ y((i+1)N+m-1)]^T$ is a N-element column vector which, according to (6.4), can be expressed as

$$\mathbf{y}_m(i) = \sum_{k=1}^{3K} \bar{A}_k \bar{b}_k \bar{\mathbf{h}}_k^m + \mathbf{n}_c^m(i) \tag{6.6}$$

In (6.6), $\bar{\mathbf{h}}_k^m = [\bar{\mathbf{h}}_k(iN+m)\ \bar{\mathbf{h}}_k(iN+m+1)\ \cdots\ \bar{\mathbf{h}}_k((i+1)N+m-1)]^T$ and $\mathbf{n}_c^m(i) = [n_c(iN+m)\ n_c(iN+m+1)\ \cdots\ n_c((i+1)N+m-1)$ are truncated versions of $\bar{\mathbf{h}}_k$ and $\mathbf{n}_c(i)$ in (6.4), respectively.

According to (6.4)-(6.6), new detectors can be obtained by solving the optimization problem

$$\text{minimize} \quad \mathrm{E}\left[||\mathbf{w}^H\mathbf{Y}(i)||^2 - \alpha^2\right]^2 \tag{6.7a}$$

$$\text{subject to:} \quad \mathbf{C}^H\mathbf{w} = \mathbf{u} \tag{6.7b}$$

where $\mathbf{Y}(i)$ is a Toeplitz matrix defined as

$$\begin{aligned}\mathbf{Y}(i) &= \begin{bmatrix} y(iN+1) & y(iN+2) & \cdots & y(iN+M) \\ y(iN+2) & y(iN+3) & \cdots & y(iN+M+1) \\ \vdots & \vdots & \ddots & \vdots \\ y((i+1)N) & y((i+1)N+1) & \cdots & y((i+1)N+M-1) \end{bmatrix} \\ &= [\mathbf{y}_1(i)\ \mathbf{y}_2(i)\ \cdots\ \mathbf{y}_M(i)]\end{aligned} \tag{6.8}$$

$\alpha^2 = \bar{A}_1^2$ denotes the modulus of the signal of the desired equivalent user, $\mathbf{C}$ is a $N \times (2M-1)$ Toeplitz matrix given by

$$\mathbf{C} = \begin{bmatrix} s_1(M) & \cdots & s_1(1) & \cdots & 0 \\ & \ddots & \vdots & \ddots & \vdots \\ \vdots & & s_1(M) & & s_1(1) \\ & & \vdots & & \\ s_1(N) & & s_1(N-M) & & \vdots \\ \vdots & \ddots & \vdots & \ddots & \\ 0 & \cdots & s_1(N) & \cdots & s_1(N-M) \end{bmatrix} \tag{6.9}$$

and $\mathbf{u}$ is a $(2M-1)$-element column vector with its Mth component being one and all other components being zeros.

The linear constraints in (6.7b) are introduced into the problem primarily for two reasons: first, the projection of the discrete-time nominal signature of the desired user on the detection vector $\mathbf{w}$ is fixed to unity; and second, $\mathbf{w}$ is forced to be orthogonal to all other shifted and truncated versions of the discrete-time nominal signature of the desired user. If the signature distortion due to aliasing is temporarily ignored, the quantity $\mathbf{w}^H\bar{\mathbf{h}}_1^m$ implicitly included in the objective function in (6.7a) can be expressed as

$$\mathbf{w}^H\bar{\mathbf{h}}_1^m = g_1(m) \tag{6.10}$$

Since $\sum_{m=1}^{M} |g_1(m)|^2 = 1$, it can be shown that minimizing the objective function in (6.7a) may lead to

$$|\mathbf{w}^H\bar{\mathbf{h}}_k^m|^2 \approx 0 \qquad \text{for } k = 2,\ \ldots,\ 3K,\ m = 1,\ \ldots,\ M$$

Note that $\bar{\mathbf{h}}_k^m$ is a truncated version of the discrete-time signature of the kth equivalent user. By comparing (6.5), (6.6), and (6.10), the minimization of the objective function in (6.7a) may lead to the suppression of the MUI of equivalent signals.

Once the solution of the optimization problem in (6.7) is obtained, the information bit of the desired user can be determined using the *maximum ratio combination* (MRC) criterion [4]

$$\hat{b}_1(i) = \text{sgn}\left[\text{Re}(\mathbf{w}^H\mathbf{Y}\cdot\hat{\mathbf{g}}_1^*)\right] \tag{6.11}$$

where $\text{Re}(\cdot)$ denotes the real part of a complex quantity, $\text{sgn}(\cdot)$ denotes the sign of a scalar, and $\hat{\mathbf{g}}_1^* = [\hat{\mathbf{g}}_1^*(1)\ \hat{\mathbf{g}}_1^*(2)\ \cdots\ \hat{\mathbf{g}}_1^*(M)]^T$ is an approximation for the channel impulse response of the first user, which can be computed as

$$\hat{\mathbf{g}}_1^*(m) = \text{E}\left|\mathbf{w}^H\mathbf{y}_m(i)\right|\exp(j\theta_{1m}) \quad \text{for} \quad m = 1,\ 2,\ \ldots,\ M \tag{6.12}$$

We conclude this section with two remarks, as follows:

1) Channel Order Selection: Although it is assumed that the maximum channel length for all users is M, the assumption does *not* imply that the channels should be of the maximum length exactly. In fact, if the number of nonzero components in $\mathbf{g}_1$ is less than M and their positions are known a *priori*, then some constraints can be removed from (6.7b) in order to reduce the amount of computation for solving the problem in (6.7).

2) Group-Blind Detectors: In uplink CDMA systems, the nominal signatures of other users may be known at the base station. In such cases, the performance of the proposed detector can be improved by expanding the linear constraints in (6.7b) such that $\mathbf{w}$ is forced to be orthogonal to the shifted and truncated versions of the nominal signatures of the other users known at the receiver (see [98] for more details).

6.4 Adaptation Algorithms

In this section, two adaptation algorithms, namely, the constrained stochastic gradient (CSG) algorithm, and the recursive VCM (RVCM) algorithm, are proposed for solving the optimization problem in (6.7).

In the CSG algorithm, the detection vector $\mathbf{w}$ is initialized as $\mathbf{w}(0) = \mathbf{C}(\mathbf{C}^H\mathbf{C})^{-1}\mathbf{u}$, which can be shown to satisfy the equality constraint in (6.7b). In each iteration of the CSG algorithm, we first compute the instantaneous gradient of the objective function, which is denoted as $\mathbf{g}(i)$. Then $\mathbf{g}(i)$ is projected onto an orthogonal matrix to $\mathbf{C}$ to ensure that the updated vector still satisfies the equality constraint in (6.7b) in the next iteration. The step size used for the adaptation algorithm is normalized to improve the convergence of the algorithm. A step-by-step description of the algorithm is summarized in Table 6.2.

Because the objective function in (6.7a) involves fourth-order statistics of the received signal, the convergence rate of the stochastic gradient type algorithm can be rather slow [34]. When communication channels experience dramatic changes, the

Table 6.2. *Constrained Stochastic Gradient Algorithm*

Step 1: Compute the initial solution as $\mathbf{w}(0) = \mathbf{C}(\mathbf{C}^H\mathbf{C})^{-1}\mathbf{u}$.

Step 2: Compute $\mathbf{\Pi}_{\mathbf{C}}^{\perp} = \mathbf{I} - \mathbf{C}(\mathbf{C}^H\mathbf{C})^{-1}\mathbf{C}^H$.

Step 3: For $i = 0,\ 1,\ 2,\ \ldots$

(1) Compute $e(i) = ||\mathbf{w}^H(i)\mathbf{Y}(i)||^2 - A_1^2$.

(2) Compute the stochastic gradient as $\mathbf{g}(i) = e(i) \cdot \mathbf{Y}(i)\mathbf{Y}^H(i)\mathbf{w}(i)$ and project it onto $\mathbf{\Pi}_{\mathbf{C}}^{\perp}$ as $\tilde{\mathbf{g}}(i) = \mathbf{\Pi}_{\mathbf{C}}^{\perp}\ \mathbf{g}(i)$.

(3) Compute a step-size as $\mu(i) = ||\tilde{\mathbf{g}}(i)||^2 / \left[e(i) \cdot ||\tilde{\mathbf{g}}^H(i)\mathbf{Y}(i)||^2\right]$

(4) Update the detection vector as $\mathbf{w}(i+1) = \mathbf{w}(i) - \mu(i) \cdot \tilde{\mathbf{g}}(i)$

CGS algorithm may fail to track the variation of the received signal. In what follows, a recursive VCM (RVCM) algorithm is proposed which offers faster convergence at the cost of increased amount of computation.

The RVCM algorithm is developed on the basis of the well-known recursive least square (RLS) algorithm [34]. The initialization for the RVCM algorithm is the same as that for the CGS algorithm. Two key formulas for the RVCM algorithm are given by

$$\mathbf{k}(i) = \frac{1}{\lambda + \mathbf{s}^H(i)\mathbf{P}(i-1)\mathbf{s}(i)} \cdot \mathbf{P}(i-1)\ \mathbf{s}(i) \tag{6.13a}$$

$$\mathbf{P}(i) = \frac{1}{\lambda} \cdot \left[\mathbf{P}(i-1) - \mathbf{k}(i)\mathbf{s}^H(i)\mathbf{P}(i-1)\right] \tag{6.13b}$$

where $\mathbf{s}(i) = \mathbf{\Pi}_{\mathbf{C}}^{\perp}\mathbf{Y}(i)\mathbf{Y}^H(i)\mathbf{w}(i)$, $\mathbf{P}(i)$ is a matrix to approximate the inverse of the crosscorrelation matrix of $\mathbf{s}(i)$, and $0 < \lambda \leq 1$ is a forgetting factor. A step-by-step description of the RVCM algorithm is presented in Table 6.3.

Table 6.3. *Recursive VCM Algorithm*

Step 1: Initialize $\mathbf{P}(0) = \delta\mathbf{I}$ with δ being a positive scalar and $\mathbf{w}(0) = \mathbf{C}(\mathbf{C}^H\mathbf{C})^{-1}\mathbf{u}$.

Step 2: Compute $\mathbf{\Pi}_{\mathbf{C}}^{\perp} = \mathbf{I} - \mathbf{C}(\mathbf{C}^H\mathbf{C})^{-1}\mathbf{C}^H$.

Step 3: For $i = 0,\ 1,\ 2,\ \ldots$

(1) Compute $e(i) = ||\mathbf{w}(i)^H\mathbf{Y}(i)||^2 - A_1^2$.

(2) Compute $\mathbf{s}(i) = \mathbf{\Pi}_{\mathbf{C}}^{\perp}\mathbf{Y}(i)\mathbf{Y}^H(i)\mathbf{w}(i)$.

(3) Update $\mathbf{k}(i)$ as $\mathbf{k}(i) = \mathbf{P}(i)\mathbf{s}(i)/\left[\lambda + \mathbf{s}^H(i)\mathbf{P}(i)\mathbf{s}(i)\right]$.

(4) Update the detection vector as $\mathbf{w}(i+1) = \mathbf{w}(i) - e(i)\cdot\mathbf{k}(i)$.

(5) Update $\mathbf{P}(i+1) = (1/\lambda)\cdot\left[\mathbf{P}(i) - \mathbf{k}(i)\mathbf{s}^H(i)\mathbf{P}(i)\right]$.

6.5 Analysis of the Proposed Adaptation Algorithms

In this section, we investigate the interference suppression efficiency of the proposed adaptation algorithms. For this purpose, we first assume a noise-free channel, i.e., $\sigma_v^2 \approx 0$. Using (6.10), the objective function in (6.7a) can be expressed as

$$\mathcal{J}(\mathbf{w}) = \mathrm{E}\left[\sum_{m=1}^{M}\left|\bar{A}_1\bar{b}_1(i)(g_1(m) + \mathbf{w}^H\mathbf{e}_1) + \mathbf{w}^H\left(\sum_{k=2}^{3K}\bar{A}_k\bar{b}_k(i)\bar{\mathbf{h}}_k^m\right)\right|^2 - A_1^2\right]^2 \quad (6.14)$$

Note that if the detection vector $\mathbf{w}$ satisfies

$$\mathbf{w}^H\bar{\mathbf{h}}_k^m \approx 0 \quad (6.15)$$

for $k = 2,\ldots,3K$ and $m = 1,\ \ldots,\ M$ and $\mathbf{w}^H\mathbf{e}_1 \approx 0$, then as can be seen in (6.14) that $\mathcal{J}(\mathbf{w}) \approx 0$, which is the smallest value that can be assumed by $\mathcal{J}(\mathbf{w})$.

By studying the first and second derivatives of the objective function in (6.7a), it is shown in Appendix C that a sufficiency condition for global convexity in the optimization problem in (6.7) is given by

$$\sum_{\substack{l=1\\ l\neq k}}^{3K}\bar{A}_l^2\mathbf{P}_{ll} - \bar{A}_1^2\mathbf{P}_{11} - \bar{A}_k^2\mathbf{P}_{kk} \succeq \mathbf{0} \quad \text{for } k = 1,\ \ldots,\ 3K \quad (6.16)$$

where '$\succeq \mathbf{0}$' denotes the positive semidefinite and $\mathbf{P}_{kk} = 2\sum_{m=1}^{M} \bar{\mathbf{h}}_k^m (\bar{\mathbf{h}}_k^m)^H$ is a positive semidefinite matrix. Therefore, if the condition in (6.16) is satisfied, then the problem in (6.7) is a convex programming problem which has a unique and global optimal solution. In such a case, the solution obtained by using any gradient based algorithm will satisfy (6.15). In other words, the detection vector obtained by using the CGS and the RVCM algorithms can effectively suppress the ISI and MUI present in the received signal.

The derivation of the condition in (6.16) is based on the assumption that σ_v^2 is negligible, which is not true in general. In addition, when the sufficiency condition in (6.16) is not satisfied, the above analysis cannot be applied directly.

Monte-Carlo simulations were conducted to examine the interference suppression performance of the proposed algorithms. In the simulations, the measurement of interest is the bit-error-rate (BER) which was averaged over 100 runs, each of which entails the detection of 10^5 information bits. For comparison purposes, the BERs obtained by using the constrained optimization method (denoted as the COM detector) and the subspace method (denoted as the SUB detector) are also presented. Note that the interference suppression efficiency of the proposed detector is comparable to that of the COM and SUB detectors if the BERs obtained by the proposed detector are sufficiently close to that obtained by the two detectors. The system parameters that are related to the sufficiency condition in (6.16) were randomly generated in each run. More explicitly, $\mathbf{s}_k$ and $\mathbf{g}_k$ were vectors of zero-mean Gaussian variables of unit norm, d_k was an integer selected from $\{0,\ 1,\ \ldots,\ (N-1)\}$ with equal probability, and A_k for $k = 1,\ 2,\ \ldots,\ K$ were assumed to log-normally distributed random variables whose log-arithmitic variance is denoted as σ_a^2. These parameters remained unchanged in a single run but were regenerated for different runs. For a fair comparison, we assumed that $\mathbf{e}_k = 0$, $k = 1, \ldots, K$ in the simulations.

The first example considered a six-user system with a reduced near-far problem by setting $\sigma_a^2 = 10$. Parameters N and M were assumed to be 63 and 4, respectively. The

second example involved an eight-user system with a more severe near-far problem by setting $\sigma_a^2 = 1000$. Parameters N and M were assumed to be 127 and 5, respectively. The BERs obtained for the two examples are plotted in Figs. 6.1 and 6.2, respectively.

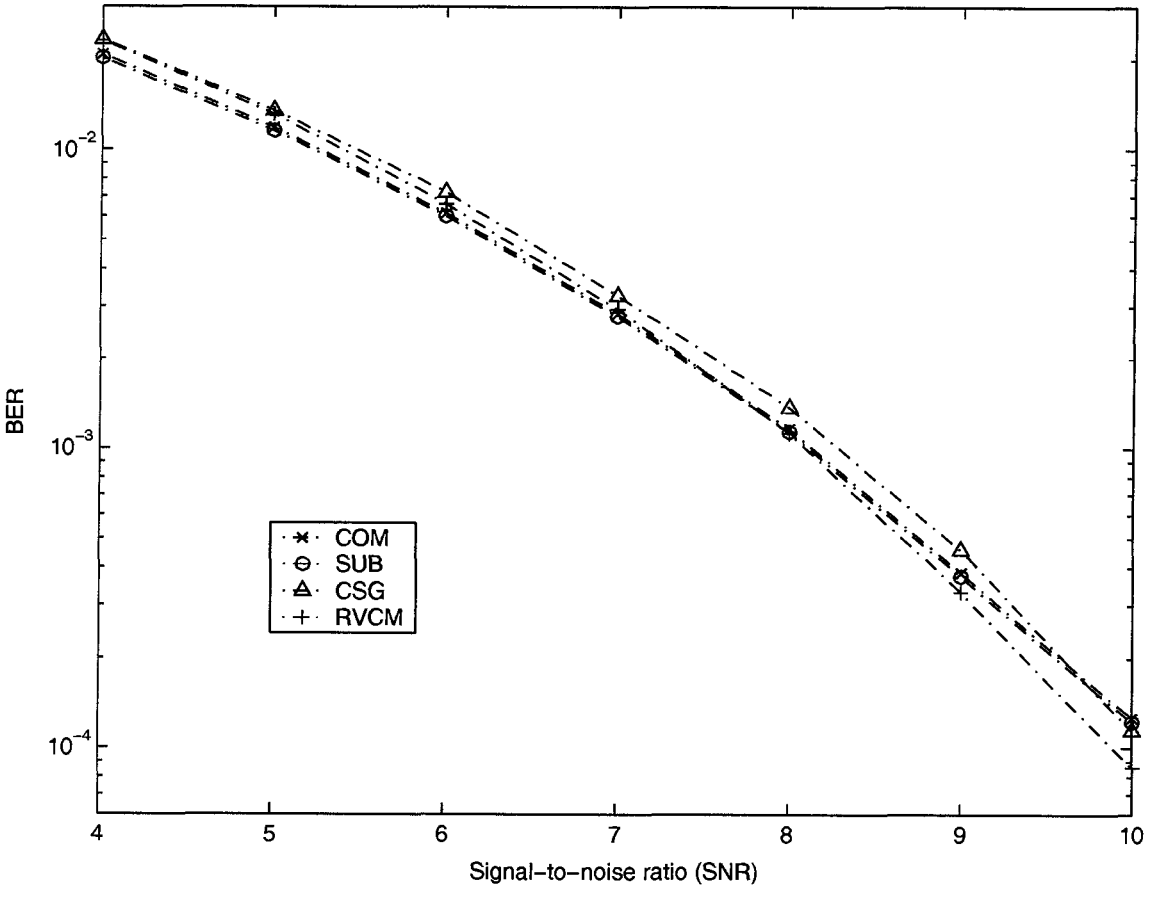

Figure 6.1. *The BERs of various detectors in the first example.*

It is observed in the figures that the BERs obtained by using the CSG and RVCM adaptation algorithms (denoted as the CSG and RVCM detectors, respectively) are very close to those obtained by the COM and SUB detectors. These simulations imply that when aliasing distortion is not present at the receiver, the interference suppression efficiency of the proposed detectors is comparable to that of the COM and SUB detectors.

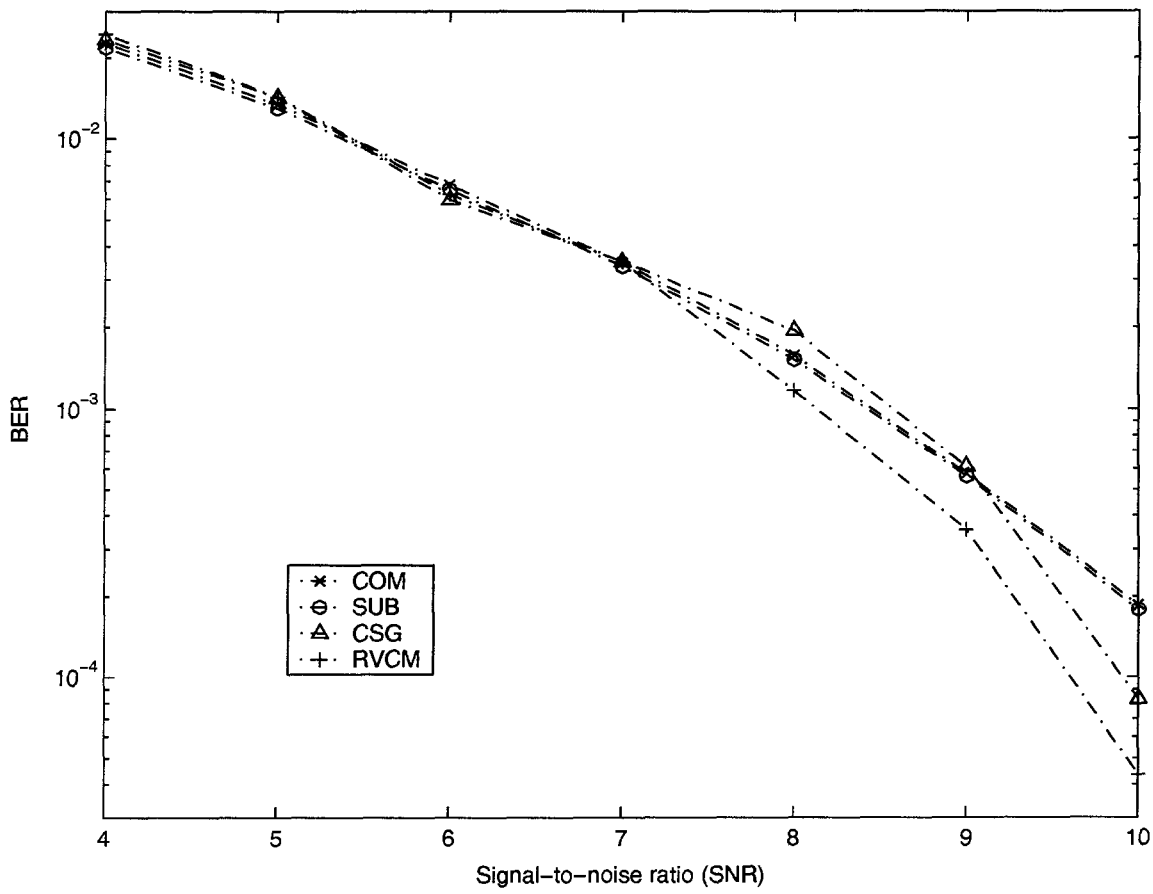

Figure 6.2. *The BERs of various detectors in the second example.*

6.6 Simulation Results

Two computer simulations were conducted to investigate the performance of VCM detectors with aliasing present at the receiver. In the simulations, $\gamma = 0.01, 0.05,$ and 0.08 were assumed. The other system parameter values were assumed to be the same as those in the first and the second examples in Sec. 6.5. The BERs of various detectors versus the magnitude of γ obtained in the two examples are plotted in Figs. 6.4 and 6.5 where the dash-dot, dot, and dash lines denote the BERs obtained for $\gamma = 0.01, 0.05,$ and 0.08, respectively.

It can be observed in Figs. 6.3 and 6.4 that the VCM detectors offer significantly

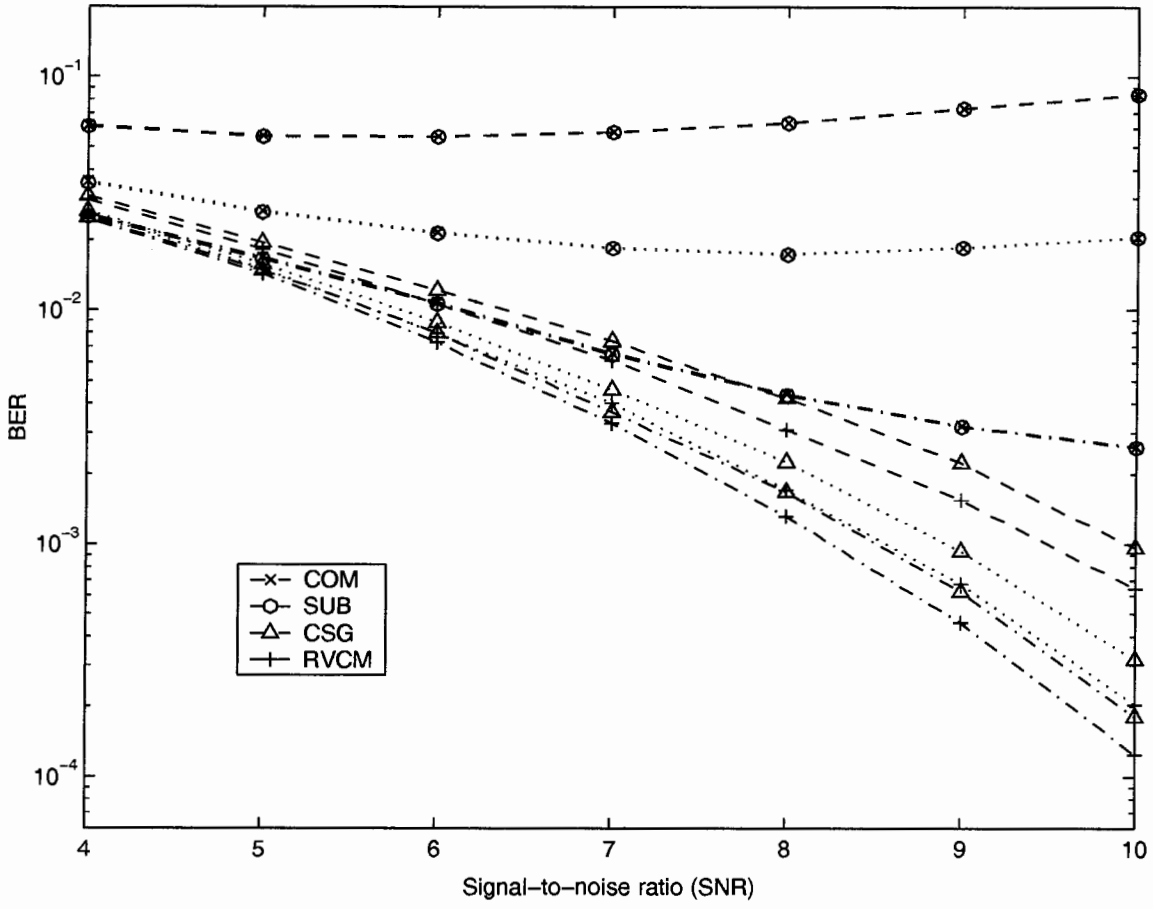

Figure 6.3. *Demodulation BERs obtained in the first example.*

improved BER performance relative to the other two detectors for nonzero values of γ. In addition, although an increase of γ leads to severe degradation in the performance of the COM and SUB detectors, it causes only mild degradation in the performance of the proposed detectors. It can also be seen that the BER performance offered by the VCM detector using the RVCM algorithm is slightly better relative to that of the VCM detector using the CGS algorithm.

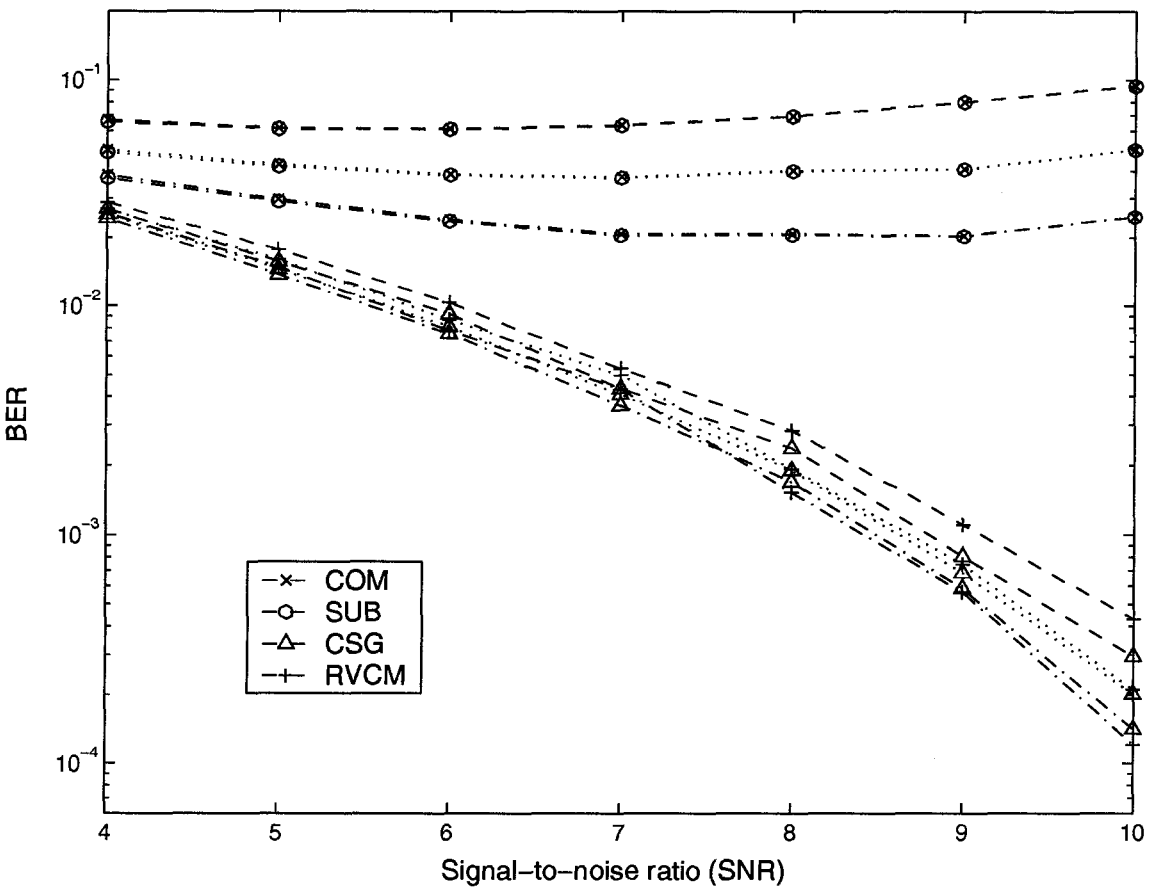

Figure 6.4. *Demodulation BERs obtained in the second example.*

6.7 Conclusions

New multiuser detectors based on the VCM criterion have been proposed for DS-CDMA systems with multipath propagation channels. Two adaptation algorithms have been developed and the interference suppression efficiency of the proposed detectors has been investigated. Computer simulations have been conducted to evaluate the performance of the VCM detector. It has been shown that the proposed detectors can effectively suppress the MUI and ISI present in the received signal. More importantly, these detectors have been shown to offer robust performance against the discrete-time signature distortion caused by aliasing at the receiver.

Chapter 7

Conclusions and Future Work

7.1 Conclusions

Four multiuser detectors have been proposed in Chapters 3 to 6 for different mobile communications environments. They are the semidefinite programming relaxation (SDPR) detector, the recursive convex programming (RCP) detector, the subspace-estimation based (SED) detector, and the vector constant modulus (VCM) detector. The SDPR and RCP detectors are designed for base stations aimed at providing joint detection for the information bits of all users, and the SED and VCM detectors are designed for mobiles where the information bit of only one user needs to be detected.

7.1.1 SDPR Detector

In Chapter 3, we have proposed a multiuser detector to approximate the maximum likelihood (ML) detection by using a semidefinite programming relaxation method. In this detector, the combinatorial optimization problem associated with the ML detection is reformulated by expressing the binary constraints as a number of linear equality constraints and a rank constraint on a positive semidefinite matrix. It has been shown that by neglecting the rank constraint on the positive semidefinite matrix, the combinatorial problem can be relaxed into a semidefinite programming (SDP) problem whose solution can be obtained with much reduced computational complexity relative to that involved in the combinatorial problem.

In order to further reduce the amount of computation involved, an efficient algorithm has been proposed based on duality theory. This algorithm is composed of three steps: first, the primal SDP problem is reformulated to a dual SDP problem; second, the dual problem is solved by using the projective method; and third, the solution of the primal SDP problem is expressed in terms of the solution of the dual SDP problem based on the KKT conditions and the central path concept. Since the number of variables involved in the dual SDP problem is reduced by an order of magnitude relative to that involved in the primal SDP problem, the implementation efficiency of the SDPR detector can be considerably improved by using such an algorithm.

Computer simulations have been presented to demonstrate that the demodulation performance of the SDPR detectors is comparable to that of the ML detector, and is significantly better relative to those of other suboptimal detectors such as the decorrelating detector and the MMSE detector. However, the computational complexity involved in the SDPR detectors is of polynomial order with respect to the number of users by contrast with that involved in the ML detector which grows exponentially. A comparison of the SDPR detectors has shown that the dual SDPR detector is much more efficient than the primal SDPR detector owing to the significant reduction in the number of variables involved. Furthermore, it has also been shown that these improvements in efficiency are brought about without degrading the performance relative to that achieved by the ML detector.

7.1.2 RCP Detector

Our attention in Chapter 4 was focused on the design of a multiuser detector using a recursive convex programming (RCP) approach. In the proposed detectors, the combinatorial problem associated with ML detection is relaxed to a convex programming problem and then a recursive approach is exploited to approximate the solution of ML detection. It has been shown that the recursive approach used in the proposed detectors is analogous to the interference cancellation approaches that have been ap-

plied in many other multiuser detectors. However, since the order of cancellation and the decisions of the information bits in the RCP detector are based on the solutions of CP problems, the RCP detector outperforms those of other detectors using interference cancellation approaches. A comparison of the RCP detector with the SDPR detector has been presented to demonstrate that the RCP detector and the SDPR detector belong to two distinct ways in approximating the ML detector. In order to further reduce the computational complexity involved in the RCP detector, an efficient unconstrained relaxation (UR) approach has been proposed, and its effect on the implementation efficiency of the RCP detector has been investigated.

Computer simulations have been presented to demonstrate that the demodulation performance of the RCP detector is superior relative to many other suboptimal detectors such as the successive interference cancellation (SIC) detector, the GMMSE detector, and the BC detector. In DS-CDMA systems suffering strong MUI, the demodulation performance of the RCP detector has been shown still comparable to that of the ML detector, and slightly better relative to that of the SDPR detector. Comparisons of the computational complexity involved in the ML, the SDPR, and the RCP detector have indicated that the RCP detector entails a significantly lower computation burden relative to that of the other two detectors.

7.1.3 SED Detector

In Chapter 5, we focused on the design of multiuser detectors for DS-CDMA systems with frequency-selective channels. In such a channel environment, the effective signature waveform can be distorted during multipath propagation and can thus become unknown to the receiver. It has been shown that a mismatched signature used at receiver may lead to significant degradation in the performance of the constrained minimum output energy (CMOE) detector. Multiuser detectors based on subspace and constrained optimization methods have been proposed to alleviate the problem effectively by several researchers. However, both types of detectors have some disad-

ventages: i) the detector based on constrained optimization methods offers worse performance than the detector based on subspace methods, and ii) the detector based on subspace methods require more computation than the detector based on constrained optimization methods.

In Chapter 5, we have also shown that the existing subspace and constrained optimization methods can be related to each other via the bridge of estimation of the noise subspace. Based on this observation, a new approach has been proposed for a more accurate estimation of the noise subspace. The estimation of the noise subspace offered by the new approach is comparable to that offered by the existing subspace methods despite the channel noise level. Based on the new approach, a subspace estimation based detector has been proposed for DS-CDMA systems. The performance of the proposed detector can approach that of the existing subspace methods while requiring a much reduced computational complexity. Relative to existing detectors based on constrained optimization methods, the proposed detector offers a significantly improved performance while requiring a comparable amount of computation.

7.1.4 VCM Detector

In Chapter 6, our attention was focused on the design of multiuser detectors for DS-CDMA systems with frequency-selective channels where the discrete-time effective signature is distorted not only by multipath propagation but also by aliasing at the receiver. In the presence of aliasing, the discrete-time effective signature is a linear convolution of the discrete-time versions of the nominal signature and the channel impulse response plus a additive term representing aliasing distortion. Our simulation results have shown that the detectors described in Chapter 5 are very sensitive to aliasing.

In Chapter 6, new multiuser detectors have been proposed. In the proposed detectors, the detection is carried out by solving a linear-constrained optimization problem

whose objective function is formulated based on the vector constant modulus (VCM) criterion. It has been shown by analysis and simulation results that minimization of the objective function of the optimization problem leads to effective suppression of multiuser interference (MUI) and intersymbol interference (ISI). Two adaptation algorithms, namely, the constrained stochastic gradient (CSG) algorithm and the recursive vector constant modulus (RVCM) algorithm, have been developed for solving the optimization problem. The effective maximum ratio combination (MRC) approach has been applied to make binary decisions for the information bits transmitted.

Computer simulations have been presented to demonstrate that the performance of the VCM detector is comparable to that of the detectors described in Chapter 5 when aliasing is not present at the receiver. When aliasing distortion is present, however, the VCM detector has been shown to offer significantly better demodulation performance relative to that of the detectors described in Chapter 5. In addition, it has also been shown that the VCM detector based on the RVCM algorithm offers slightly better performance relative to the VCM detector based on the CSG algorithm.

7.2 Future Work

In what follows, three research topics are suggested that can extend the work presented.

7.2.1 RCP Detectors

Although the RCP detectors described offer near-optimal demodulation performance, the computational complexity involved in both detectors is still rather high relative to that required by linear multiuser detectors. Since the recursive approach utilized in the RCP detector is very similar to the interference cancellation approaches used for other detectors which involve considerably lower computational complexity relative

to that of the RCP detector, it would be natural to ask whether the RCP detectors can be implemented with linearly increased computational complexity with respect to the number of users? In addition, a thorough study on the error probability of the RCP detector is required.

7.2.2 RCP Detectors for Asynchronous DS-CDMA Systems

In asynchronous DS-CDMA systems, the number of variables involved in the CP problem can be increased significantly, which leads to a dramatic increase in the computational complexity. Therefore, it is of particular importance to design asynchronous versions of RCP detectors without dramatically increasing the computational complexity. In fact, the design of the ML detector for asynchronous DS-CDMA systems has been considered and an efficient Viterbi algorithm has been proposed. However, the Viterbi algorithm was developed based on a trellis structure, which cannot be applied directly to the SDPR and the RCP detectors. Once the design of the RCP detector for asynchronous DS-CDMA detectors has been achieved, it would be natural to consider extensions for multipath propagation channels.

7.2.3 SED Detector

Recall that although improved performance has been achieved for both low and high SNR AWGN channels by using the method proposed in Chapter 6, the improvement is limited when the approximation of the data correlation matrices is imperfect or the background noise is not white Gaussian. In this regard, it is worthwhile to extend the current work to overcome the above mentioned limitations. These extensions could include (a) develop more robust detectors based on the proposed method for DS-CDMA systems where the data crosscorrelation matrices are imperfect; (b) develop approaches for DS-CDMA systems where more realistic noise models are considered; and (c) develop adaptive algorithms for the above systems to improve the imple-

mentation efficiency. Together with the current work, the proposed extensions will constitute a feasible solution for multiuser detection in wideband DS-CDMA systems.

Bibliography

[1] T. S. Rappaport, *Wireless Communications: Principles & Practice*, Prentice-Hall, NJ, 1996.

[2] M. Zeng, A. Annamalai, and V. K. Bhargava, "Recent advances in cellular wireless communications," *IEEE Commun. Mag.*, vol. 37, pp. 128-138, Sept. 1999.

[3] A. J. Viterbi, *CDMA: Principles of spread spectrum communication*, Addison-Wesley, MA, 1995.

[4] J. G. Proakis, *Digital Communications*, 3rd ed., McGraw-Hill, NY, 1995.

[5] R. Price, "A conversation with Claude Shannon," *IEEE Commun. Mag.*, vol. 22, pp. 123-126, May 1984.

[6] R. Scholtz, "The origins of spread-spectrum communications," *IEEE Trans. Commun.*, vol. 30, pp. 822-854, May 1982.

[7] M. Simon, J. Omura, R. Scholtz, and B. Levitt, *Spread Spectrum Communications Handbook*, McGraw-Hill, NY, 1994.

[8] Telecommunications Industry Association, "Mobile station-base station compatibility standard for dual-mode wideband spread spectrum cellular system," Tech. Rep. TIA/EIA/IS-95, Electronic Industries Association, July 1993.

[9] N. Suehiro and M. Hatori, "Modulatable orthogonal sequences and their application to SSMA systems," *IEEE Trans. Inform. Theory*, vol. 34, pp. 93-100, Jan. 1988.

[10] T. Kasami, "Weight distribution formula for some class of cyclic codes," *Tech. Report R-285, Coordinated Science Laboratory*, University of Illinois, Urbana, IL, Apr. 1966.

[11] R. Gold, "Optimum Binary sequences for spread spectrum multiplexing," *IEEE Trans. Inform. Theory*, vol. 14, pp. 154-156, Oct. 1967.

[12] E. H. Dinam and B. Jabbari, "Spreading codes for direct sequence CDMA and wideband CDMA cellular networks," *IEEE Commun. Magazine*, pp. 48-54, Sept. 1998.

[13] S. W. Wales, "Techniques for cochannel interference suppression in TDMA mobile radio systems," *IEE Proc.-Communications*, vol. 142, pp. 106-114, Apr. 1995.

[14] R. Kohno, M. Hatori and H. Imai, "Cancellation techniques of co-channel interference in asynchronous spread spectrum multiple access systems," *Elect. and Commun. in Japan*, Vol. 66-A, No. 5, pp. 20-29, 1983.

[15] G. Caire, G. Taricco, J. Ventura-Traveset, and E. Biglieri, "A multiuser approach to narrowband cellular communication," *IEEE Trans. Inform. Theory*, vol. 43, pp. 1503-1517, Sept. 1997.

[16] R. Price and P. Green, "A communication technique for multipath channels," *Proc. IRE*, vol. 46, pp. 555-570, Mar. 1958.

[17] S. Verdú, *Multiuser Detection*, Cambridge University Press, Cambridge, UK, 1998.

[18] A. Duel-Hallen, J. Holtzman, and Z. Zvonar, "Multiuser detection for CDMA systems," *IEEE Personal Commun.*, vol. 2, pp. 46-58, Apr. 1995.

[19] S. Moshavi, "Multi-user detection for DS-CDMA communications," *IEEE Commun. Magazine*, pp. 124-136, Oct. 1996.

[20] S. Verdú, "Minimum probability of error for asynchronous Gaussian multiple-access channels," *IEEE Trans. Inform. Theory*, vol. 32, pp. 85-96, Jan. 1986.

[21] P. Kempf, "A nonorthogonal synchronous DS-CDMA case where successive cancellation and maximum-likelihood detectors are equivalent," *Proc. IEEE Int. Symp. Inform. Theory*, pp. 321, Whistler, BC, Canada, Sept. 1995.

[22] K. Schneider, "Optimum detection of code division multiplexed signals," *IEEE Trans. Aerospace and Electronics Systems*, vol. 15, pp. 181-185, Jan. 1979.

[23] R. Kohno, H. Imai, and M. Hatori, "Optimum receiver using canceller of co-channel interference in SSMA," *Proc. IECE Conference, Spring*, pp. 7-201, 1982.

[24] T. Kailath and H. V. Poor, "Detection of stochastic process," *IEEE Trans. Inform. Theory*, vol. 44, pp. 2230-2259, Oct. 1998.

[25] C. Sankaran and A. Ephremides, "Solving a class of optimum multiuser detection problems with polynomial complexity," *IEEE Trans. Inform. Theory*, vol. 44, pp. 1958-1961, Sept. 1998.

[26] A. J. Paulraj and C. B. Papadias, "Space-Time Processing for wireless Communications," *IEEE Signal Proc. Mag.*, vol. 14, pp. 49-83, Nov. 1997.

[27] A. J. Viterbi, "Error bounds for convolutional codes and an asymptotically optimal decoding algorithm," *IEEE Trans. Inform. Theory*, vol. 13, pp. 260-269, 1967.

[28] R. Lupas and S. Verdú, "Linear multiuser detectors for synchronous code-division

multiple-access channels," *IEEE Trans. Inform. Theory*, vol. 35, pp. 123-136, Jan. 1989.

[29] R. Lupas and S. Verdú, "Near-far resistance of multiuser detectors in asynchronous channels," *IEEE Trans. Commun.*, vol. 38, no. 4, pp. 496-508, 1990.

[30] Z. Xie, R. Short, and C. Rushforth, "A family of suboptimum detectors for coherent multiuser communications," *IEEE Journal on Selected Areas in Communications*, vol. 8, pp. 683-690, May 1990.

[31] P. B. Rapajic and B. S. Vucetic, "Adaptive receiver structures for asynchronous CDMA systems," *IEEE J. Select. Areas Commun.*, vol. 12, no. 4, pp. 685-697, May 1994.

[32] U. Madhow and M. L. Honig, "MMSE interference suppression for direct-sequence spread spectrum CDMA," *IEEE Trans. Commun.*, vol. 42, pp. 3178-3188, Dec. 1994.

[33] H. V. Poor and S. Verdú, "Probability of error in MMSE multiuser detection," *IEEE Trans. Inform. Theory*, vol. 43, pp. 858-871, May 1997.

[34] S. Haykin, *Adaptive Filter Theory*, 3rd ed., Prentice-Hall, NJ, 1996.

[35] M. Honig, U. Madhow and S. Verdù, "Blind adaptive multiuser detection," *IEEE Trans. Inform. Theory*, vol. 41, pp. 944-960, July 1995.

[36] P. B. Rapajic and B. S. Vucetic, "Application of fast adaptive algorithms in asynchronous CDMA systems," *Int. Symp. on Inform. Theory and Its Applications*, pp. 97-102, Nov. 1994.

[37] D. S. Chen and S. Roy, "An adaptive multiuser receiver for CDMA systems," *IEEE J. Select. Areas Commun.*, Vol. 12, No. 5, pp. 808-816, June 1994.

[38] S. L. Miller, "An adaptive direct-sequence code-division multiple-access receiver for multiuser interference rejection," *IEEE Trans. Commun.*, vol. 43, no. 2/3/4, pp. 1746-1755, Feb/March/April 1995.

[39] X. Wang and H. V. Poor, "Blind multiuser detection: a subspace approach," *IEEE Trans. Inform. Theory*, vol. 44, pp. 677-690, Mar. 1998.

[40] H. Liu and G. Xu, "A subspace method for signature waveform estimation in synchronous CDMA systems," *IEEE Trans. Commun.*, vol. 44, pp. 1346-1354, Oct. 1996.

[41] S. E. Bensley and B. Aazhang, "Subspace-based channel estimation for code division multiple access communication systems," *IEEE Trans. Commun.*, vol. 44, pp. 1009-1020, Aug. 1996.

[42] M. K. Tsatsanis and Z. Xu, "Performance analysis of minimum variance CDMA receivers," *IEEE Trans. Signal. Processing*, vol. 46, pp. 3014-3022, Nov. 1998.

[43] Z. Xu, "Improved constrained optimization method for CDMA systems," *Proc. of 34th Asilomar Conference*, pp. 1293-1297, 2000.

[44] Z. Xu and M. K. Tsatsanis, "Blind adaptive algorithms for minimum variance CDMA receivers," *IEEE Trans. Commun.*, vol. 49, pp. 180-194, Jan. 2001.

[45] A. J. Viterbi, "Very low rate convolutional codes for maximum theoretical performance of spread-spectrum multiple-access channels," *IEEE J. Select. Areas Commun.*, vol.8, pp.641-649, May 1990.

[46] R. Kohno, H. Imai, M. Hatori and S. Pasupathy, "Combination of an adaptive array and a canceller of interference for direct sequence spread spectrum multiple access system," *IEEE J. Select. Areas Commun.*, vol. 8, pp. 675-682, May 1990.

[47] D. N. Godard, "Self-recovering equalization and carrier tracking in two dimensional data communication systems," *IEEE Trans. Commun.*, vol. COMM-28, pp. 1867-1875, Nov. 1980.

[48] J. R. Treichler and B. G. Agee, "A new approach to multipath correction of constant modulus signals," *IEEE Trans. Acoust., Speech, and Signal Processing*, vol. ASSP-31, pp. 459-472, Apr. 1983.

[49] J. Yang, J. J. Werner, and G. A. Dumont, "The multimodulus blind equalization algorithm," *Proc. 13th Int'l. Conf. Digital Sig. Proc.*, vol. 1, pp. 127-130, July 1997.

[50] V. Y. Yang and D. L. Jones, "A vector constant modulus algorithm for shaped constellation equalization," *IEEE Sigal Processing Letters*, vol. 5, No. 4, pp. 89-91, Apr. 1998.

[51] R. Kohno, "Pseudo-noise sequences and interference cancellation techniques for spread spectrum systems - spread spectrum theory and techniques in Japan," *IEICE Trans.*, vol. E74, pp. 1083-1092, May 1991.

[52] P. R. Patel and J. M. Holtzman, "Analysis of a simple successive interference cancellation scheme in a DS/CDMA system," *IEEE J. Select. Areas Commun.*, vol. 12, pp.796-807, June 1994.

[53] D. Divsalar, M. K. Simon and D. Raphaeli, "Improved parallel interference cancellation for CDMA," *IEEE Trans. Commun.*, vol. 46, pp. 258-268, Feb. 1998.

[54] G. Xue, J. Weng, T. Le-Ngoc and S. Tahar, "Adaptive multistage parallel interference cancellation for CDMA," *IEEE J. Select. Areas Commun.*, vol. 17, no. 10, pp. 1815-1827, Oct. 1999.

[55] M.K. Varanasi and B. Aazhang, "Multistage detection in asynchronous code-division multiple-access communications," *IEEE Trans. Commun.*, vol. 38, no. 4, pp. 509-519, 1990.

[56] M.K. Varanasi and B. Aazhang, "Near-optimal detection in synchronous code-division multiple-access systems," *IEEE Trans. Commun.*, vol. 39, no. 5, pp. 725-735, May 1991.

[57] A. Duel-Hallen, "Decorrelating decision-feedback multi-user detector for synchronous code-division multiple access channel," *IEEE Trans. Commun.*, vol. 41, pp. 285-290, Feb. 1993.

[58] A. Duel-Hallen, "A family of multi-user decision-feedback detectors for asynchronous code-division multiple access channels," *IEEE Trans. Commun.*, vol. 43, pp. 421-434, Feb./Mar./Apr. 1995.

[59] A. Yener, R. D. Yates, and S. Ulukus, "CDMA multiuser detection: a nonlinear programming approach," *IEEE Trans. Commun.*, vol. 50, pp. 1016-1024, June 2002.

[60] H. T. Peng, L. K. Rasmussen, and T. J. Lim, "Constrained Maximum-Likelihood Detection in CDMA," *IEEE Trans. Commun.*, vol. 49, pp. 142-152, Jan. 2002.

[61] A. Nemirovskii and P. Gahinet, "The projective method for solving linear matrix inequalities," *Math. Programming Series B*, 77:163-190, 1997.

[62] W.-K. Ma, T.N. Davidson, K.M. Wong, Z.-Q. Luo, and P.C. Ching, "Quasi-maximum-likelihood multiuser detection using semi-definite relaxation with applications to synchronous CDMA," *IEEE Trans. Signal Processing*, vol. 50, no. 4, pp. 912-922, 2002.

[63] M. Abdi, H. El Nahas, A. Jard, and E. Moulines, "Semidefinite positive relaxation of the maximum-likelihood criterion applied to multiuser detection in a CDMA contex," *IEEE Signal Processing Letters*, vol. 9, no. 6, pp. 165-167, 2002.

[64] H. T. Peng and L. K. Rasmussen, "The application of semidefinite programming for detection in CDMA," *IEEE Journal on Selected Areas in Communications*, vol. 19, pp. 1442-1449, Aug. 2001.

[65] X. M. Wang, W.-S. Lu and A. Antoniou, "A near-optimal multiuser detector for CDMA channels using semidefinite programming relaxation," *Proc. ISCAS 2001*, vol. 4, pp. 298-301, May 2001.

[66] J. C. Liberti, Jr. and T. S. Rappaport, *Smart Antennas for Wireless Communications: IS-95 and Third Generation CDMA Applications*, Prentice-Hall, 1999.

[67] V. G. Subramanian and U. Madhow, "Blind demodulation of Direct-Sequence

CDMA signals using an antenna array," *Proc. CISS '96*, pp. 74-79, Mar. 1996.

[68] F. Wijk, G. M. J. Janssen and R. Prasad, "Groupwise successive interference cancellation in a DS/CDMA system," *Proc. 1995 Int. Symp. Personal, Indoor and Mobile Radio Communications (PIMRC'95)*, pp. 742-746, 1995.

[69] F. Adachi, M. Feeney, A. Williamson, and J. Parsons, "Crosscorrelation between the envelopes of 900 Mhz signals received at a mobile radio base station," *Proc. IEE*, 133(6):506-512, Oct., 1986.

[70] W. R. Braun and U. Dersch, "A physical mobile radio channel model," *IEEE Trans. Vehicular Technology*, VT-40(2): 472-482, May, 1991.

[71] L. Vandenberghe and S. Boyd, "Semidefinite programming," *SIAM Review*, vol. 38, pp. 49-95, 1996.

[72] K. C. Toh, M. J. Todd, and R. H. Tütüncü, *"SDPT3 Version 2.1–a MATLAB Software for Semidefinite Programming"*, Sept. 1999.

[73] P. Gahinet, A. Nemirovski, A. J. Laub, and M. Chilali, *Manual of LMI Control Toolbox*, MathWorks Inc., Natick, May 1990.

[74] H. Wolkowicz, R. Saigal, and L. Vandenberghe, *Handbook on Semidefinite Programming*, Kluwer Academic, MA, 2000.

[75] M. X. Geomans and D. P. Williamson, "Improved approximation algorithms for maximum cut and satisfiability problem using semidefinite programming," *J. ACM*, vol. 42, pp. 1115-1145, 1995.

[76] M. X. Geomans and D. P. Williamson, ".878-approximation algorithms for MAX-CUT and MAX-2SAT," *Proc. 26th ACM Symposium on Theory of Computing*, pp. 422-431, 1994.

[77] R. A. Horn and C. R. Johnson, *Matrix Analysis*, Cambridge University Press, Cambridge, UK, 1990.

[78] G. W. Stewart, *Introduction to Matrix Computations*, Academic Press, NY, 1973.

[79] J. H. Wilkinson, *The Algebraic Eigenvalue Problem*, Oxford University Press, 1965.

[80] G. H. Golub and C. F. Vanloan, *Matrix Computations*, 3rd ed., The Johns Hopkins University Press, Baltimore, MD, 1996.

[81] C. Helmberg, *Semidefinite Programming for Combinatorial Optimization*, Konrad-Zuse-Zentrum, Berlin, Oct. 2000.

[82] B. Hassibi and H. Vikalo, "On the expected complexity of integer least squares problems," *Proc. ICASSP*, pp. 1497-1500, Orlando, Florida, May 2002.

[83] J. Luo, K. R. Pattipati, P. K. Willett, and L. Brunel, "Branch-and-bound-based fast optimal algorithm for multiuser detection in synchronous CDMA," *Proc. Int. Conf. Communications*, pp. 3336-3340, Alaska, May 2003.

[84] X. M. Wang, W.-S. Lu, and A. Antoniou, "A near-optimal multiuser detector for DS-CDMA using semidefinite programming relaxation," *IEEE Trans. Signal Processing*, vol. 51, pp. 2446–2450, Sept. 2003.

[85] R. Kohno, H. I, M. Hatori, and S. Pasupathy, "An adaptive canceller of cochannel interference for spread-spectrum multiple-access communication networks in a power line," *IEEE Journa on Select. Areas Commun.*, vol. 8, no. 4, pp. 691-699, Apr. 1990.

[86] F. Rendl, R.J. Vanderbei, and H. Wolkowicz, "Max-min eigenvalue problems, primal-dual interior point algorithms, and trust region subproblems," *Optimization Methods and Software*, vol. 5, pp. 1-16, 1995.

[87] C. Helmberg, F. Rendl, R.J. Vanderbei, and H. Wolkowicz, "An interior-point method for semidefinite programming," *SIAM J. Optim.*, vol. 6, no. 2, pp. 342-361, 1996.

[88] R. Fletcher, *Practical Methods of Optimization*, 2nd ed., Wiley, NY, 1987.

[89] H. Vikalo and B. Hassibi, "Towards closing the capacity gap on multiple antenna channels," *Proc. ICASSP*, pp. 2385-2388, Orlando, Florida, May 2002.

[90] B. Steingrimsson, Z.-Q. Luo, and K. M. Wong, "Soft-quasi-maximum-likelihood detection for multiantenna wireless channels," *IEEE Trans. Signal Processing*, vol. 51, pp. 2710-2719, Nov. 2003.

[91] B. M. Hochwald and S. ten Brink, "Achieving near-capacity on a multiple-antenna channel," *IEEE Trans. Communications*, vol. 51, pp. 389-399, Mar. 2003.

[92] M. Varanasi, "Decision feedback multiuser detection: A systematic approach," *IEEE Trans. Information Theory*, vol. 45, no. 1, pp. 219-240, Jan. 1999.

[93] P. R. Patel and J. M. Holtzman, "Analysis of a simple successive interference cancellation scheme in a DS/CDMA system," *IEEE J. Select. Areas Commun.*, vol. 12, no. 5, pp. 796-807, June 1994.

[94] P. E. Gill, W. Murray, and M. H. Wright, *Practical Optimization*, Academic Press, NY, 1981.

[95] D. Goldfarb and A. Idnani, "A numerical stable dual method for solving strictly convex quadratic programs," *Math. Prog.*, vol. 27, pp. 1-33, 1983.

[96] R. Fletcher, *Practical Methods of Optimization*, 2nd ed., Wiley, NY, 1987.

[97] A. Okounkov, *Brunn-Minkowski inequality for multiplicities*, Invent. Math. 125, pp. 405-411, 1996.

[98] X. Wang and A. Host-Madsen, "Group-blind Multiuser Detection for Uplink CDMA," *IEEE Journal on Selected Areas in Commun.*, vol. 17, no. 11, Nov. 1999.

Appendix A

Proof of Propostion 4.2

We prove this proposition by induction with respect to K.

(i) It is easy to see that for any scalar x that satisfies the inequality $|x|^m - 1 \leq 0$ for $m \geq 1$, we have $x \in [-1, 1]$. Hence, $|x|^n - 1 \leq 0$ for $n \geq 1$ and the proposition holds for $K = 1$.

(ii) Assume that the proposition holds for $K = k$. That is, for any k-component vector $\mathbf{x} \in \mathcal{R}_m$, if

$$\sum_{i=1}^{k} |x_i|^m - k \leq 0 \quad \text{for } m \geq 1, \tag{A.1}$$

$$\text{then} \quad \sum_{i=1}^{k} |x_i|^n - k \leq 0 \quad \text{for } m \geq n \geq 1 \tag{A.2}$$

We can now show that the proposition also holds for $K = k+1$. That is, if $m \geq n \geq 1$ and

$$|x_1|^m + |x_2|^m + \cdots + |x_{k+1}|^m - (k+1) \leq 0 \tag{A.3a}$$

for any vector $\mathbf{x} \in \mathcal{R}_m$, then

$$|x_1|^n + |x_2|^n + \cdots + |x_{k+1}|^n - (k+1) \leq 0 \tag{A.3b}$$

Denoting x_i as the component of $\mathbf{x}$ in (A.3a) that has the least absolute value, it is easy to see that $|x_i| \leq 1$. Then (A.3a) can be expressed as

$$\sum_{\substack{j=1 \\ j \neq i}}^{k+1} |x_j|^m \leq k + 1 - |x_i|^m \tag{A.4}$$

By introducing a positive scalar

$$t = [k/(k+1-|x_j|^m)]^{1/m}$$

the inequality in (A.4) is equivalent to

$$\sum_{\substack{j=1 \\ j\neq i}}^{k+1} |tx_j|^m \leq k \tag{A.5}$$

Since there are only k variables involved on the left-hand side of (A.5), according to the assumption, we have

$$\sum_{\substack{j=1 \\ j\neq i}}^{k+1} |tx_j|^n - k \leq 0 \tag{A.6}$$

which can be expressed as

$$\sum_{\substack{j=1 \\ j\neq i}}^{k+1} |x_j|^n \leq k^{1-n/m}(k+1-|x_i|^m)^{n/m} \tag{A.7}$$

Next we define a function

$$f(x) = (k+1-x^n) - \left[k^{(1-n/m)}(k+1-x^m)^{n/m}\right]$$

whose first derivative is given by

$$f'(x) = -nx^{n-1} + n \cdot k^{(1-n/m)}(k+1-x^m)^{n/m-1}x^{m-1} \tag{A.8}$$

For $x \in [0,1]$ and $m \geq 1$, it can be verified that

$$0 \leq x \leq \left(1 + \frac{1}{k} - \frac{x^m}{k}\right)^{1/m} \tag{A.9}$$

If we take the $(m-n)$th power for both sides of (A.9), then for $m \geq n \geq 1$ the above inequality becomes

$$0 \leq \frac{x^{(m-1)}}{x^{(n-1)}} \leq \frac{(k+1-x^m)^{(m-n)/m}}{k^{(m-n)/m}} \tag{A.10}$$

which leads to

$$k^{(m-n)/m}(k+1-x^m)^{-(m-n)/m} \cdot x^{(m-1)} \leq x^{(n-1)} \tag{A.11}$$

Using (A.11), $f'(x)$ in (A.8) can be shown to be non-positive for $0 \leq x \leq 1$. That is, $f(x)$ is monotonically decreasing on interval [0, 1]. Since $f(1) = 0$, we have $f(x) \geq 0$ for $x \in [0,\ 1]$. Hence,

$$k^{(1-n/m)}(k+1-|x_i|^m)^{n/m} \leq (k+1-|x_i|^n) \quad \text{for} \quad 0 \leq |x_i| \leq 1 \tag{A.12}$$

From (A.7) and (A.12), we have

$$|x_1|^n + |x_2|^n + \cdots + |x_{k+1}|^n \leq k+1 \tag{A.13}$$

which implies that the inequality in (A.3) is satisfied.

Appendix B

Proof of Proposition 4.4

The following lemma will be used in the proof.

Lemma B.1: If $\mathbf{A}$ is an $n \times n$ matrix composed of four block matrices as

$$\mathbf{A} = \begin{bmatrix} \mathbf{A}_{11} & \mathbf{A}_{12} \\ \mathbf{A}_{21} & \mathbf{A}_{22} \end{bmatrix} \tag{B.1}$$

where $\mathbf{A}_{11} \in \mathcal{C}^{k \times k}$, $\mathbf{A}_{12} \in \mathcal{C}^{k \times (n-k)}$, $\mathbf{A}_{21} \in \mathcal{C}^{(n-k) \times k}$, and $\mathbf{A}_{22} \in \mathcal{C}^{(n-k) \times (n-k)}$, then the inverse of $\mathbf{A}$ is given by

$$\mathbf{A}^{-1} = \begin{bmatrix} \mathbf{B} & -\mathbf{B} \cdot \mathbf{A}_{12}\mathbf{A}_{22}^{-1} \\ -\mathbf{C} \cdot \mathbf{A}_{21}\mathbf{A}_{11}^{-1} & \mathbf{C} \end{bmatrix} \tag{B.2}$$

where

$$\mathbf{B} = (\mathbf{A}_{11} - \mathbf{A}_{12}\mathbf{A}_{22}^{-1}\mathbf{A}_{21})^{-1}$$
$$\mathbf{C} = (\mathbf{A}_{22} - \mathbf{A}_{21}\mathbf{A}_{11}^{-1}\mathbf{A}_{12})^{-1}$$

This lemma can be easily verified by showing that $\mathbf{A}^{-1} \cdot \mathbf{A} = \mathbf{I}$.

To simplify the notation, the solution of the problem in (4.36), $\mathbf{x}_j^*$, is expressed as

$$\mathbf{x}_j^* = \begin{bmatrix} \hat{\mathbf{x}}_j^* \\ \check{\mathbf{x}}_j^* \end{bmatrix} \tag{B.3}$$

where $\check{\mathbf{x}}_j^*$ is composed of the variables corresponding to the information bits that are detected in the jth iteration and $\hat{\mathbf{x}}_j^*$ is composed of the variables corresponding to the

other information bits. According to the RCP algorithm in Table 4.2, we have

$$|\hat{\mathbf{x}}_j^*(i)| < \xi_j \quad \text{and} \quad |\check{\mathbf{x}}_j^*(i)| \geq \xi_j \tag{B.4}$$

where $\mathbf{x}(i)$ denotes the ith component of $\mathbf{x}$. Note that according to the assumption in (B.3), $\mathbf{H}_j$ in (4.36) can be decomposed into submatrices as

$$\mathbf{H}_j = \begin{bmatrix} \mathbf{H}_{j+1} & \hat{\mathbf{H}}_j \\ \hat{\mathbf{H}}_j^T & \check{\mathbf{H}}_j \end{bmatrix} \tag{B.5}$$

where $\mathbf{H}_{j+1}$ is defined in (4.22) and $\hat{\mathbf{H}}_j$ and $\check{\mathbf{H}}_j$ are defined in (4.40).

Note that the constraint $c_j(\mathbf{x}_j^*, p) < 0$ implies that the constant of this problem is inactive; hence, the solution of the problem in (4.34) can be obtained as

$$\mathbf{x}_j^* = \begin{bmatrix} \hat{\mathbf{x}}_j^* \\ \check{\mathbf{x}}_j^* \end{bmatrix} = -\frac{1}{2} \begin{bmatrix} \mathbf{H}_{j+1} & \hat{\mathbf{H}}_j \\ \hat{\mathbf{H}}_j^T & \check{\mathbf{H}}_j \end{bmatrix}^{-1} \left(\mathbf{p}_j + 2\tilde{\mathbf{H}}_j \bar{\mathbf{b}}_j \right) \tag{B.6}$$

According to Lemma B.1, $\hat{\mathbf{x}}_j^*$ in (B.6) can be expressed as

$$\hat{\mathbf{x}}_j^* = \boldsymbol{\Delta} \cdot (\mathbf{r} - \bar{\mathbf{S}}_j \bar{\mathbf{A}}_j \bar{\mathbf{b}}_j) = \mathbf{b}_{j+1} + \boldsymbol{\Delta}_j \cdot (\bar{\mathbf{S}}_j \bar{\mathbf{A}}_j \bar{\delta}_{b,j} + \mathbf{n}_c) \tag{B.7}$$

where $\boldsymbol{\Delta}$ is defined by

$$\boldsymbol{\Delta}_j = \left(\mathbf{H}_{j+1} - \hat{\mathbf{H}}_j \check{\mathbf{H}}_j^{-1} \hat{\mathbf{H}}_j^T \right)^{-1} \cdot \left(\mathbf{A}_{j+1} \mathbf{S}_{j+1}^T - \hat{\mathbf{H}}_j \check{\mathbf{H}}_j^{-1} \check{\mathbf{A}}_j \check{\mathbf{S}}_j^T \right) \tag{B.8}$$

$\bar{\mathbf{S}}_j$, $\bar{\mathbf{A}}_j$, $\mathbf{S}_{j+1}$, and $\mathbf{A}_{j+1}$ are defined in (4.22), $\check{\mathbf{S}}_j$ denotes the signature matrix obtained by removing the columns of $\mathbf{S}_j$ whose indices are not in Ω_{j+1}, $\check{\mathbf{A}}_j$ denotes the amplitude matrix obtained by removing the rows and columns of $\mathbf{A}_j$ whose indices are not in Ω_{j+1}, and $\bar{\delta}_{\mathbf{b},j}$ denotes the vector composed of the decision errors of the information bits that are detected before the jth iteration.

Next we define vector $\mathbf{x}_{j+1}^\dagger$ as

$$\begin{aligned} \mathbf{x}_{j+1}^\dagger &= -\frac{1}{2} \mathbf{H}_{j+1}^{-1} (\mathbf{p}_{j+1} + 2\tilde{\mathbf{H}}_{j+1} \bar{\mathbf{b}}_{j+1}) = \mathbf{H}_{j+1}^{-1} \mathbf{A}_{j+1} \mathbf{S}_{j+1}^T (\mathbf{r} - \bar{\mathbf{S}}_{j+1} \bar{\mathbf{A}}_{j+1} \bar{\mathbf{b}}_{j+1}) \\ &= \mathbf{b}_{j+1} + \mathbf{H}_{j+1}^{-1} \mathbf{A}_{j+1} \mathbf{S}_{j+1} \left(\bar{\mathbf{S}}_j \bar{\mathbf{A}}_j \bar{\delta}_{\mathbf{b},j} + \check{\mathbf{S}}_j \check{\mathbf{A}}_j \check{\delta}_{\mathbf{b},j} + \mathbf{n}_c \right) \end{aligned} \tag{B.9}$$

where $\check{\delta}_{\mathbf{b},j}$ denotes the vector composed by the decision errors of the information bits that are detected in the jth iteration. It is easy to verify that

$$\delta_{\mathbf{x},j} = \hat{\mathbf{x}}_j^* - \mathbf{x}_{j+1}^\dagger = \mathbf{\Sigma}_j \cdot \mathbf{n}_c + \mathbf{\Sigma}_j \cdot \bar{\mathbf{S}}_j \; \bar{\mathbf{A}}_j \bar{\delta}_{\mathbf{b},\,j} - \mathbf{H}_{j+1}^{-1} \; \hat{\mathbf{H}}_j \; \check{\delta}_{\mathbf{b},\,j} \tag{B.10}$$

where $\mathbf{\Sigma}$ is defined as

$$\mathbf{\Sigma}_j = \mathbf{\Delta}_j - \mathbf{H}_{j+1}^{-1} \mathbf{A}_{j+1} \mathbf{S}_{j+1}^T \tag{B.11}$$

When the decisions of the ith information bits for $i \in \Omega_{i+1}$ are determined correctly, $\bar{\delta}_{\mathbf{b},\,j}$ and $\check{\delta}_{\mathbf{b},\,j}$ become zero vectors, and (B.10) can be simplified to

$$\delta_{\mathbf{x},j} = \hat{\mathbf{x}}_j^* - \mathbf{x}_{j+1}^\dagger = \mathbf{\Sigma}_j \cdot \mathbf{n}_c \tag{B.12}$$

Hence

$$\mathrm{P}\left[\mathbf{x}_{j+1}^* = \mathbf{x}_{j+1}^\dagger\right] \geq \prod_{i \notin \Omega_{j+1}} \mathrm{P}\left(|\mathbf{x}_{j+1}^\dagger(i)| \leq 1\right) \tag{B.13}$$

$$\geq \prod_{i \notin \Omega_{j+1}} \mathrm{P}\left(|\mathbf{n}_{\Sigma,j}(i)| < 1 - \xi_j\right) \tag{B.14}$$

where $\mathbf{n}_{\Sigma,j} = \mathbf{\Sigma}_j \mathbf{n}_c$ and $\mathbf{n}_{\Sigma,j}(i)$ denotes the ith component of $\mathbf{n}_{\Sigma,j}$. Note that the inequality in (B.13) is obtained by letting $p \to \infty$ and thus is satisfied for any scalar $p \geq 1$. Since $\mathbf{n}_{\Sigma,j}(i)$ is a zero-mean Gaussian variable whose variance is $\sigma^2 \rho_i^2$ with ρ_i being defined in (4.37), we obtain

$$\mathrm{P}\left(|\mathbf{n}_\Sigma(i)| < 1 - \xi_j\right) = \frac{1}{\sqrt{2\pi}\sigma\rho_i} \int_{-(1-\xi_j)}^{1-\xi_j} \exp\left(-\frac{t^2}{2\sigma^2\rho_i^2}\right) dt = \mathrm{erf}\left(\frac{1-\xi_j}{\sqrt{2}\sigma\rho_i}\right) \tag{B.15}$$

Substituting (B.15) into (B.14), we have

$$\mathrm{P}\left[\mathbf{x}_{j+1}^* = -\frac{1}{2}\mathbf{H}_{j+1}^{-1}(\mathbf{p}_{j+1} + 2\tilde{\mathbf{H}}_{j+1}\bar{\mathbf{b}}_{j+1})\right] \geq \prod_{i \notin \Omega_{j+1}} \mathrm{erf}\left(\frac{1-\xi_j}{\sqrt{2}\sigma\rho_i}\right) \tag{B.16}$$

Appendix C

A Sufficient Condition for Global Convexity of the Problem in (6.19)

Based on the assumption $||\mathbf{g}_1||^2 = 1$, the objective function in (6.19a) can be expressed as

$$\begin{aligned}\mathcal{J}(\mathbf{w}) &= \mathrm{E}\left[\sum_{m=1}^{M}\left(|\mathbf{w}^H\mathbf{y}_m|^2 - A_1^2 g_1^2(m)\right)\right]^2 \\ &= \sum_{m=1}^{M}\sum_{n=1}^{M}\mathrm{E}\left(|\mathbf{w}^H\mathbf{y}_m|^2 - r_m\right)\left(|\mathbf{w}^H\mathbf{y}_n|^2 - r_n\right) \\ &= \sum_{m=1}^{M}\sum_{n=1}^{M}\mathcal{J}_{m,n}(\mathbf{w}) \qquad \text{(C.1)}\end{aligned}$$

where $r_m = A_1^2 g_1^2(m)$ and $\mathcal{J}_{m,n}(\mathbf{w}) = \mathrm{E}\left(|\mathbf{w}^H\mathbf{y}_m|^2 - r_m\right)\left(|\mathbf{w}^H\mathbf{y}_n|^2 - r_n\right)$. In (C.1), $\mathbf{y}_m(i)$ is replaced by $\mathbf{y}_m$ to simplify the notation. By defining $\bar{\mathbf{H}}^m = [\bar{\mathbf{h}}_1^m\ \bar{\mathbf{h}}_2^m\ \cdots\ \bar{\mathbf{h}}_{3K}^m]$, $\bar{\mathbf{A}} = \mathrm{diag}\{\bar{A}_1\ \bar{A}_2\ \cdots\ \bar{A}_{3K}\}$ and $\bar{\mathbf{b}} = [\bar{b}_1\ \bar{b}_2\ \cdots\ \bar{b}_{3K}]^T$, (6.18) can be expressed as

$$\mathbf{y}_m = \bar{\mathbf{H}}_m\bar{\mathbf{A}}\bar{\mathbf{b}} + \mathbf{v}_m \qquad \text{(C.2)}$$

where $\mathbf{v}_m(i)$ is replaced by $\mathbf{v}_m$ for the same reason. When $m = n$, $\mathcal{J}_{m,m}(\mathbf{w})$ can be simplified as

$$\mathcal{J}_{m,m}(\mathbf{w}) = \mathrm{E}(|\mathbf{w}^H\mathbf{y}_m|^4) - 2r_m\mathrm{E}(|\mathbf{w}^H\mathbf{y}_m|^2) + r_m^2 \qquad \text{(C.3)}$$

Note that each component of $\bar{\mathbf{b}}$ can assume +1 and -1 with equal probability and $\mathbf{v}_m$ is a vector of complex-valued zero-mean white Gaussian variables. It can be shown

that

$$\mathrm{E}(\bar{\mathbf{b}}\bar{\mathbf{b}}^H) = \mathbf{I} \qquad \mathrm{E}|\mathbf{w}^H\mathbf{v}_m|^2 = \sigma_v^2(\mathbf{w}^H\mathbf{w}) \qquad \mathrm{E}|\mathbf{w}^H\mathbf{v}_m|^4 = 3\sigma_v^4(\mathbf{w}^H\mathbf{w})^2$$
$$\mathrm{E}(\mathbf{v}_m\mathbf{v}_m^T) = 0 \qquad \mathrm{E}(\mathbf{v}_m\mathbf{v}_n^H) = 0 \quad \text{for } m \neq n \tag{C.4}$$

By using (C.4), we compute

$$\mathrm{E}\left(|\mathbf{w}^H\mathbf{y}_m|^2\right) = \mathbf{w}^H(\mathbf{Q}_m + \sigma_v^2\mathbf{I})\mathbf{w} = \mathbf{w}^H\mathbf{R}_m\mathbf{w} \tag{C.5}$$

$$\begin{aligned}\mathrm{E}|\mathbf{w}^H\mathbf{y}_m|^4 &= \mathrm{E}\left|\mathbf{w}^H\bar{\mathbf{H}}_m\bar{\mathbf{A}}\bar{\mathbf{b}}\right|^4 + \mathrm{E}\left[\mathbf{w}^H(\mathbf{v}_m\bar{\mathbf{b}}^T\bar{\mathbf{A}}^T\bar{\mathbf{H}}_m^H + \bar{\mathbf{H}}_m\bar{\mathbf{A}}\bar{\mathbf{b}}\mathbf{v}_m^H)\mathbf{w}\right]^2 \\ &\quad + \mathrm{E}|\mathbf{w}^H\mathbf{v}_m|^4 + 2(\mathbf{w}^H\mathbf{Q}_m\mathbf{w})\mathrm{E}|\mathbf{w}^H\mathbf{v}_m|^2 \\ &= \mathrm{E}\left|\mathbf{w}^H\bar{\mathbf{H}}_m\bar{\mathbf{A}}\bar{\mathbf{b}}\right|^4 + 3\sigma_v^4(\mathbf{w}^H\mathbf{w})^2 + 4\sigma_v^2(\mathbf{w}^H\mathbf{Q}_m\mathbf{w})\cdot\mathbf{w}^H\mathbf{w}\end{aligned} \tag{C.6}$$

where $\mathbf{Q}_m = \bar{\mathbf{H}}_m\bar{\mathbf{A}}\bar{\mathbf{A}}^H\bar{\mathbf{H}}_m^T$ and $\mathbf{R}_m = \mathbf{Q}_m + \sigma_v^2\mathbf{I}$. The first term in (C.6) can be written as

$$\begin{aligned}\mathrm{E}\left|\mathbf{w}^H\bar{\mathbf{H}}_m\bar{\mathbf{A}}\bar{\mathbf{b}}\right|^4 = (\mathbf{w}^H\mathbf{Q}_m\mathbf{w})^2 + \sum_{k=1}^{3K}\sum_{\substack{l=1\\l\neq k}}^{3K}\bar{A}_k^2\bar{A}_l^2\left[|\mathbf{w}^H\bar{\mathbf{h}}_k^m|^2|\mathbf{w}^H\bar{\mathbf{h}}_l^m|^2\right. \\ \left. + (\mathbf{w}^H\bar{\mathbf{h}}_k^m)^2[(\mathbf{w}^H\bar{\mathbf{h}}_l^m)^H]^2\right]\end{aligned} \tag{C.7}$$

Substituting (C.5), (C.6), and (C.7) into (C.3), $\mathcal{J}_{m,m}(\mathbf{w})$ in (C.3) can be expressed as

$$\begin{aligned}\mathcal{J}_{m,m}(\mathbf{w}) &= (\mathbf{w}^H\mathbf{R}_m\mathbf{w} - r_m)^2 + 2\sigma_v^4(\mathbf{w}^H\mathbf{w})^2 + 2\sigma_v^2\ \mathbf{w}^H\mathbf{Q}_m\mathbf{w}\cdot\mathbf{w}^H\mathbf{w} \\ &\quad + \sum_{k=1}^{3K}\sum_{\substack{l=1\\l\neq k}}^{3K}\bar{A}_k^2\bar{A}_l^2\left[|\mathbf{w}^H\bar{\mathbf{h}}_k^m|^2|\mathbf{w}^H\bar{\mathbf{h}}_l^m|^2 + (\mathbf{w}^H\bar{\mathbf{h}}_k^m)^2[(\mathbf{w}^H\bar{\mathbf{h}}_k^m)^H]^2\right]\end{aligned} \tag{C.8}$$

When $m \neq n$, $\mathcal{J}_{m,n}(\mathbf{w})$ can be derived in a similar way as

$$\begin{aligned}\mathcal{J}_{m,n}(\mathbf{w}) = (\mathbf{w}^H\mathbf{R}_m\mathbf{w} - r_m)(\mathbf{w}^H\mathbf{R}_n\mathbf{w} - r_n) + \sum_{k=1}^{3K}\sum_{\substack{l=1\\l\neq k}}^{3K}\bar{A}_k^2\bar{A}_l^2\left[(\mathbf{w}^H\bar{\mathbf{h}}_k^m)(\mathbf{w}^H\bar{\mathbf{h}}_k^n)\cdot\right. \\ \left.(\mathbf{w}^H\bar{\mathbf{h}}_l^m)^H\ (\mathbf{w}^H\bar{\mathbf{h}}_l^n)^H + (\mathbf{w}^H\bar{\mathbf{h}}_k^m)(\mathbf{w}^H\bar{\mathbf{h}}_k^n)^H\ (\mathbf{w}^H\bar{\mathbf{h}}_l^m)^H(\mathbf{w}^H\bar{\mathbf{h}}_l^n)\right]\end{aligned} \tag{C.9}$$

Substituting (C.8) and (C.9) into (C.1), the objective function in (C.1) becomes

$$\begin{aligned}\mathcal{J}(\mathbf{w}) &= 2\sigma_v^2(\mathbf{w}^H\mathbf{Q}\mathbf{w})(\mathbf{w}^H\mathbf{w}) + 2\sigma_v^4\, M(\mathbf{w}^H\mathbf{w}) + \frac{1}{2}\sum_{k=1}^{3K}\sum_{l=1}^{3K}\bar{A}_k^2\bar{A}_l^2(\mathbf{w}^H\mathbf{P}_{kl}\mathbf{w})^2 \\ &\quad + (\mathbf{w}^H\mathbf{R}\mathbf{w} - A_1^2)^2 - \frac{1}{2}\sum_{k=1}^{3K}\bar{A}_k^4(\mathbf{w}^H\mathbf{P}_{kk}\mathbf{w})^2 \\ &= \sum_{i=1}^{5}\mathcal{J}_i(\mathbf{w}) \end{aligned} \tag{C.10}$$

where $\mathbf{Q} = \sum_{m=1}^{M}\mathbf{Q}_m$, $\mathbf{R} = \sum_{m=1}^{M}\mathbf{R}_m$ are positive semidefinite matrices, $\mathbf{P}_{kl}$ is a Hermitian matrix which is defined as $\mathbf{P}_{kl} = \sum_{m=1}^{M}\left[\bar{\mathbf{h}}_k^m(\bar{\mathbf{h}}_l^m)^H + \bar{\mathbf{h}}_l^m(\bar{\mathbf{h}}_k^m)^H\right]$. Note that $\mathcal{J}_i(\mathbf{w})$ is defined as the ith term in (C.10).

Next, we compute the Hessian of the objective function, which is given by $\mathcal{J}''(\mathbf{w}) = \sum_{i=1}^{5}\mathcal{J}_i''(\mathbf{w})$. In what follows, $\mathbf{x}$ denotes an arbitrary nonzero vector.

i) The Hessian of $\mathcal{J}_1(\mathbf{w})$ is given by

$$\begin{aligned}\mathcal{J}_1''(\mathbf{w}) &= \left[2\sigma_v^2(\mathbf{w}^H\mathbf{Q}\mathbf{w})(\mathbf{w}^H\mathbf{w})\right]'' \\ &= 8\sigma^2\left[(\mathbf{w}^H\mathbf{w})\mathbf{Q} + \mathbf{w}\mathbf{w}^H\mathbf{Q} + (\mathbf{w}^H\mathbf{Q}\mathbf{w})\mathbf{I} + \mathbf{Q}\mathbf{w}\mathbf{w}^H\right]\end{aligned} \tag{C.11}$$

According to the Cauchy-Schwarz inequality, we obtain

$$\mathbf{x}^H\mathcal{J}_1''\mathbf{x} \geq 8\sigma^2\left|\sqrt{\mathbf{w}^H\mathbf{w}}\sqrt{\mathbf{x}^H\mathbf{Q}\mathbf{x}} - \sqrt{\mathbf{x}^H\mathbf{x}}\sqrt{\mathbf{w}^H\mathbf{Q}\mathbf{w}}\right|^2 \geq 0 \tag{C.12}$$

ii) The Hessian of $\mathcal{J}_2(\mathbf{w})$ is given by

$$\mathcal{J}_2''(\mathbf{w}) = \left[2M\sigma^4(\mathbf{w}^H\mathbf{w})^2\right]'' = 16M\sigma^4(\mathbf{w}^H\mathbf{w}\cdot\mathbf{I} + \mathbf{w}\mathbf{w}^H) \tag{C.13}$$

It is easy to see that $\mathbf{x}^H\mathcal{J}_2''\mathbf{x} = 16M\sigma^4\left(||\mathbf{w}||^2||\mathbf{x}||^2 + |\mathbf{x}^H\mathbf{w}|^2\right) > 0$

iii) The Hessian of $\mathcal{J}_3(\mathbf{w})$ is given by

$$\begin{aligned}\mathcal{J}_3''(\mathbf{w}) &= \left[\frac{1}{2}\sum_{k=1}^{3K}\sum_{l=1}^{3K}\bar{A}_k^2\bar{A}_l^2(\mathbf{w}^H\mathbf{P}_{kl}\mathbf{w})^2\right]'' \\ &= 4\sum_{k=1}^{3K}\sum_{l=1}^{3K}\bar{A}_k^2\bar{A}_l^2\left[\mathbf{P}_{kl}\mathbf{w}\mathbf{w}^H\mathbf{P}_{kl}^H + (\mathbf{w}^H\mathbf{P}_{kl}\mathbf{w})\mathbf{P}_{kl}\right]\end{aligned} \tag{C.14}$$

iv) The Hessian of $\mathcal{J}_4(\mathbf{w})$ is given by

$$\mathcal{J}_4''(\mathbf{w}) = \left[(\mathbf{w}^H\mathbf{R}\mathbf{w} - A_1^2)^2\right]'' = 8\mathbf{R}\mathbf{w}\mathbf{w}^H\mathbf{R} + 8(\mathbf{w}^H\mathbf{R}\mathbf{w} - A_1^2)\mathbf{R} \tag{C.15}$$

v) The Hessian matrix of $\mathcal{J}_5(\mathbf{w})$ is given by

$$\begin{aligned}\mathcal{J}_5''(\mathbf{w}) &= -\frac{1}{2}\left[\sum_{k=1}^{3K} \bar{A}_k^4(\mathbf{w}^H\mathbf{P}_{kk}\mathbf{w})^2\right]'' \\ &= -4\sum_{k=1}^{3K} \bar{A}_k^4\left[\mathbf{P}_{kk}\mathbf{w}\mathbf{w}^H\mathbf{P}_{kk}^H + (\mathbf{w}^H\mathbf{P}_{kk}\mathbf{w})\mathbf{P}_{kk}\right]\end{aligned} \tag{C.16}$$

Since $\mathcal{J}_1''(\mathbf{w})$ and $\mathcal{J}_2''(\mathbf{w})$ are positive semidefinite matrices, we have to find the condition so that $\sum_{i=3}^{5}\mathcal{J}_i''(\mathbf{w})$ is positive semidefinite as well. After some manipulations, it can be shown that

$$\mathbf{x}^H\left[4\sum_{k=1}^{3K}\sum_{l=1}^{3K}\bar{A}_k^2\bar{A}_l^2(\mathbf{P}_{kl}\mathbf{w}\mathbf{w}^H\mathbf{P}_{kl}^H) - 4\sum_{k=1}^{3K}\bar{A}_k^4(\mathbf{P}_{kk}\mathbf{w}\mathbf{w}^H\mathbf{P}_{kk}^H)\right]\mathbf{x}$$

$$= 4\sum_{k=1}^{3K}\sum_{\substack{l=1\\l\neq k}}^{3K}\bar{A}_k^2\bar{A}_l^2|\mathbf{x}^H\mathbf{P}_{kl}\mathbf{w}|^2 \geq 0 \tag{C.17}$$

$$\mathbf{x}^H\left(4\sum_{k=1}^{3K}\sum_{l=1}^{3K}\bar{A}_k^2\bar{A}_l^2(\mathbf{w}^H\mathbf{P}_{kl}\mathbf{w})\mathbf{P}_{kl}\right)\mathbf{x}$$

$$= 16\sum_{m=1}^{M}\sum_{n=1}^{M}\left|\sum_{k=1}^{3K}\bar{A}_k^2(\mathbf{w}^H\bar{\mathbf{h}}_k^m)(\mathbf{x}^H\bar{\mathbf{h}}_k^n)\right|^2 \geq 0 \tag{C.18}$$

$$\mathbf{x}^H\left(8\mathbf{R}\mathbf{w}\mathbf{w}^H\mathbf{R}\right)\mathbf{x} = 8|\mathbf{x}^H\mathbf{R}\mathbf{w}|^2 \geq 0 \tag{C.19}$$

Then based on the constraint (6.19b), we have

$$\mathbf{w}^H\mathbf{R}\mathbf{w} \geq \bar{A}_1^2 + \sigma^2\mathbf{w}^H\mathbf{w} > \bar{A}_1^2 \tag{C.20}$$

which leads to

$$\mathbf{x}^H \left[8(\mathbf{w}^H\mathbf{R}\mathbf{w} - \bar{A}_1^2)\mathbf{R} - 4\sum_{k=1}^{3K} \bar{A}_k^4(\mathbf{w}^H\mathbf{P}_{kk}\mathbf{w})\mathbf{P}_{kk} \right] \mathbf{x} \tag{C.21}$$

$$> \mathbf{x}^H \left[8(\mathbf{w}^H\mathbf{Q}\mathbf{w} - \bar{A}_1^2)\mathbf{Q} - 4\sum_{k=1}^{3K} \bar{A}_k^4(\mathbf{w}^H\mathbf{P}_{kk}\mathbf{w})\mathbf{P}_{kk} \right] \mathbf{x}$$

$$= 2\sum_{k=1}^{3K} \bar{A}_k^2\mathbf{x}^H\mathbf{P}_{kk}\mathbf{x} \left(\sum_{\substack{l=1 \\ l\neq k}}^{3K} \bar{A}_l^2\mathbf{w}^H\mathbf{P}_{ll}\mathbf{w} - \bar{A}_1^2\mathbf{w}^H\mathbf{P}_{11}\mathbf{w} - \bar{A}_k^2\mathbf{w}^H\mathbf{P}_{kk}\mathbf{w} \right) \tag{C.22}$$

$$= 2\sum_{k=1}^{3K} \bar{A}_k^2\mathbf{x}^H\mathbf{P}_{kk}\mathbf{x} \cdot \mathbf{w}^H \left(\sum_{\substack{l=1 \\ l\neq k}}^{3K} \bar{A}_l^2\mathbf{P}_{ll} - \bar{A}_1^2\mathbf{P}_{11} - \bar{A}_k^2\mathbf{P}_{kk} \right) \mathbf{w} \tag{C.23}$$

Note that the equality in (C.22) is based on the observation $\mathbf{w}^H\mathbf{P}_{11}\mathbf{w} = 2 \cdot |\mathbf{g}_1|^2 = 2$. In addition, since $\mathbf{P}_{kk}$ in (C.23) is a positive semidefinite matrix, we have $\mathbf{x}^H\mathbf{P}_{kk}\mathbf{x} \geq 0$. Hence, if

$$\sum_{\substack{l=1 \\ l\neq k}}^{3K} \bar{A}_l^2\mathbf{P}_{ll} - \bar{A}_1^2\mathbf{P}_{11} - \bar{A}_k^2\mathbf{P}_{kk} \succeq 0 \quad \text{for} \quad k = 1,\ 2,\ \ldots,\ 3K \tag{C.24}$$

then the quantity in (C.23) is non-negative.

Therefore, if the condition in (C.24) is satisfied, then the Hessian of the objective function is globally convex and thus the problem in (6.19) has a unique global optimal solution.